Jordan Journal of Mechanical and Industrial Engineering (JJMIE)

JJMIE is a high-quality scientific journal devoted to fields of Mechanical and Industrial Engineering. It is published by Hashemite University in cooperation with the Jordanian Scientific Research and Innovation Support Fund, Ministry of Higher Education and Scientific Research.

SUBMISSION ADDRESS:

Prof. Moh'd Sami Ashhab, Editor-in-Chief
Jordan Journal of Mechanical & Industrial Engineering,
Hashemite University,
PO Box 330127, Zarqa, 13133 , Jordan
E-mail: jjmie@hu.edu.jo

Hashemite Kingdom of Jordan

Hashemite University

Jordan Journal of Mechanical and Industrial Engineering

JJMIE

An International Peer-Reviewed Scientific Journal

Financed by Scientific Research Support Fund

http://jjmie.hu.edu.jo/

ISSN 1995-6665

Jordan Journal of Mechanical and Industrial Engineering (JJMIE)

JJMIE is a high-quality scientific journal devoted to fields of Mechanical and Industrial Engineering. It is published by Hashemite University in cooperation with the Jordanian Scientific Research and Innovation Support Fund, Ministry of Higher Education and Scientific Research.

Introduction: The Editorial Board is very committed to build the Journal as one of the leading international journals in mechanical and industrial engineering sciences in the next few years. With the support of the Ministry of Higher Education and Scientific Research and Jordanian Universities, it is expected that a heavy resource to be channeled into the Journal to establish its international reputation. The Journal's reputation will be enhanced from arrangements with several organizers of international conferences in publishing selected best papers of the conference proceedings.

Aims and Scope: *Jordan Journal of Mechanical and Industrial Engineering* (JJMIE) is a refereed international journal to be of interest and use to all those concerned with research in various fields of, or closely related to, mechanical and industrial engineering disciplines. *Jordan Journal of Mechanical and Industrial Engineering* aims to provide a highly readable and valuable addition to the literature which will serve as an indispensable reference tool for years to come. The coverage of the journal includes all new theoretical and experimental findings in the fields of mechanical and industrial engineering or any closely related fields (Materials, Manufacturing, Management, Design, Thermal, Fluid, Energy, Control, Mechatronics, and Biomedical). The journal also encourages the submission of critical review articles covering advances in recent research of such fields as well as technical notes.

Guide for Authors

Manuscript Submission:
High-quality submissions to this new journal are welcome now and manuscripts may be either submitted online or email.

Online: For online and email submission upload one copy of the full paper including graphics and all figures at the online, submission site, accessed via http://jjmie.hu.edu.jo. The manuscript must be written in MS Word Format. All correspondence including notification of the Editor's decision and requests for revision, takes place by e-mail and via the Author's homepage, removing the need for a hard-copy paper trail

Submission address and contact :

Prof. Moh'd Sami Ashhab
Editor-in-Chief
Jordan Journal of Mechanical & Industrial Engineering, Hashemite University
PO Box 330127, Zarqa, 13115, Jordan
E-mail: jjmie@hu.edu.jo

Types of contributions*:* Original research papers and Technical reports

Corresponding author: Clearly indicate who is responsible for correspondence at all stages of refereeing and publication, including post-publication. Ensure that telephone and fax numbers (with country and area code) are provided in addition to the e-mail address and the complete postal address. Full postal addresses must be given for all co-authors.

Original material: Submission of an article implies that the work described has not been published previously (except in the form of itstan abstract or as part of a published lecture or academic thesis), that it is not under consideration for publication elsewhere, tha publication is approved by all authors and that, if accepted, it will not be published elsewhere in the same form, in English or in any other language, without the written consent of the Publisher. Authors found to be deliberately contravening the submission guidelines on originality and exclusivity shall not be considered for future publication in this journal.

Withdrawing: If the author chooses to withdraw his article after it has been assessed, he shall reimburse JJMIE with the cost of reviewing the paper.

Manuscript Preparation:

General: Editors reserve the right to adjust style to certain standards of uniformity. Original manuscripts are discarded after .publication unless the Publisher is asked to return original material after use. Please use MS Word for the text of your manuscript

Structure: Follow this order when typing manuscripts: Title, Authors, Authors title, Affiliations, Abstract, Keywords, Introduction, Main text, Conclusions, Acknowledgements, Appendix, References, Figure Captions, Figures and then Tables. Please supply figures imported into the text AND also separately as original graphics files. Collate acknowledgements in a separate section at the end of the article and do not include them on the title page, as a footnote to the title or otherwise.

Text Layout: Use 1.5 line spacing and wide (3 cm) margins. Ensure that each new paragraph is clearly indicated. Present tables and figure legends on separate pages at the end of the manuscript. If possible, consult a recent issue of the journal to become familiar with layout and conventions. All footnotes (except for table and corresponding author footnotes) should be identified with superscript Arabic numbers. To conserve space, authors are requested to mark the less important parts of the paper (such as records of experimental results) for printing in smaller type. For long papers (more than 4000 words) sections which could be deleted without destroying either the sense or the continuity of the paper should be indicated as a guide for the editor. Nomenclature should conform to that most frequently used in the scientific field concerned. Number all pages consecutively; use 12 or 10 pt font size and standard fonts.

Corresponding author: Clearly indicate who is responsible for correspondence at all stages of refereeing and publication, including post-publication. The corresponding author should be identified with an asterisk and footnote. Ensure that telephone and fax numbers (with country and area code) are provided in addition to the e-mail address and the complete postal address. Full postal addresses must be given for all co-authors. Please consult a recent journal paper for style if possible.

Abstract: A self-contained abstract outlining in a single paragraph the aims, scope and conclusions of the paper must be supplied.

Keywords: Immediately after the abstract, provide a maximum of six keywords (avoid, for example, 'and', 'of'). Be sparing with abbreviations: only abbreviations firmly established in the field may be eligible.

Symbols: All Greek letters and unusual symbols should be identified by name in the margin, the first time they are used.

Units: Follow internationally accepted rules and conventions: use the international system of units (SI). If other quantities are mentioned, give their equivalent quantities in SI

Maths: Number consecutively any equations that have to be displayed separately from the text (if referred to explicitly in the text).

References: All publications cited in the text should be presented in a list of references following the text of the manuscript.

Text: Indicate references by number(s) in square brackets in line with the text. The actual authors can be referred to, but the reference number(s) must always be given.

List: Number the references (numbers in square brackets) in the list in the order in which they appear in the text.

Examples:
Reference to a journal publication:
[1] M.S. Mohsen, B.A. Akash, "Evaluation of domestic solar water heating system in Jordan using analytic hierarchy process". Energy Conversion & Management, Vol. 38 (1997) No. 9, 1815-1822.

Reference to a book:
[2] Strunk Jr W, White EB. The elements of style. 3rd ed. New York: Macmillan; 1979.

Reference to a conference proceeding:
[3] B. Akash, S. Odeh, S. Nijmeh, "Modeling of solar-assisted double-tube evaporator heat pump system under local climate conditions". 5th Jordanian International Mechanical Engineering Conference, Amman, Jordan, 2004.

Reference to a chapter in an edited book:
[4] Mettam GR, Adams LB. How to prepare an electronic version of your article. In: Jones BS, Smith RZ, editors. Introduction to the electronic age, New York: E-Publishing Inc; 1999, p. 281-304

Free Online Color : If, together with your accepted article, you submit usable color and black/white figures then the journal will ensure that these figures will appear in color on the journal website electronic version.

Tables: Tables should be numbered consecutively and given suitable captions and each table should begin on a new page. No vertical rules should be used. Tables should not unnecessarily duplicate results presented elsewhere in the manuscript (for example, in graphs). Footnotes to tables should be typed below the table and should be referred to by superscript lowercase letters.

Notification: Authors will be notified of the acceptance of their paper by the editor. The Publisher will also send a notification of receipt of the paper in production.

Copyright: All authors must sign the Transfer of Copyright agreement before the article can be published. This transfer agreement enables Jordan Journal of Mechanical and Industrial Engineering to protect the copyrighted material for the authors, but does not relinquish the authors' proprietary rights. The copyright transfer covers the exclusive rights to reproduce and distribute the article, including reprints, photographic reproductions, microfilm or any other reproductions of similar nature and translations.

Proof Reading: One set of page proofs in MS Word format will be sent by e-mail to the corresponding author, to be checked for typesetting/editing. The corrections should be returned within **48 hours**. No changes in, or additions to, the accepted (and subsequently edited) manuscript will be allowed at this stage. Proofreading is solely the author's responsibility. Any queries should be answered in full. Please correct factual errors only, or errors introduced by typesetting. Please note that once your paper has been proofed we publish the identical paper online as in print.

Author Benefits:

No page charges: Publication in this journal is free of charge.

Free offprints: One journal issues of which the article appears will be supplied free of charge to the corresponding author and additional offprint for each co-author. Corresponding authors will be given the choice to buy extra offprints before printing of the article.

JJMIE

Volume 13, Number 4, December. 2019
ISSN 1995-6665

Jordan Journal of Mechanical and Industrial Engineering

PAGES	PAPERS

JJMIE

Volume 13, Number 4, December. 2019
ISSN 1995-6665
Pages 221 - 230

Jordan Journal of Mechanical and Industrial Engineering

Numerical Simulation of Forced Convection Flows over a Pair of Circular Cylinders in Tandem Arrangement

Oyewola, O.M[a*] , Ismail, O. S[b] , Abu, K.[b]

[a] *School of Mechanical Engineering, Fiji National University, Suva, Fiji*
[b] *Department of Mechanical Engineering, University of Ibadan, Ibadan, Nigeria*

Received 17 October. 2019

Abstract

Numerical simulation of time-dependent 2-dimensional forced convection flow over a pair of tandem circular cylinders in a rectangular channel has been carried out. An air stream of Prandtl number (Pr) of 0.702 flows over the cylinders with heated walls. The influence of spacing ratios S/D at 1.1, 1.8, 2.0, 2.2, 2.4, 3.0, 4.0 and 5.0 at Reynolds number based on cylinder diameter (ReD) = 23 500 on the heat transfer and flow parameters, such as isothermal contours, Nusselt number, vortices, drag and lift coefficients over the cylinders were determined using the finite-element based software (COSMOL Multiphysics), taking into considerations the governing equations (Continuity, Momentum and Energy) and the boundary conditions. The results show that the dynamics of the flow is altered by the spacing ratios. Further, the temperature between the cylinders drops significantly as S/D increases. The local Nusselt number on the four portions of the cylinders is found to increase as S/D increases. The shear layers and the vortices about the cylinders at S/D = 2, 3 and 4 present different flow structures. At S/D = 2, the shear layers shed from the upstream cylinder re-attach to the downstream cylinder, but no vortex shedding takes place. However, small vortices are formed between the cylinders and behind the downstream cylinder at S/D = 3. At S/D = 4, the vortices from the two cylinders combine and progress in vortex street behind the downstream cylinder. This work suggests that in minimizing the vibration of the tubes and enhancing effective heat transfer by the heat exchangers, the aforementioned parameters and conditions should be taken into consideration.

Keywords: Nusselt number, vortex shedding, shear layers, forced convection, tandem;

Nomenclature

C_D is drag coefficient; C_L is lift coefficient.
D is diameter of the cylinder in m.
h_θ is local convective heat transfer coefficient in W/m^2K.
k is the turbulent kinetic energy.
Nu_θ is local Nusselt number.
P is pressure in Pa.
Pr is Prandtl number.
q'' is heat flux in W/m^2.
q''' is heat generation per unit volume.
Re is Reynolds number while Re_D is the Reynolds number based on diameter.
S is centre-to-centre distance between the two cylinders.
S/D is centre-to-centre spacing to diameter ratio.
S_{ij} is strain deformation.
t is time in s.
T is temperature in K.
T_m is the bulk temperature of the fluid.
T_w is the temperature at the cylinder wall.
U_∞ is free stream velocity in m/s.
V means velocity.
δ_{ij} means kronecker delta.
ε is the rate of dissipation of kinetic energy
λ is thermal conductivity of the fluid in W/mK.
μ is molecular dynamic viscosity in Pa.s
μ_t is the turbulent (eddy) viscosity.
ρ is density in kg/m^3.
τ_{ij} is Reynolds shear stress in Pa

1. Introduction

Flow over cylinders has been extensively studied from both experimental and numerical points of view (Ishigai and Nishikawa, 1975; King and Johns, 1976; Zdravkovich, 1977; Kim and Durbin, 1988; Zhao *et al.*, 2015) due to its vast applications. For instance, Zdravkovich (1977) reviewed different arrangements of cylinders as well as the influence of spacing between them on the force coefficients and Strouhal number, and highlighted different applications which include chimney stacks in wind and jetties; offshore structures in high seas; vibration of two conductor transmission lines; vibration of heat exchanger tubes etc. It should be mentioned that thermal effects of flow about pair of cylinders at different gap spaces and Reynolds numbers (Mohsenzadeh *et al*., 2010; Moshkin and Sompong, 2009) has also received some

* Corresponding author e-mail: oooyewola001@gmail.com

considerable attentions. This is not surprising since this field of research is useful in accounting for loss of heat from high-rise buildings, cooling towers, offshore risers, nuclear reactor rods, cooling of electrical components, etc.

To understand the fluid-structure interaction, Zdravkovich (1985) classified fluid-static responses in a discontinuous change of flow regimes, where there are large amplitude oscillations of cylinders. He noted that there were instabilities that built up to extremely large amplitude mainly in the streamwise direction, instability which developed to certain level in the streamwise direction and instability which built up gradually predominantly in the transverse direction. For better understanding of the interaction between cylinders in tandem arrangement, Xu and Zhou (2004) in their experimental investigation at Re = 800 – 4.2 × 10^4observed that formation of shears layers separate from upstream cylinder and do not re-attach to the downstream cylinder to form vortex street at 1< S/D < 2. They also found that the shear layers separating from the upstream cylinder reattach on the upstream side of the downstream cylinder and then separate at 2< S/D < 5; and that both cylinders generate vortices at S/D=4. Further, Zhou and Yiu (2006) conducted experimental study of two cylinders in tandem arrangement with wake spacing ratios of 1.3, 2.5, 4.0 and 6.0, and uncovered two distinct flow structures which depend upon re-attachment of shear layers from the upstream cylinder to the downstream cylinder.

In order to have a clear picture of the interaction and overcome experimental limitations, numerical approaches have been used to study the flow interference as well as heat transfer between two cylinders. For example, Liu *et al.* (1998) developed a numerical approach which addressed the major issues of spatial resolution and temporal resolution to ensure computational efficiency in unsteady flow simulation. Interestingly, they were able to obtain solution for 2D unsteady laminar flows. Similarly, Farrant *et al.* (2000) adopted the cell boundary element method based on unstructured mesh to solve two-dimensional Navier-Stokes equations for laminar flow over four equispaced circular cylinders for various gap spaces of 2.0 and 4.0. For their arrangement of the four circular cylinders in square configuration at gap spacing of 2.0, in-phase vortex shedding was observed as against dominant anti-phase vortex shedding for gap spacing of 4.0. Lacovides *et al.* (2014) assessed the results of Large Eddy Simulation (LES) and four Unsteady Reynold-Averaged Navier Stokes equations (URANS), at Re_D = 41 000, of flow and heat transfer through in-line tube banks. They reported that for close-pitched large in-line tube banks, where pitch size-to-diameter ratio ≤ 1.6, flow would seek the path of least resistance and travel in a diagonal manner, but the URANS except for k-ε Linear Production model showed that straight-through flow would be returned.

Furthermore, Juncu (2007a) examined flow over two tandem cylinders at Reynolds number ranging from 1 to 30, using compact higher order finite difference method to solve the Navier-Stokes equations on bipolar cylindrical coordinates. They reported that interference effects are higher on the trailing cylinder than that on the leading cylinder, with marked increase as the Reynolds number was increased. In addition, they found that drag on each of the two cylinders is smaller than that of an isolated cylinder. Moreover, Eswaram *et al.* (2013) concluded that Strouhal numbers for two tandem cylinders are smaller than that of a single cylinder at Reynolds numbers of 200 and 15000 with spacing of 2 and 4. Kitagawa and Ohta (2008) adopted Large Eddy Simulation (LES) in the examination of two tandem cylinders at Re = 2.2 × 10^4 and S/D ranging from 2 to 5. They reported how the shear layers and vortices are formed and shed around the cylinders, as well as re-attachment of shear layers on the downstream cylinder. Dehkordi *et al.* (2011) simply repeated the simulation of the work by Kitagawa and Ohta (2008) using cartesian-based finite volume method and it was found that the two authors' results were in good agreement.

Mahir and Altac (2008) used FLUENT to determine the effects of centre-to-centre spacing ratio ranging from 2 to10 on unsteady flow past two tandem cylinders at Re_D = 100 and 200. They reported that Nusselt number of the upstream cylinder approaches that of a single isothermal cylinder at S/D > 4, and the mean Nusselt number of the downstream cylinder is about 80% of the upstream cylinder. Similarly, Juncu (2007b) reported that the Nusselt number of the upstream cylinder was greater than that of the downstream cylinder, and that it increased as the Reynolds number increased for all the Prandtl numbers of 0.1, 1, 10, and 100 considered. Also, Hamiri and Saghafian (2012) studied the effect of spacing ratio at 2, 3, 4, 5, 7 and 10 for Prandtl numbers of 0.7 and 7 with Reynolds numbers of 100 and 200 on three tandem circular cylinders. They reported that Nusselt number over the cylinders increased with increasing spacing ratio. In addition, it was observed that Nusselt number was higher at Reynolds number of 200 and Prandtl number of 7 than at Reynolds number of 100 and Prandtl number of 0.7. In their study of a mixed convection flow over two tandem cylinders, Salcedo *et al*. (2016) reported that overall Nusselt number of the downstream cylinder decreased monotonically within -1 ≤ Ri ≤ 1, but increased monotonically within 1.5 ≤ Ri ≤ 4, where Ri is Richardson number.

Some engineering applications, such as nuclear reactors which involve internal heat generation may require investigation of heat transfer over them. For instance, Wang and Georgiadis (1996) reported that for an array of cylinders volumetrically heated at constant rate in a laminar flow, the temperature difference in the cylinder blocks monotonically decreases with increasing Re, whereas it increases as the fluid-to-solid conductivity increases. Furthermore, Buyruk *et al.* (1998) reported that the heat transfer from a cylindrical tube in cross flow at Re = 120 and Re = 390 increases when blockage ratio and Reynolds number increases. Buyruk (2002) extended the work of Buyruk *et al*. (1998) by examined the influence of gap spaces on tandem cylinders at Re = 300, Pr = 0.7 and S/D = 1.3 and 6. He concluded that low temperature drop occurred for the two cylinders with S/D = 1.3 while higher temperature drop occurred for the case of S/D = 6.

It is evidenced in the literature that flow-induced vibrations and interferences in the wake of two circular cylinders have great effect on the flow structure. Although a lot of studies has been conducted on two-cylinder wakes at various low and high Reynolds numbers in order to achieve a certain target, this present work examines the influence of spacing ratios S/D = 1.1, 1.8, 2.0, 2.2, 2.4, 3.0, 4.0 and 5.0 on the hydrodynamic force coefficients and heat transfer characteristics across two tandem circular cylinders at intermediate Reynolds number of 23 500. This work will complement existing work and improve our understanding on the flow-structure interaction taking into considerations the hydrodynamic force, heat transfer phenomenon and Reynolds number involve. This work will be relevant especially in heat exchanger application and other related systems. The governing equations with appropriate boundary conditions were implemented using a Finite Element based Software (COSMOL Multiphysics 5.0)

2. Problem Description, Geometry and Physics

Stream of air of Pr = 0.702 flows at free stream velocity U_∞ (4.139m/s) and free stream temperature T_∞ (25^{o}C) into a rectangular channel. Two circular cylinders are placed in-line along the centerline of the channel at some points away from the inlet. They are separated from each other by a distance of S. The centerline of the channel coincides with the centre of the cylinders. The two cylinders are heated to surface temperature T_w (70 ^{o}C) such that $T_w > T_\infty$. The bulk temperature of the fluid T_m, given by $(T_w + T_\infty)/2$ is 47.5 ^{o}C. The fluid properties such as viscosity and density of the dry air are taken at the bulk temperature. At the surface or wall of the cylinders, velocity is zero (no-slip condition) for laminar flow consideration. However, wall function is applied to the boundary condition at the solid wall for a turbulent flow. Initially, temperature of the bulk of the flow domain is assumed to be the same before heating up the cylinders. The reason for heating up the cylinders is to investigate the thermal effects around them as flow takes place over them.

Spacing ratios (S/D) of 1.1, 1.8, 2.0, 2.2, 2.4, 3.0, 4.0 and 5.0 were used for the in-line arrangement of the cylinders as shown in Fig.1. The fluid domain is rectangular, and the length of the domain is 22D (where D is diameter = 0.1 m) and the height is 4D. The first cylinder is placed at distance 2D downstream of the inlet where a parabolic velocity profile is established, while the other is placed at distance S behind it. Computational studies were carried out for the different spacing ratios at the Reynolds number Re_D = 23500. The effects of the S/D ratios on isotherms, temperature field, average Nusselt number, vortices, streamlines, drag and lift coefficients around the two cylinders were studied.

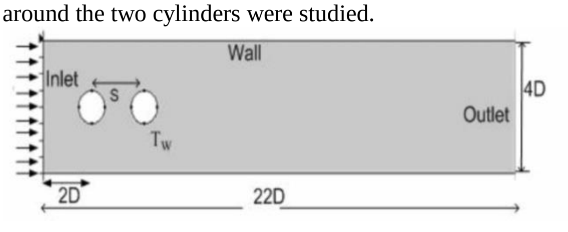

Figure 1. Tandem arrangement.

3. Governing Equations and Boundary Conditions

3.1. Governing Equations

The differential equations that govern unsteady incompressible turbulent flow are given by the continuity and momentum equations (Versteeg and Malalasekera, 2007), expressed as

$$\frac{\partial(\bar{v}_i)}{\partial x_i} = 0 \qquad (1)$$

$$\frac{\partial(\bar{v}_i)}{\partial t} + \frac{\partial(\bar{v}_i\bar{v}_j)}{\partial x_j} = -\frac{1}{\bar{\rho}}\frac{\partial \bar{P}}{\partial x_i} + \frac{1}{\bar{\rho}}\frac{\partial}{\partial x_j}\left((\mu + \mu_t)\frac{\partial v_i}{\partial x_j} + \tau_{ij}\right) \qquad (2)$$

where i =1, 2; $\tau_{ij} = -\overline{\rho v_i v_j} = 2\mu_t S_{ij} - \frac{2}{3}\bar{\rho}k\delta_{ij}$; $S_{ij} = \frac{1}{2}\left(\frac{\partial \bar{v}_i}{\partial x_j} + \frac{\partial \bar{v}_j}{\partial x_i}\right)$; k is the turbulent kinetic energy per unit mass; μ_t is the turbulent (eddy) viscosity; μ is molecular dynamic viscosity; and t is time. The overhead bar signifies average.

The energy equation is given as

$$\frac{\partial(\bar{T})}{\partial t} + \frac{\partial(\bar{v}_i\bar{T})}{\partial x_i} = \frac{\partial}{\partial x_i}\left\{\alpha\frac{\partial \bar{T}}{\partial x_i} + q_i\right\} + q''' \qquad (3)$$

where $q_i = -\overline{v_i T}$, α is thermal diffusivity and q''' is heat generation per unit volume.

The turbulence is modelled using the standard k-ε model represented by the following equations (Versteeg and Malalasekera, 2007).

$$\frac{\partial(\rho k)}{\partial t} + \nabla.(\rho k\vec{v}) = \nabla.\left[\frac{\mu_t}{\sigma_k}\nabla k\right] + 2\mu_t S_{ij}.S_{ij} - \rho\varepsilon \qquad (4)$$

$$\frac{\partial(\rho\varepsilon)}{\partial t} + \nabla.(\rho\varepsilon\vec{v}) = \nabla.\left[\frac{\mu_t}{\sigma_\varepsilon}\nabla\varepsilon\right] + c_{1\varepsilon}\frac{\varepsilon}{k}2\mu_t S_{ij}.S_{ij} - c_{2\varepsilon}\rho\frac{\varepsilon^2}{k} \qquad (5)$$

Turbulence viscosity is given by $\mu_t = \rho C_\mu \frac{k^2}{\varepsilon}$; $c_{1\varepsilon} = 1.44$, and $c_{2\varepsilon} = 1.92$; $c_\mu = 0.09$; $\sigma_k = 1.00$; $\sigma_\varepsilon = 1.30$ are constants and $\vec{v}$ is the velocity vector.

The lift and drag coefficients are evaluated using the following equations (Cengel and Cimbala, 2006).

$$C_D = \frac{F_D}{\frac{1}{2}\rho U_\infty^2 D} \qquad (6)$$

$$C_L = \frac{F_L}{\frac{1}{2}\rho U_\infty^2 D} \qquad (7)$$

The heat transfer q″ over the cylinders is evaluated as follows (Lienhard and Lienhard, 2006).

$$q'' = -\lambda_{fluid}\frac{dT}{dx}\Big|_{x=0} \qquad (8)$$

$$q'' = h_\theta(T_w - T_\infty) \qquad (9)$$

$$h_\theta = \frac{-\lambda_{fluid}\frac{dT}{dx}\big|_{x=0}}{(T_w - T_\infty)} \qquad (10)$$

where λ is thermal conductivity of the fluid.

In order to measure the convective heat transfer at a solid surface of the cylinder, a dimensionless number called Nusselt number is defined based on diameter. It is given as

$$Nu_\theta = \frac{h_\theta D}{\lambda} \qquad (11)$$

3.2. Choice of standard k-ε model over k- ω turbulence model

Both standard k-ε model and k- ω turbulence model are available for simulating fluid flow in COMSOL Multiphysics. COMSOL User Manual (2014) compares the strength and weakness of the two models. Standard k-ε model is suitable for flows over bodies (external flow), has good convergence rate and requires low computational memory. However, k- ω turbulence model is more suited to internal flow and cases of strong curvature or separated flows, but it requires more time for convergence.

Furthermore, dependent of k- ω turbulence model on the assumed free stream value of ω makes it less suitable for external flows (Menter, 1992). This current study is about external flow problem, thus the choice of standard k-ε model for the simulation.

3.3. Boundary conditions

The boundary conditions adopted for this study are described as follows.

1. Inlet: u= U_∞, T = T_∞. The inlet is 2D away from the cylinders
2. Outlet:$\frac{\partial u}{\partial x} = 0$; $\frac{\partial v}{\partial x} = 0$; $\frac{\partial T}{\partial x} = 0$; and pressure p=0.
3. The top and bottom sides as well as the cylinder walls use the slip wall boundary condition.

The slip wall boundary condition ensures that fluid does not leave the domain or does not penetrate through the cylinder. Mathematically, the constraint is defined in COMSOL 5.0 (2014b) as:

$$\vec{\boldsymbol{v}} \cdot \boldsymbol{n} = 0 \quad (12)$$

and

$$\boldsymbol{K} - (\boldsymbol{K}.\boldsymbol{n})\boldsymbol{n} = 0 \quad (13)$$

where

$$\boldsymbol{K} = \mu(\nabla\vec{\mathbf{v}} + (\nabla\vec{\mathbf{v}})^T)\boldsymbol{n} \quad (14)$$

4. The temperature at the upper and bottom surfaces is T = T∞, while the cylinder wall temperature is set to T=Tw.

COMSOL Multiphysics 5.0 is used to solve the governing differential equations along with the defined boundary conditions.

4. Mesh Generation

4.1. Geometry Discretization

The governing equation and boundary conditions are solved by first dividing the problem geometry into smaller elements. Mesh generation is the step-in numerical simulation with which a set of elements are obtained. The equations are then solved for each of the elements in the mesh generated to obtain pressure, velocity and temperature at every node in the computational domain.

The mesh size determines the accuracy of the solution that will be obtained. COMSOL Multiphysics has pre-defined meshes which include, 'coarse', 'normal', 'fine', 'finer', and allows for users to define mesh sizes according to the desirable level of accuracy expected. It is important to state that the memory of the computational facility may limit the user from defining very small and fine mesh sizes. More so for very complex problems, the use of very fine mesh imposes more constraints on the requirement of the computational facility.

4.2. 4.2 Mesh Dependency

Few simulations were run for a forced convection flow over a single cylinder, using different COMSOL physics-defined mesh sizes known as 'normal', 'fine' and 'finer'. Table 1 shows and compares that the Nusselt number values obtained from the three mesh sizes are close to each other, with only less than 5% discrepancy between normal size and fine size, and between fine size and finer size. Normal mesh size is just enough for the single cylinder, but we select fine mesh size for the present work as it offers results most stable and which are in good agreement with literature (Table 3 in section 5.1). Moreover, fine mesh uses much less average computational time and memory than finer mesh.

Table 1. Impact of quality of mesh on Nusselt number for a single cylinder

	Normal Mesh Size (6522 elements)		Fine Mesh Size (12690 elements)		Finer Mesh Size (29178 elements)	
Re_D	Nu	Time (s)	Nu	Time (s)	Nu	Time (s)
200	8.006	1314	8.008	1947	7.990	3249
300	9.758	1460	9.940	2102	9.7415	3226
400	11.119	1562	11.520	5340	11.397	5104
500	12.208	1593	12.804	4860	12.789	5516

A typical meshing of the two tandem cylinders in rectangular domain at S/D = 5.0 is shown in Fig. 2. The mesh statistics including domain elements, boundary elements, number of degree of freedoms (DOFs) and solution time are shown in Table 2, as computed using the default physics defined 'fine' mesh.

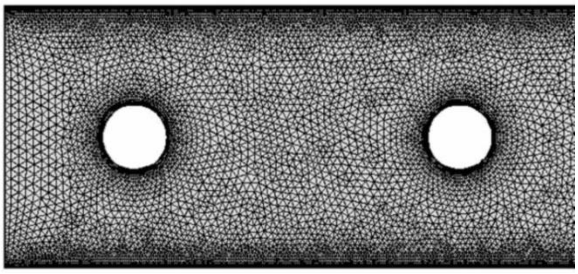

Figure 2. Fine mesh generated at S/D = 5.0.

Table 2. Mesh Statistics for Tandem Arrangement at Re_D =23500

S/D	Mesh Type	Domain Elements	Boundary Elements	†nDOF(plus 1074DOFs)	Solution Time(s)
1.1	Fine	30328	1062	109622	6184
2.0	Fine	30530	1062	110228	4891
2.2	Fine	30564	1062	110330	7038
2.4	Fine	30410	1062	109868	7348
3.0	Fine	30394	1062	109820	7934
4.0	Fine	30620	1062	110498	28979
5.0	Fine	30660	1062	110618	7613

†nDOF means number of degree of freedoms.

5. Results and Discussion

5.1. Validation of solution method

In order to validate the solution obtained in this study, simulation of forced convective heat transfer was carried out for a single cylinder. The results obtained for a single cylinder, using normal mesh size, was compared with the analytical result of Khan *et al.* (2004), and numerical results of Salcedo *et al.* (2016) and Mettu *et al*. (2006) as in Table 3.

Table 3. Comparison of mean Nusselt number for a single cylinder for Re = 200 – 500

Re_D	Nu			
	Present	Salcedo et al (2016)	Khan et al. (2004)	Mettu et al. (2006)
200	8.006	8.003	7.747	7.592
300	9.758	9.563	9.489	9.326
400	11.119	10.795	10.950	10.910
500	12.208	12.108	12.210	12.130

5.2. Heat transfer characteristics

The heat transfer patterns over the cylinders are shown by the means of isotherm contours, surface temperature plot, and Nusselt number. Figure 3 shows the heat transfer characteristics over the cylinders and downstream of the flow channel. Figures 3a and 3c show the isotherm contours over the cylinders at S/D = 1.1 and 2.0. Figures 3b and 3d show the temperature surface plots for the temperature variation between the cylinders and behind the downstream cylinder at the same S/D ratios. There are significant changes in the flow patterns as reflected both in the isotherm contours as well as in the surface plot. It can be inferred that the heat transfer is being caused by the flow. This is also true for S/D = 3 and 4, shown in Fig. 4. Comparing the temperature contour and surface plots in Figs. 3 and 4 at S/D =1.1, 2.0, 3.0 and 4.0, it can be deduced that the temperature drop between the cylinders increases as the spacing ratios increases. This was also reported by Buyruk (2002). This is likely due to turbulent activities being strongly aggravated by the cylinders. The present result suggests that the closer the cylinders the more the turbulent activities

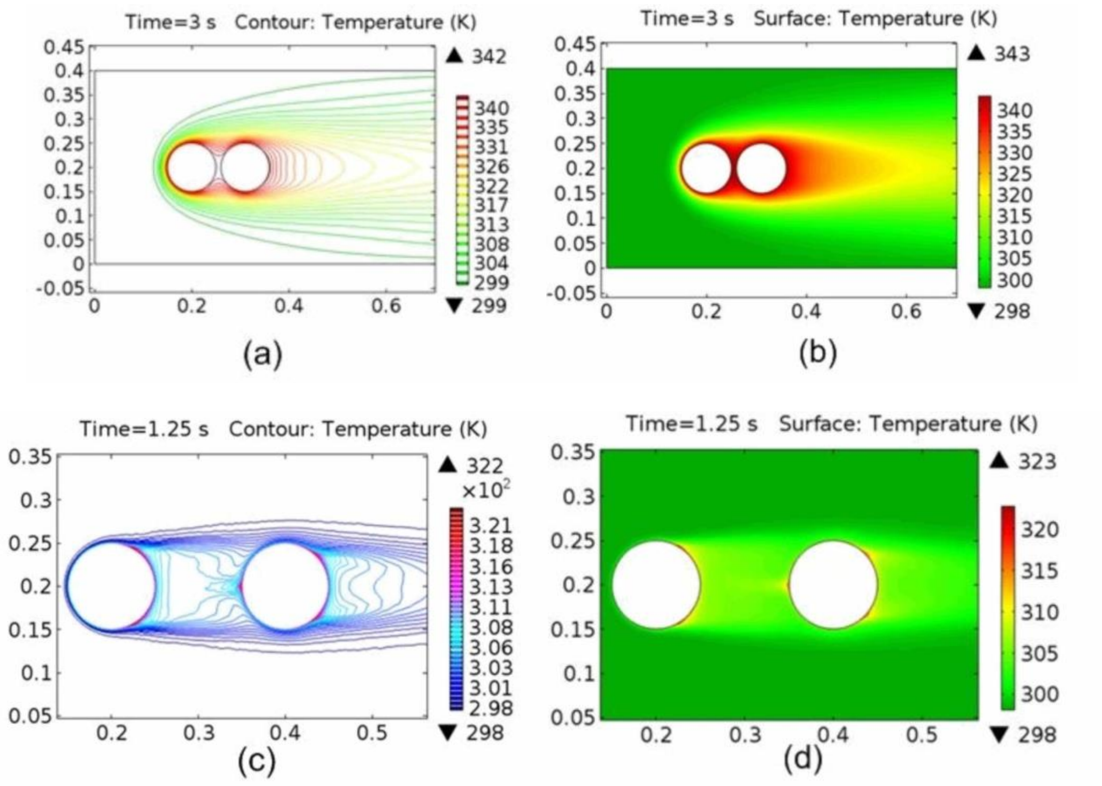

Figure 3. The Isotherms and surface temperature plots around the cylinders at S/D = 1.1 (aand b) and S/D = 2 (c and d).

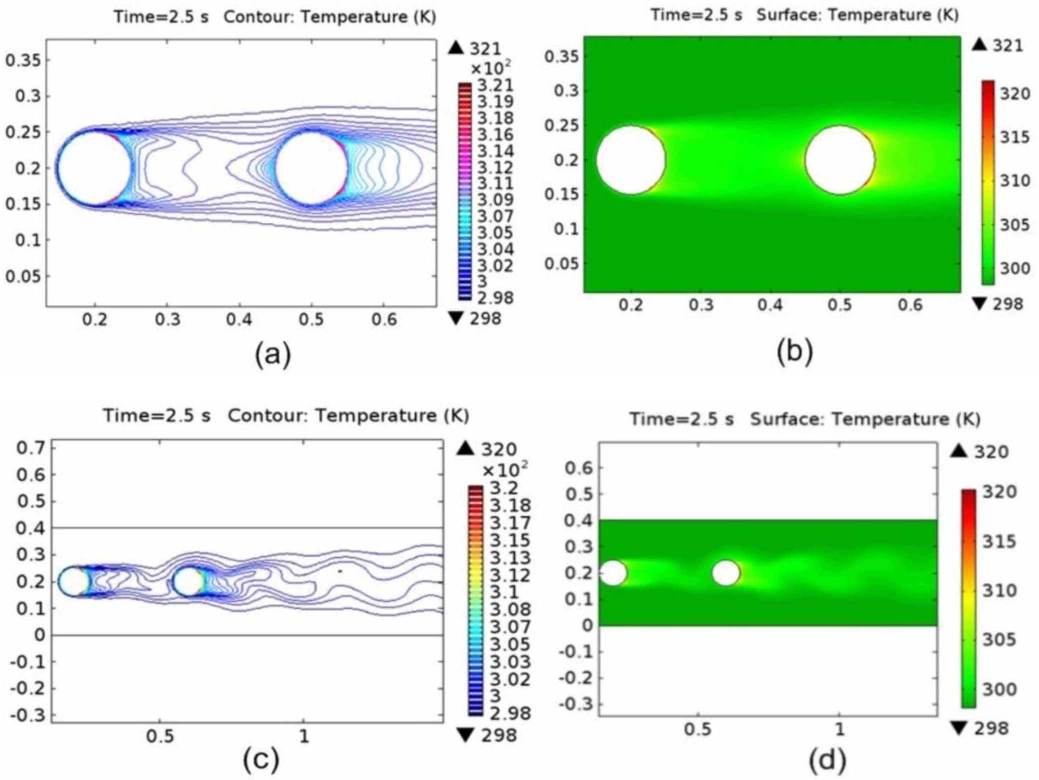

Figure 4. The Isotherms and temperature plot around the cylinders at S/D = 3 (a and b) and S/D = 4 (c and d).

Moreover, since there are different heat characteristics on the various parts of the cylinders, the variation of Nusselt number with S/D ratio should reflect the heat transfer phenomenon between the cylinders. This is presented in Fig. 5. Figure 5a illustrates the relationship of the mean Nusselt number (by considering the two cylinders simultaneously) of each of the four surfaces recognized on the cylinders with the spacing ratio. The Nusselt number increases for increasing S/D ratio within 1<S/D≤4, but sharply decreases for S/D = 5. Similar relationship holds for the mean value of the whole two cylinders. Figure 5b shows the variation of the mean Nusselt number of the two whole cylinders with the spacing ratio. Therefore, it can be deduced from Fig. 5 that the mean Nusselt number is greatest at the front portions of the cylinders. Similarly, Rosales *et al.* (2001) also reported that Nusselt number of the front face of a heated square cylinder at Reynolds number of 500 has the highest surface-averaged Nusselt number compared to other portions of the cylinder

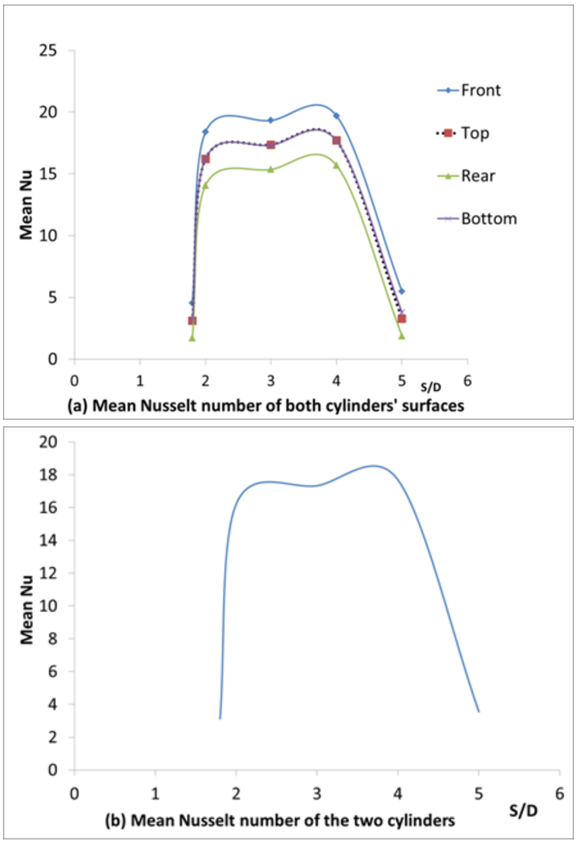

Figure 5. The variation of Mean Nusselt number with spacing ratio (a) for four surfaces; (b) for two cylinders.

5.3. Vortex structure and flow pattern

Figure 6 shows the flow pattern over two cylinders in tandem arrangement for S/D = 2.0 at dimensionless time tU_∞ /D = 55. The shear layers shed from the upstream cylinder reattach to the downstream cylinder. It should be noted that there is no vortex shedding at S/D =2 as shown in Fig. 6a and the streamline plot (Fig. 6b) shows a stable flow pattern. At S/D = 3, the shear layers shed from the upstream cylinder re-attach symmetrically to the downstream cylinder (Fig. 6c). Further, as time progresses, tiny and small vortices are formed between the cylinders, and vortex shedding takes place for a short time behind the downstream cylinder at S/D = 3.

However, the flow phenomenon is entirely different for S/D >3. The streamlines in Fig. 7 shows that there is an unstable flow pattern at S/D = 4 as reflected in the streamlines at tU/D = 75 and 83. This is not surprising, as Fig. 8 vividly confirms this incident. Figure 8 shows that vortices shed from the upstream cylinder reattach to the downstream cylinder. It should be mentioned that these vortices combine, and progress in the vortex street behind the downstream cylinder which eventually results in the strong agitation of the layer. The behavior suggests that these vortices are responsible for the high instability in the flow. The vortex structure and shear layers described for S/D = 2,3 and 4 are consistent with those reported by Xu and Zhou (2004) and Kitagawa and Ohta(2008). However, vortex shedding did not occur at S/D > 4 at Re_D = 23500.

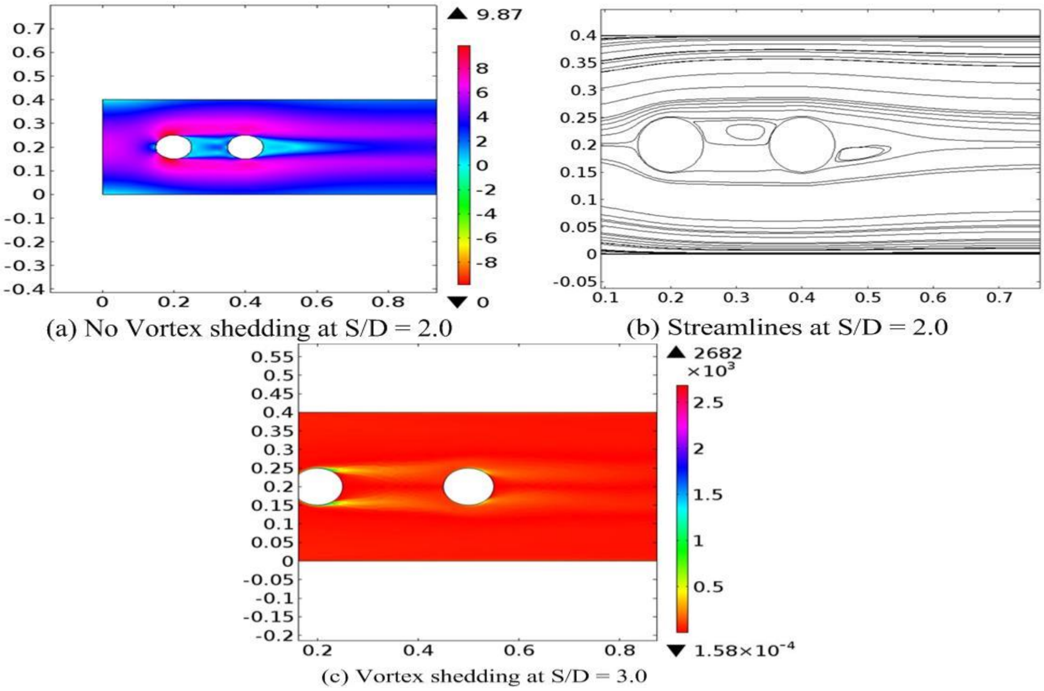

Figure 6. Flow pattern over two cylinders for S/D = 2.0 and 3.0 at tU/D = 56.

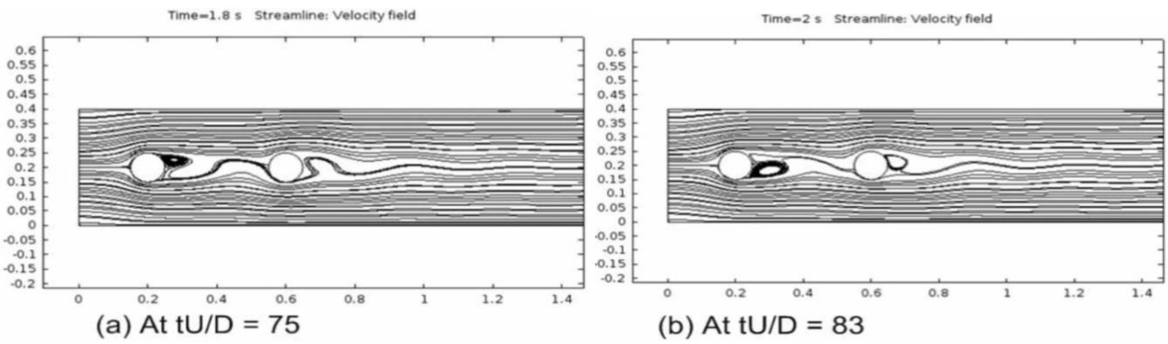

Figure 7. Streamlines over two cylinders in tandem arrangement for S/D= 4.0.

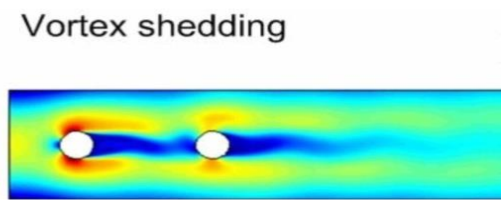

Figure 8. Vortex shedding over two cylinders in tandem arrangement for S/D = 4.0.

5.4. Lift and drag coefficients

The previous results indicated that the dynamics of the layer is influenced by the spacing ratios between the two cylinders. The effect of the spacing ratios on the lift and drag coefficients should shed more light on these changes. At S/D = 4 (Fig. 9), the drag coefficients for the upstream and downstream cylinders are positive but of different magnitudes. Figures 9a and 9b also show that lift coefficients CL_1 and CL_2 oscillate about the mean zero level. It should be noted that the vortices shed from the upstream cylinder at the S/D = 4 cause vortices in the wake of the downstream cylinder and hence, result in high flow instability. This invariably led to high fluctuation in the lift and drag coefficients. Figure 10 shows the variation of mean drag coefficients of the two cylinders with the spacing ratios.

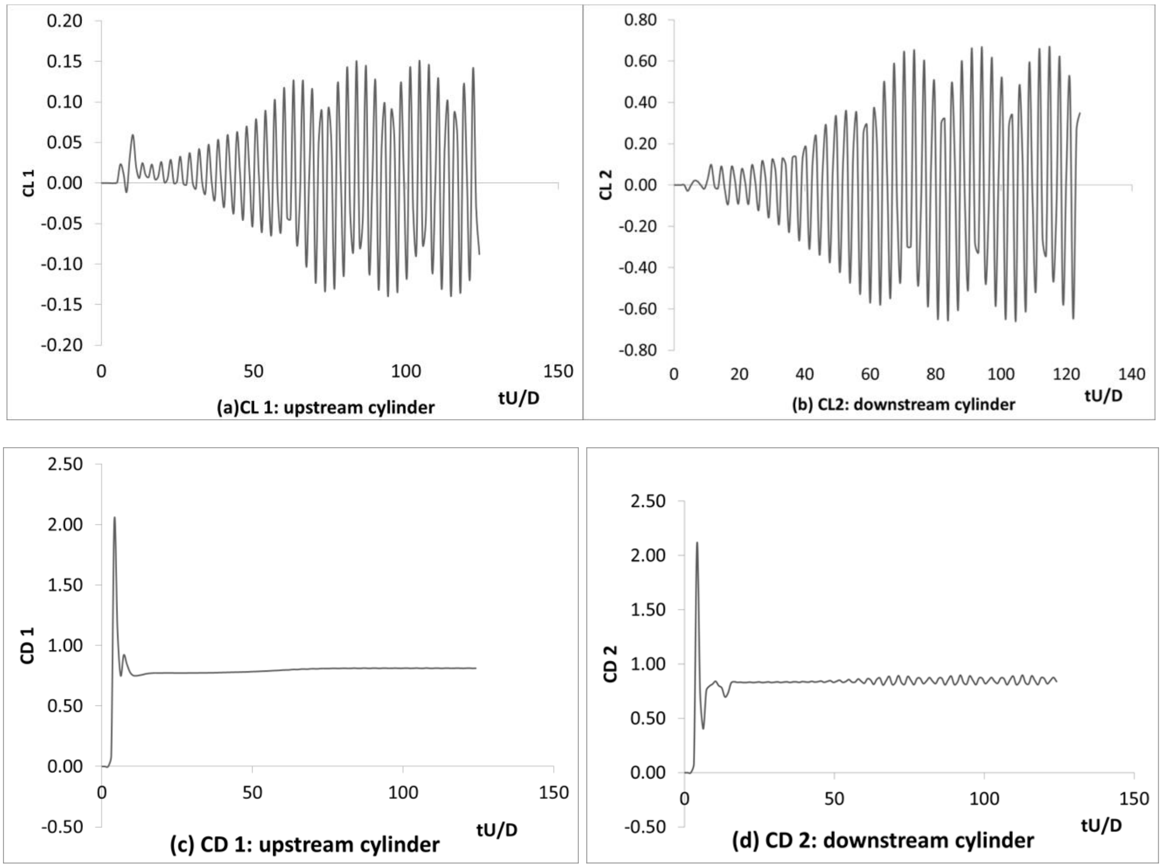

Figure 9. Lift and drag coefficient fluctuations at S/D =4.

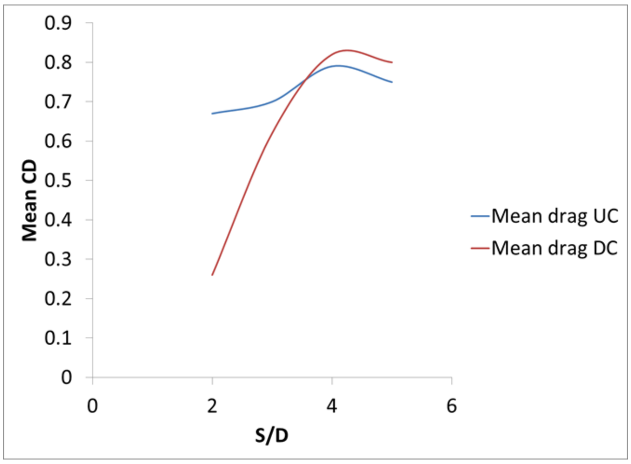

Figure 10. Variation of mean drag coefficient with the spacing ratios.

It can be deduced that the mean drag coefficient of the cylinders increases linearly for 2≤S/D≤4 and later decreases. The mean drag coefficient of the upstream cylinder is higher than those of the downstream cylinder for 2≤S/D<3. Surprisingly, the peak values occur at the same S/D (= 4), where $CL_1 > CL_2$. The result suggests that while the dynamics of the layer alter the magnitude of the mean lift coefficients of the two cylinders in an unequal manner, the oscillations are similar. The drag coefficients and the Strouhal number for these spacing ratios at Re_D = 23500 are presented in Table 4.

Table 4. Drag coefficients and Strouhal number of the cylinders at Re_D = 23500

S/D		C_D	St
2	*UC	0.67	0.193
	**DC	0.26	0.242
3	UC	0.70	0.269
	DC	0.62	0.269
4	UC	0.79	0.338
	DC	0.82	0.338
5	UC	0.75	-
	DC	0.80	-

*UC = Upstream Cylinder; **DC =Downstream Cylinder.

6. Conclusion

The influence of spacing ratios on the heat transfer and flow parameters in a 2-dimensional forced convection flow of air over a pair of tandem circular cylinders in a rectangular channel has been carried out numerically at Re_D= 23 500. The results revealed that the dynamics of the flow depend strongly on the spacing ratios taking into consideration the flow and the initial conditions. It was discovered that the temperature drop within the gap between the cylinders is higher at larger spacing ratios where high vortex-induced vibration also occurred. The mean Nusselt number over the tandem cylinders generally increases (directly) with increasing spacing ratios for 1<S/D≤4. Shear layers shed from the upstream cylinder re-attached to the downstream cylinder, and there is no vortex shedding at S/D = 2. There is re-attachment of the shear layers shed from the upstream cylinder onto the downstream cylinder at S/D = 3. At this ratio, vortex shedding takes place within the gap as well as behind the downstream cylinders. The flow pattern is highly unstable for S/D = 4, and vortices shed from the upstream cylinder impinged on the downstream cylinder, and this progresses in vortex street behind the downstream cylinder. This causes high fluctuations in the lift and drag coefficients for the spacing ratio.

The present work suggests that the above set of parameters and conditions should be taken into considerations in the operation of heat exchangers in order to minimize the vibration of the tubes as well as to ensure efficient and effective heat transfer by the heat exchangers.

References

[1] Buyruk, E., Johnson M.W. and Owen I. Numerical and Experimental Study of Flow and Heat Transfer around a Tube in Cross-Flow at Low Reynolds Number, *Intl. J. Heat and Fluid Flow*, vol. **19**, pp. 223-232, 1998.

[2] Buyruk, E., Numerical Study of Heat Transfer Characteristics on Tandem, Inline and Staggered Tube Bank in Cross-Flow of Air, *Intl. Communications in Heat and Mass Transfer*, vol. **29**, no. 3, pp. 355-366, 2002.

[3] Cengel, Y.A. and Cimbala, J.M., *Fluid Mehanics Fundamentals and Applications*, first ed., Boston: McGraw-Hill Higher Education, pp. 562-566, 2006.

[4] COMSOL 5.0., *COMSOL Multiphysics Model Library Manual*, p. 644, 2014b.

[5] COMSOL 5.0., *COMSOL Multiphysics Reference Manual*, pp. 59-70,2014a.

[6] Dehkordi, B.G., Moghaddam, H.S. and Jafari, H.H., Numerical Simulation of Flow over Two Circular Cylinders in Tandem Arrangement, *J. Hydrodynamics*, vol. **23** no. 1, pp. 114-126, 2011.

[7] Eswaram, M., Goyal, P., Dutta, A., Reddy, G.R., Singh, R.K. and Vaze, K.K. Numerical Investigation of Strouhal Frequencies of Two Staggered Bluff Bodies, *Excerpt of The Proceedings of the 2013 COMSOL Conf*., Bangalore, 2013.

[8] Farrant, T, Tan, M. and Price, W., A Cell Boundary Element Method Applied to Laminar Vortex-Shedding From Arrays of Cylinders in Various Arrangements, *J. Fluids and Structures*, vol. **14**, pp. 375-402, 2000.

[9] Hamiri, J. and Saghafian, M., Numerical Simulation of Fluid Flow and Forced Convection Heat Transfer from Tandem Circular Cylinders Using Overset Grid Method, *J. Fluids and Structures*, vol. **28**, pp. 309 – 327, 2012.

[10] Ishigai, S., Nishikawa E., Experimental Study of Gas Flow in Tube Banks with Tube Axes Normal to Flow Part II; on the Structure of Gas Flow in Single-Column, Single-Row, and Double-Rows Tube Banks, JSME, vol. **18**, pp. 528-535, 1975.

[11] Juncu G., A Numerical Study of Momentum and Forced Convection Heat Transfer around Two Tandem Circular Cylinders at Low Reynolds Number. Part II: Forced Convection Heat Transfer, *Intl. J. Heat and Mass Transfer*, vol. **50**, pp. 3799 – 3808, 2007b.

[12] Juncu, G., A Numerical Study of Momentum and Forced Convection Heat Transfer Around Two Tandem Circular Cylinders at Low Reynolds Number. Part I: Momentum Transfer, *Intl. J. Heat and Mass Transfer*, vol. **50**, pp. 3788 – 3798, 2007a.

[13] Khan, W., Culham, J. and Yovanovich, M., Fluid Flow and Heat Transfer from a Cylinder between Parallel Planes, *J. Thermophysics and Heat Transfer*, vol. **18**, pp. 395-403, 2004.

[14] Kim, H.J. and Durbin, P.A., Investigation of the Flow betweena Pair of Circular Cylinders in the Flopping Regime, *J. Fluid Mechanics*, vol. **196**, pp. 431–448, 1988.

[15] King, R. and Johns, D., Wake Interaction Experiments with Two Flexible Circular Cylinders in Flowing Water, *J. Sound and Vibration*, vol. **45**, pp. 259–283, 1976.

[16] Kitagawa, T. and Ohta H., Numerical Investigation on Flow around Circular Cylinders in Tandem Arrangement at Subcritical Reynolds Number. *J. Fluids and Structures*, vol. **24**, no. 5, pp. 680-699, 2008.

[17] Lacovides, H., Launder, B. and West, A., A Comparison and Assessment of Approaches for Modelling Flow over In-Line Tube Banks, *Intl. J. Heat and Fluid Flow*, vol. **49**, pp. 69-79, 2014.

[18] Lienhard, J.H. IV and Lienhard, J.H. V.A., *Heat Transfer Textbook*, third ed., Massachusetts: Phlogiston Press, pp. 274-275, 2006.

[19] Liu, C., Zheng, X. and Sung, C.H., Preconditioned Multigrid Methods for Unsteady Incompressible Flow, *J. Comput. Physics*, vol. **139**, pp. 35-57, 1998.

[20] Mahir, N. and Altac, Z., Numerical Investigation of Convective Heat Transfer in Unsteady Flow Past Two Cylinders in Tandem Arrangement, *Intl. J. Heat and Fluid*, vol. **29,** pp. 1309-1318, 2008.

[21] Menter, F. R. (1992). Performance of Popular Turbulence Models for Attached and Separated Adverse Pressure Gradient Flow, AIAA J., vol. **30**, pp. 2066–2072, 1992.

[22] Mettu, S., Verma, N. and Chhabra, R., Momentum and Heat Transfer from an Asymmetrically Confined Circular Cylinder in a Plane Channel, *Heat and Mass Transf*., vol. **42**, pp. 1037-1048, 2006.

[23] Mohsenzadeh, A., Farhadi, M. and Sedighi, K., Convective Cooling of Tandem Heated Triangular Cylinders,*Thermal Science*, vol. **14**, pp. 183-197, 2010.

[24] Moshkin, N.P. and Sompong, J., Numerical Simulation of Flow and Forced Convection Heat Transfer in Cross-flow of Incompressible Fluid over Two Rotating Circular Cylinders,*SuranareJ. Science and Technology*, vol. **17**, no. 1,pp. 87–104, 2009.

[25] Rosales, J. L., Ortega, A. and Humphrey J.A.C., A Numerical Simulation of the Convective Heat Transfer in Confined Channel Flow Past Square Cylinders: Comparison of Inline and Offset Tandem Pairs, *Intl. J. Heat and Mass Transfer*, vol. **44**, pp. 587 – 603, 2001.

[26] Salcedo, E., Cajas, J.C., Trevino, C. and Martinez-Suastegui, L., Unsteady Mixed Convection Heat Transfer from Confined Isothermal Circular Cylinders in Tandem: Buoyancy and tube Spacing Effects, *Intl. J. Heat and Fluid Flow*, **vol. 60**, pp. 12-30, 2016.

[27] Versteeg, H.K. and Malalasekera, W.,*An Introduction to Computational Fluid Dynamics: The Finite Volume Method*, second ed., Edinburgh Gate: Pearson Education Limited, pp. 65, 72-76, 2007.

[28] Wang, M. and Georgiadis, J.G., Conjugate Forced Convection in Cross Flow over a Cylinder Array with Volumetric Heating, *Intl*. *J*.*Heat and Mass Transfer*, vol. **39**, pp. 1351-1361, 1996.

[29] Xu, G. and Zhou, Y., Strouhal Numbers in the Wake of Two Inline Cylinders, *Experiments in Fluids*, vol. **37**, pp. 248-256, 2004.

[30] Zdravkovich, M. Review of Flow Interference between Two Circular Cylinders in Various Arrangements, Transactions of the ASME, *J. Fluids Engineering*, vol. **99**, pp. 618–633, 1977.

[31] Zdravkovich, M., Flow Induced Oscillations of Two Interfering Circular Cylinders, *J. Sound and Vibration*, vol. **101**, no. 4, pp. 511-521, 1985.

[32] Zhao, M., Cheng, L., An, H. and Tong, F., Flow and Flow-Induced Vibration of a Square Array of Cylinders In Steady Currents, *Fluid Dynamics Research*, vol.**47**, no. 4,pp. 1-21, 2015.

[33] Zhou, Y. and Yiu, M.W., Flow Structure, Momentum and Heat Transport in a Two Tandem-cylinder Wake, *J. Fluid Mechanics*, vol. **548**, pp. 17–48, 2006.

Declaration on Conflict of Interest

The authors declare that there is no conflict of interest among them. All the authors read and approved the article. In addition, they contribute significantly to the article.

JJMIE

Volume 13, Number 4, December. 2019
ISSN 1995-6665
Pages 231 - 241

Jordan Journal of Mechanical and Industrial Engineering

Process Robustness and Effect of Process Parameters on Rapid Joining of Electrical Contacts by Ultrasonic Vibrations

Pradeep Kumar Jeyaraj

Department of Production Engineering, PSG College of Technology, Coimbatore, India

Received 18 July. 2019

Abstract

Recent technological developments in producing electrical contacts are evolving at a rapid rate, resulting in reliable functioning of a wide variety of customer durable products. Tensile strength is of a predominant requirement for an electrical contact joint to perform the satisfactory function. In this work, an effort has been taken to propose realistic joining conditions for process improvement in ultrasonic metal welding of joining an electrical contact comprising of metallic wire and a flat metallic sheet made of copper material. Taguchi's method is incorporated for the design of experiments. An experimental investigation is carried out to study the effect of process parameters such as clamping pressure, the amplitude of vibration of the sonotrode and weld time on tensile strength of the electrical contacts. Analysis of variance is performed to establish the significant effect of joining conditions on the response variable. The regression model has been developed using the results obtained from experiments to predict the strength of the joint for varying combinations of process parameters. The results of this study indicate that the clamping pressure is the significant parameter influencing the strength of the joint followed by the amplitude of vibration of the sonotrode and the weld time. The parameters identified for achieving maximum tensile strength of the joint are the clamping pressure of 2 bar, the amplitude of vibration of the sonotrode of 57 μm and the weld time of 2.5 seconds. Confirmation experiments are carried out to validate the optimum combination of process parameters for achieving the maximum strength of the joint.

Keywords: Ultrasonic metal welding, Taguchi's method, Design of experiments, Sonotrode, Clamping pressure, Amplitude of vibration of the sonotrode, Weld time, Tensile strength, Regression model;

1. Introduction

The need for rapid joining an electrical contact comprising of copper wire and a copper sheet (terminal plate, lead tab, etc.) is continually increasing in the modern world, especially in large scale manufacturing , such as home appliances, automotive components, switch gears, bus bars, fuses, circuit breakers, ignition modules, contacts, starter motors, microelectronic wires, and battery connectors. In the current industrial world, conductive materials such as aluminum and copper are extensively used for making electrical contacts and there exists a great demand for superior quality joints in various electrical contact applications at minimum cost. One of the significant alternative green manufacturing processes evolved over a period for making such electrical contacts is ultrasonic metal welding (USMW). D. Ensminger [1] stated that the ultrasonic metal welding process is one of the most advanced solid-state welding processes in which similar or dissimilar metallic components are joined rapidly in 1 to 3 seconds by the application of high - frequency vibrations (> 20 kHz) and clamping pressure (1 to 6 bar). Satpathy et al [2] reported that the process of USMW is one in which high - frequency ultrasonic vibrations create relative motion between two abrading surfaces that are held together under moderate clamping pressure. The relative motion deforms the local surface asperities, disperse oxides and contaminants at the interface and improve metal-to-metal contact resulting in effective joining between the parts to be welded. The predominant problems confronted by the industries using the ultrasonic metal welding process are the inferior quality of the weld and strength of the joints. The success of the process while joining aluminum and brass sheet specimens essentially depends on process parameters such as vibration amplitude of the sonotrode, clamping pressure and weld time. Long et al [3] estimated that the number of wires bonded per year is more than 15 trillion which corresponds to 1 million bonds per second which indicated the successful industrial adaptability of this process. Panteli et al [4] studied the effect of process parameters, such as weld energy, weld time, clamping pressure and surface preparation on lap shear strength of the joint while joining aluminum and magnesium alloys. The study revealed the following: Increase in clamping pressure result in the formation of more number of micro bonds accelerating the formation of the weld joint, Increase in the

* Corresponding author e-mail: jp.psgtech@gmail.com

amplitude of vibration result in the development of intermetallic layer from isolated areas. As the welding action progressed, those islands of weld increase in size and spread across the interface until they coalesced into a continuous layer resulting in the formation of an effective joint. T sujino et al [5] conducted experiments for joining flat copper braid wires on a terminal plate. The results from experiments disclosed that the contribution of clamping pressure was more on influencing the strength of the joint when compared with other process parameters. Tian et al [6] investigated the joining of copper wire with Au/Ni plated copper sheet and reported that the process parameters such as ultrasonic power, clamping force and weld time had a significant effect on tensile strength of the joint. Sarangapani et al [7] presented an investigation on interface morphology and metallurgical behavior of the joint formed between wire and bond pad for varying process conditions such as wire diameter and thermal aging and reported that the copper joints were found to be more reliable at elevated temperatures. T Sujino et al [8] observed rapid formation of void at the interface based on variation in clamping force resulting in poor quality of the joint while joining polyurethane - coated copper wires of 0.36 mm and copper plates of 0.3 mm thickness at optimal setting of process parameters using 40 kHz, 60 kHz and 100 kHz complex ultrasonic welding systems. This study exhibited that the strength of the welded joint was almost the strength of the copper wire. Kodama [9] made a study on the effects of vibration frequency, specimen dimensions, surface roughness and contamination of the specimens along with other process parameters while welding a metallic wire with a flat metallic sheet and proved that the joint strength obtained by USMW process was far superior to the joint strength obtained by conventional soldering and brazing process. Hisashi Imai and Shinichi Matsuoka [10] investigated the joint interface of aluminum alloy joints welded using optimal ultrasonic welding process parameters and indicated that the junction was complete after the removal of the oxide film and organic coating due to the combined action of clamping pressure and amplitude of vibration of the sonotrode. Saadat Ali Rizvi and S P Tewari [22] optimized the welding parameters using Taguchi method and employed statistical methods, such as signal to noise ratio and analysis of variance to determine the effects of various process parameters on the mechanical properties and failure modes of GMA welded joints. Shashi Dwivedi and Satpal Sharma [23] optimized and studied the effects of resistance welding process parameters based on response surface plots for welding SAW 1010 steel sheets.

Many industries and researchers primarily focus on evaluating the strength of the joints before making the joint as the procedures and processes involved in rectifying the defects are not cost - effective. Based on the literature survey, research about study on the effect of process parameters during ultrasonic welding of electrical contacts seems to be not reported. This study is carried out to fill this gap and this study also presents a systematic approach addressing the significant issues pertaining to process parametric design using Taguchi's design of experiments.

2. Details of experiments

2.1. Methodology

Taguchi's method of experimental design provides a simple, efficient and systematic approach for conducting experimental trials [14, 15, 24]. The methodology adopted in this research work is shown in Figure 1.

2.2. Selection of factors and levels

Based on initial experimental trials and literature survey predominant process parameters such as clamping pressure, the amplitude of vibration of the sonotrode and weld time are considered as control factors and these factors are varied at three levels as shown in Table 1 [18-20]. The tensile strength of the welded electrical contact joint is considered as the output quality characteristic response variable.

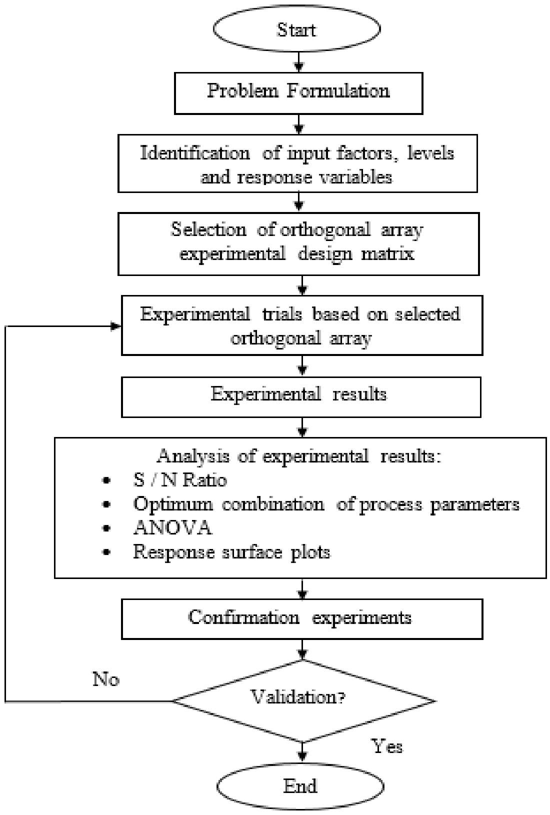

Figure 1: Taguchi Methodology

Table 1: Factors and Levels

Factors	Unit	Level 1	Level 2	Level 3
Clamping pressure (A)	bar	2	3	4
Amplitude of vibration of sonotrode (B)	µm	30	42.5	57
Weld time (C)	sec	2	2.5	3

2.3. Materials and Methods

The experiments are conducted using a conventional ultrasonic metal welding machine (National Indosonic, Bangalore, India) (2500 W, 20 kHz) for different ranges of process parameters. The specimens used in this work are the copper sheet (as received) of 100 mm length, 25 mm width, 0.3 mm thickness and the copper wire (as received) of 1.6 mm diameter and 100 mm length with an overlap length of 6 mm in lap joint configuration [11-13]. The schematic representation of the joint is shown in Figure 2. The specimens are prepared according to ASTM international codes for testing the strength of the joint under tensile loading [16,18]. The specimens are cleaned thoroughly with acetone to get rid of dirt and other impurities before welding.

The experimental trials are carried out based on Taguchi's L27 orthogonal array as shown in Table 2. The order of running the experiments is made random to reduce errors in the experimental results. Each experimental trial is repeated thrice to increase the accuracy of the experimental results. A few welded electrical contact joints thus obtained after experiments are shown in Figure 3. The welded specimens are subjected to tensile testing in a 10 kN tensile testing machine (Hitech, Coimbatore, India). During tensile testing, the wire is gripped in the upper jaw and the sheet is gripped in the lower jaw of the tensile testing machine as shown in Figure 4 to avoid errors in the measurement of the tensile strength of the joint. Minitab 16 statistical software is used for analyzing the experimental results in terms of S/N ratio calculation, ANOVA and development of response surface plots.

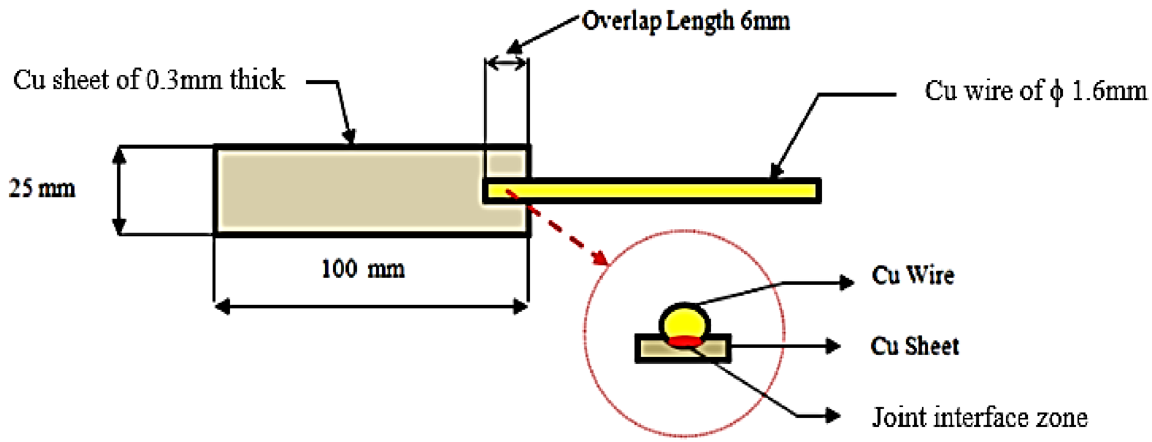

Figure 2: Schematic representation of the joint

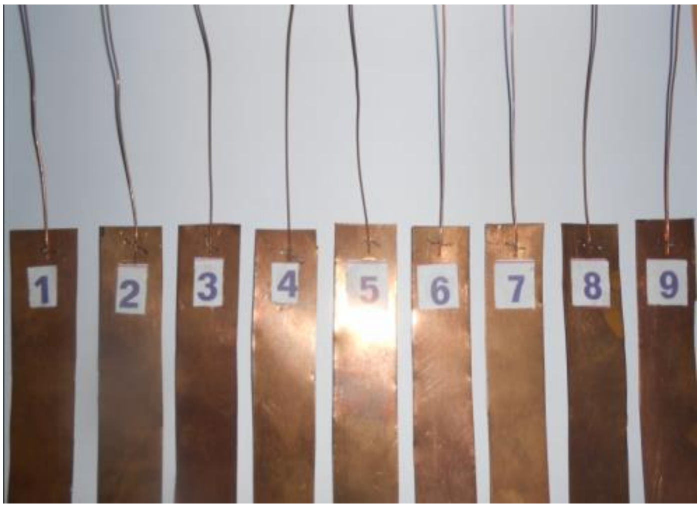

Figure 3: Welded joints

Figure 4: Tensile loading

Trial No.	Clamping pressure (A) (bar)	Amplitude of vibration of sonotrode (B) (μm)	Weld time (C) (sec)	Tensile strength of the electrical contact joint (N)				S/N ratio
				Trial I	Trial II	Trial III	Average (μ)	
1	2	30	2	224.124	224.301	224.568	224.331	47.0178
2	3	30	2	223.871	223.322	224.759	223.984	47.0043
3	4	30	2	218.545	219.241	222.109	219.965	46.8471
4	2	42.5	2.5	236.282	236.081	236.057	236.140	47.4634
5	3	42.5	2.5	228.534	228.772	228.716	228.674	47.1843
6	4	42.5	2.5	225.231	225.542	226.249	225.674	47.0696
7	2	57	3	229.992	231.016	230.693	230.567	47.2559
8	3	57	3	229.671	229.761	230.241	229.891	47.2304
9	4	57	3	227.061	225.985	227.591	226.879	47.1159
10	2	30	2.5	232.579	232.89	232.421	232.630	47.3333
11	3	30	2.5	224.899	225.864	226.298	225.687	47.0701
12	4	30	2.5	221.842	222.135	223.784	222.587	46.9500
13	2	42.5	3	225.143	225.972	224.929	225.348	47.0571
14	3	42.5	3	223.768	223.109	223.386	223.421	46.9825
15	4	42.5	3	223.190	222.765	224.332	223.429	46.9828
16	2	57	2	229.986	231.433	233.141	231.520	47.2918
17	3	57	2	229.118	228.994	227.817	228.643	47.1832
18	4	57	2	224.189	225.099	223.144	224.144	47.0105
19	2	30	3	222.899	223.282	223.782	223.321	46.9786
20	3	30	3	224.010	223.865	226.195	224.690	47.0317
21	4	30	3	217.231	216.664	216.793	216.896	46.7250
22	2	42.5	2	228.112	226.995	228.023	227.710	47.1476
23	3	42.5	2	226.124	226.953	227.593	226.890	47.1163
24	4	42.5	2	223.548	224.109	223.287	223.648	46.9913
25	2	57	2.5	236.190	236.290	236.09	236.190	47.4652
26	3	57	2.5	231.789	230.980	232.133	231.634	47.2960
27	4	57	2.5	226.892	227.546	228.656	227.698	47.1472

3. Results and Discussions

3.1. Evaluation of signal to noise ratio

In Taguchi's method, the term signal represents the desired value for the output attributes and the noise represents the undesirable value for the output attributes. There are three types of quality characteristics, such as lower–the-better (LB), the nominal –the better (NB) and the higher-the-better (HB). Since the strength

of the joint should be maximum, higher – the – better type of S/N ratio is used in this

study. The S/N ratio for the higher-the-better type is calculated as shown in Equation 1.

$$S/N_{HB} = -10 \log_{10}\left(\frac{1}{n}\sum_{i=1}^{n}\frac{1}{{y_i}^2}\right) \quad (1)$$

where, n= number of repetition in a trial y_i = tensile strength of the joint for i^{th} trial. The S/N ratio is calculated for each of the experimental trials and the results are shown in Table 2. The average values of signal to noise ratio at different levels of selected parameters are shown in Table 3. From Table 3, it is observed that the optimum combination of process parameters resulting in minimum variation of tensile strength of the joint are clamping pressure (A), amplitude of vibration of sonotrode (B) and weld time (C) at 1st, 3rd and 2nd levels respectively i.e. clamping pressure of 2 bar, the amplitude of vibration of sonotrode 57 μm and weld time of 2.5 seconds. From Table 2, it is inferred that the highest signal to noise ratio value (47.4652) corresponds to the above combination of parameters (Trial 25) which ultimately results in maximum tensile strength of the joint of 236.19 N.

3.2. Analysis of Varaince

The Analysis of variance (ANOVA) is used to interpret results from the actual experiments. The objective of ANOVA is to extract the amount of variation caused by each factor relative to the total variation observed in the actual results from experiments. ANOVA also establishes the relative significance of factors in terms of their percentage contribution to the response variable. ANOVA is performed for a confidence level of 95% and the results are shown in Table 4. The F_{Cal} value for each process parameter is calculated and compared with F_{Tab} values obtained from the F-test table [14]. A factor to be statistically significant, the calculated F_{Cal} value for each process parameter must be greater than F_{Tab} value as shown in Table 4. It reveals that the factors clamping pressure, the amplitude of vibration of sonotrode, weld time and interaction between clamping pressure and weld time are statistically significant on the tensile strength of the joint. The contributions are in the following order: Clamping pressure (34.45%), the amplitude of vibration of sonotrode (30.12%), weld time (22.03%) and interaction between clamping pressure and weld time (6.87%). The signal to noise ratio graph for interactions of process parameters is shown in Figure 5. It is seen from this figure that a significant interaction exists between clamping pressure and weld time. The average and standard deviation of experimental results are shown in Figure 6.

Table 3. Average S/N ratio for various levels of factors (Tensile strength of the joint)

Level	Clamping pressure (bar)	Amplitude of vibration of the sonotrode (µm)	Weld time (sec)
1	**47.22**	47.00	47.07
2	47.12	47.11	**47.22**
3	46.98	**47.22**	47.04
Delta	0.24	0.23	0.18
Rank	1	2	3

Table 4: ANOVA for tensile strength of the joint

Factor	DF	SS	MS	F_{Cal}	F_{Tab}^{*}	Inference	% Contribution
A	2	0.264160	0.132080	45.54	4.46	Significant	34.45
B	2	0.230830	0.115415	39.80	4.46	Significant	30.12
C	2	0.168885	0.084442	29.12	4.46	Significant	22.03
A X B	4	0.009996	0.002499	0.86	3.84	Insignificant	----
A X C	4	0.052663	0.013166	4.54	3.84	Significant	6.87
B X C	4	0.016856	0.004214	1.45	3.84	Insignificant	----
Error	8	0.023198	0.002900				6.53
Total	26	0.766587					100

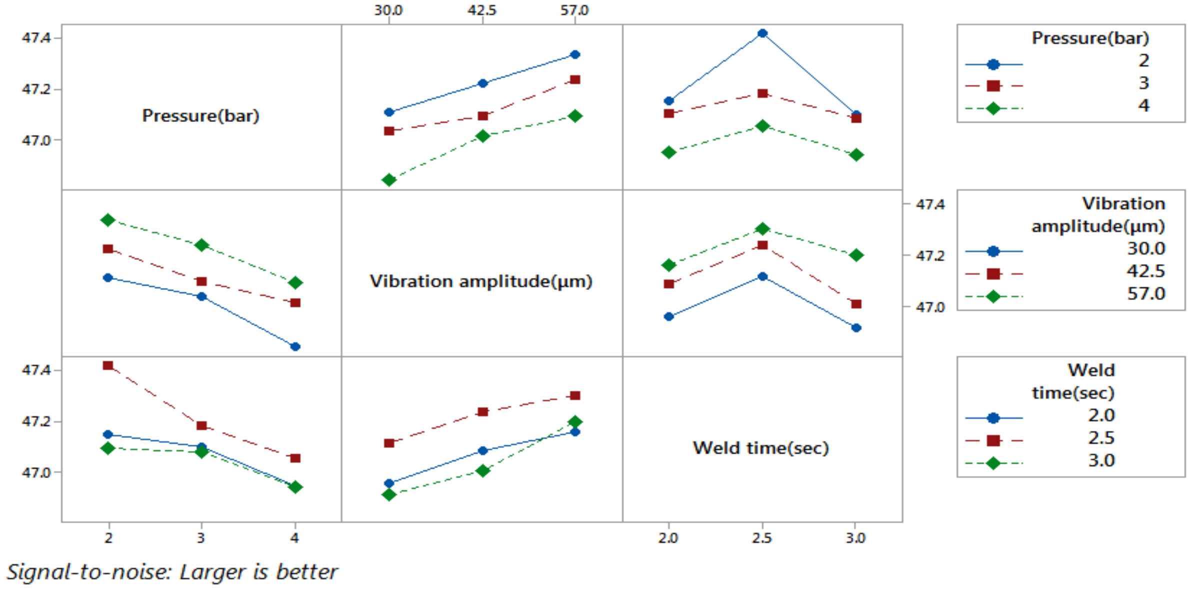

Figure 5: S/N ratio for interactions at various levels of factors

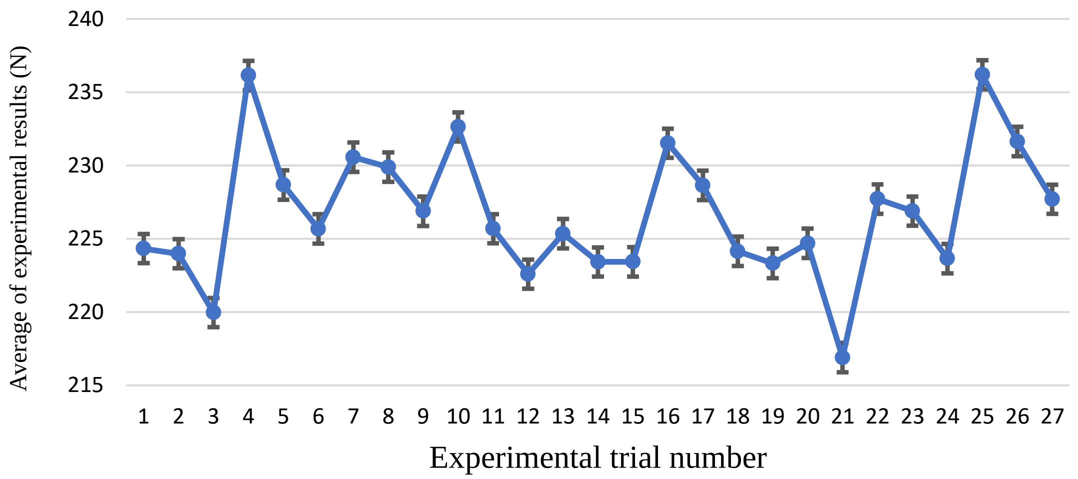

Figure 6: Average and standard deviaition of experimental results

3.3. Effect of process paramters

Response surface and contour plots are developed to understand the effect of the process parameters on the tensile strength of the joint [20]. The influence of clamping pressure and the amplitude of vibration of the sonotrode on strength of the joint is shown in Figure 7. It can be noted from this figure that, the strength of the joint decreases with the increase of clamping pressure since the increase in clamping pressure restricts the rubbing action between wire and sheet and tend to severely deform the wire resulting in the reduction of the strength of the joint. The excessive amount of pressure applied on the wire by the sonotrode makes the wire deform and penetrate considerably into the sheet resulting in the formation of cracks and tear at the interface as shown in Figure 8. An increase in clamping pressure also restricts the sliding motion between the specimens leading to reduced welding action and hence reduced strength. Hence, a low level of clamping pressure (2 bar) is found to be effective. The maximum strength of the joint of about 235 N is achieved using a lower level of clamping pressure (2 bar) and a higher level of amplitude of vibration of the sonotrode (57µm). The contour plot shows that the strength of the joint is more sensitive to changes in clamping pressure than the amplitude of vibration of the sonotrode

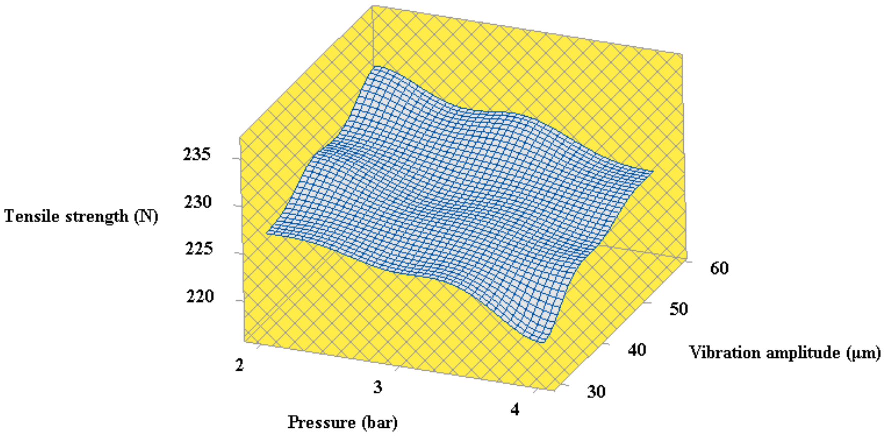

a) Response surface plot

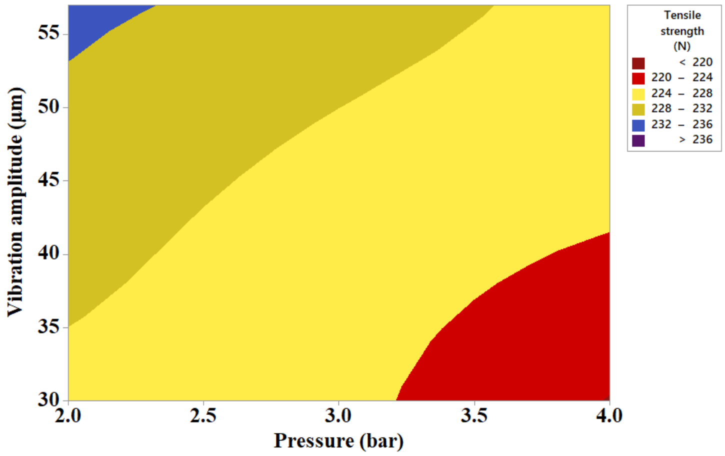

b) Contour plot

Figure 7: Effect of clamping pressure and amplitude of vibration of the sonotrode on strength of the joint (a) Response surface plot (b) Contour plot

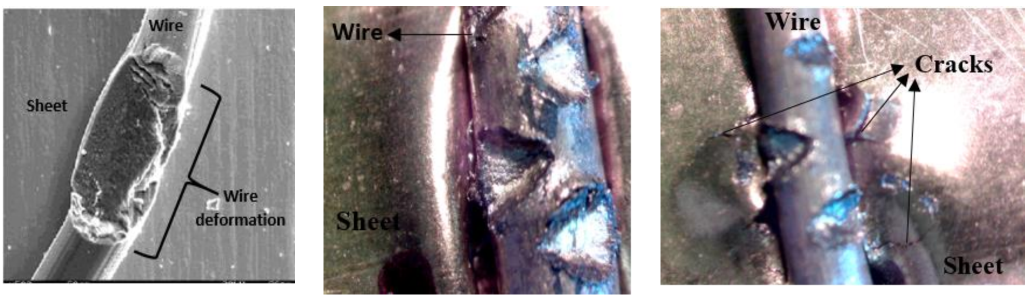

(a) Wire deformation (b) Wire penetration into the sheet (c) Cracks at the joint interface

Figure 8: Electrical contact joint defects

The effect of clamping pressure and weld time on strength of the joint shown in Figure 9. It can be seen from this figure that the lower level of clamping pressure (2 bar) and a medium level of weld time (2.5 seconds) result in maximum strength of the joint (235 N). The strength of the joint increases up to 2.5 seconds, a further increase in weld time results in the reduction of the strength of the joint. Initially, the asperities between wire and sheet join to make pure metal-to-metal contact. Due to prolonged rubbing action, the previously formed bond between wire and sheet is disturbed resulting in minimization of the strength of the joint. This can be further investigated by extending the scope of this work in the future through microstructural studies [21]. The contour plot shows that the strength of the joint is more sensitive to the changes in weld time than clamping pressure.

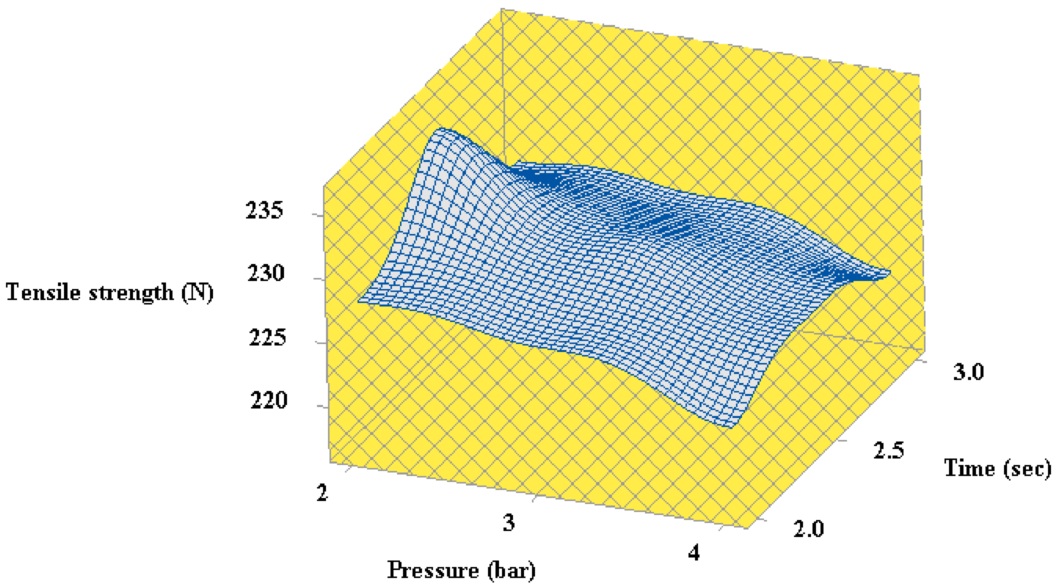

a) Response surface plot

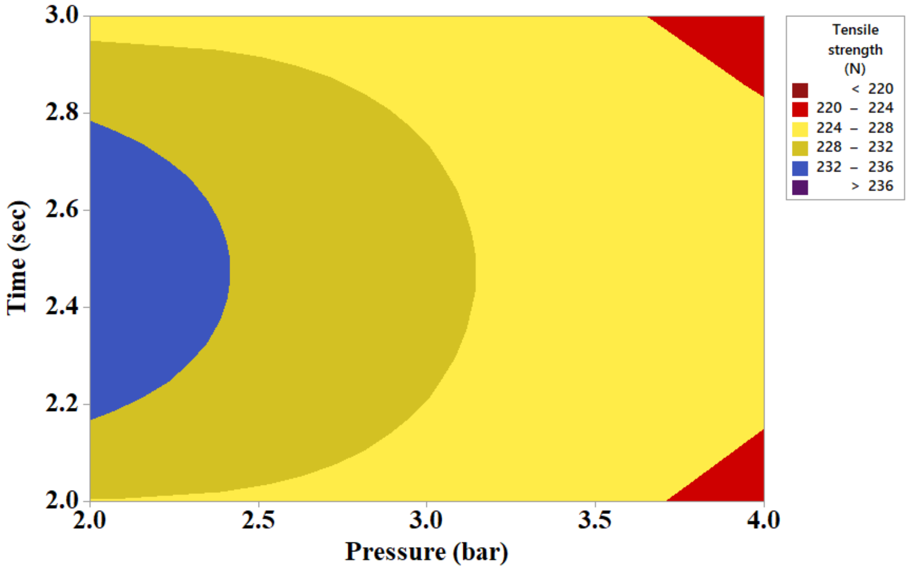

b) Contour plot

Figure 9: Effect of clamping pressure and weld time on strength of the joint

The effect of the amplitude of vibration of the sonotrode and weld time on tensile strength of the joint is shown in Figure 10. It can be observed from this figure that, the strength of the joint increases with an increase in the amplitude of vibration of the sonotrode [19, 20]. since the increase in amplitude of vibration of the sonotrode facilitates effective abrading action between wire and sheet leading to better bonding and a substantial increase in strength of the joint. The maximum strength of the joint is obtained at a higher level of amplitude of vibration of the sonotrode (57µm) and a medium level of weld time (2.5 seconds). The contour plot shows that the strength of the joint in more sensitive to changes in weld time than the amplitude of vibration of the sonotrode.

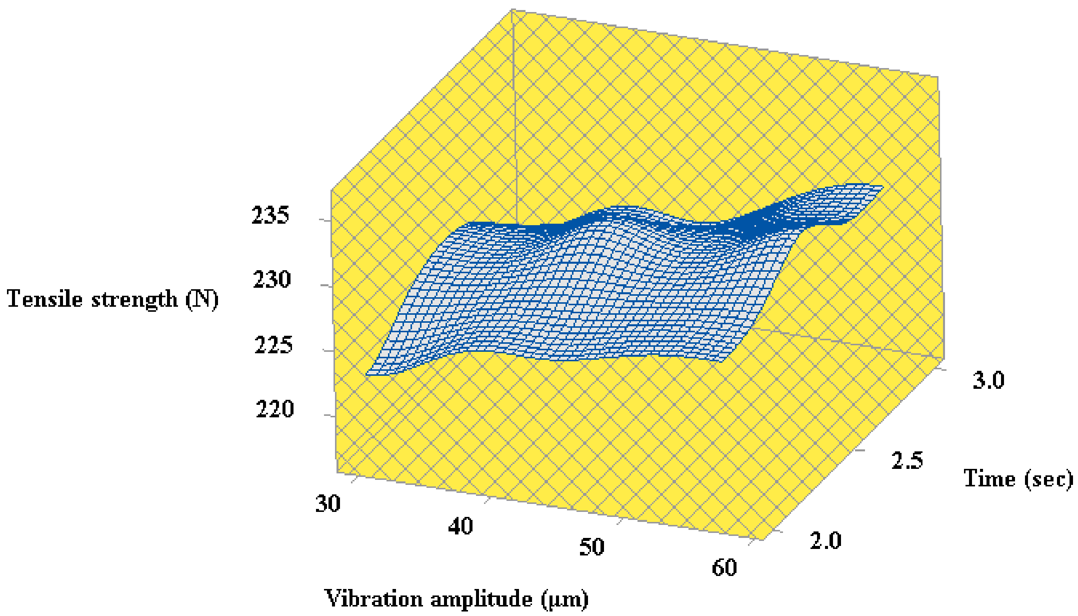

a) Response surface plot

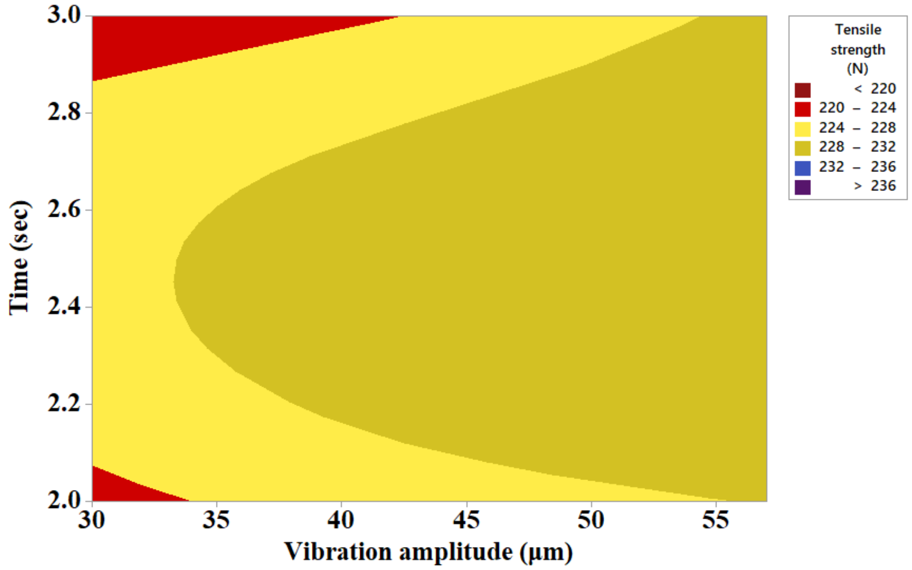

b) Contour plot

Figure 10: Effect of amplitude of vibration of the sonotrode and weld time on tensile strength of the joint.

3.4. Confirmation experiments

Confirmation experiments are to be carried out to validate the optimum combination of process parameters for achieving the maximum strength of the joint. After identification of the optimum combination of process parameters, the mean of response(μ) is estimated using Equation 2.

$$\mu = T + (A_1 - T) + (B_3 - T) + (C_2 - T) \quad (2)$$

where, T is the overall mean of response and has a value of 226.748N. The estimated mean for the optimum parameters treatment condition (A_1, B_3, and C_2) is calculated as 235.704 N. The estimated mean is calculated based on the average results of the experiments. Hence, a confidence interval for the predicted mean on a confirmation treatment condition is calculated using Equation 3 [14,15].

$$CI = \left(F_{\alpha,1,v_e} V_e \left[\frac{1}{\eta_{eff}} + \frac{1}{R}\right]\right)^{1/2} \quad (3)$$

where, $F_{\alpha,1,v_e}$ is the value of 'F' from F-Tables, α is the risk level= 0.05, V_e is the error variance = 0.0029, v_e is the degrees of freedom(DOF) for the error, R is the number of repetitions for confirmation experiments = 5, η_{eff} is the effective number of replications and calculated using Equation 4.

$$\eta_{eff} = \frac{N}{(1+U)} \quad (4)$$

where, N is the total number of experiments = 54, U is the degree of freedom associated with the estimate of mean response =10, Substituting these values in Equation 4.3, η_{eff} is calculated as 4.91, $F_{0.05,1,8}$. = 5.32. Thus, the confidence interval (CI) calculated using Equation 5 is ±0.079. The 95% confidence level of the predicted optimum strength of the joint is given by

$$[\mu - CI] < \mu < [\mu + CI] \quad (5)$$

=> 233.625< 235.704 < 235.783

A successful confirmation experiment is one that is carried out with the optimum combination of process parameters (clamping pressure 2 bar, the amplitude of vibration of the sonotrode 57 µm, weld time 2.5 seconds) and the strength of the joint fall within the calculated confidence interval. The number of experimental trials carried out for validating the combination of process parameters is 5. The strength of the joints thus obtained for five confirmation experiments along with average and standard deviation are shown in Table 5. The average of all the responses of the confirmation experiments is 235.694 which is found to be well within 95% of the confidence interval of the true mean. Therefore, the optimal settings of process parameters and their levels are found to be significant.

Table 5: Results from Confirmation experiments

Trial No	Tensile strength of the joint(N)
1	235.712
2	235.689
3	235.654
4	235.709
5	235.723
Mean	235.694
Std. dev.	0.028

t-statistic test is carried out to validate the results from confirmation experiments. The mean and standard deviation are claculated as shown in Table 5. The standard error of the mean is calculated using Equation 6.

$$\text{Std. Error} = \text{Std. deviation} \;/\; \sqrt{n} \quad (6)$$

where n is the number of observations.

Std. Error = 0.028 / √5 = 0.0125

The standard error of the mean has n-1 degrees of freedom. So 5-1 = 4 degrees of freedom. For 95% confidence interval

t(4; 0.05) = 2.132

The confidence interval is calculated as

235.694 ± (2.132 x 0.0125) N

=> 235.667 < 235.694 < 235.721

The mean of confirmation experimental results lies within the confidence intervals. Hence the validation.

3.5. Regression model

In this work, a regression model has been developed based on results from experiments to characterize the relationship between independent and dependent variables. The response variable tensile strength of the joint is dependent on independent variables such as clamping pressure (A), the amplitude of vibration of the sonotrode (B) and weld tine (C). The regression model developed for prediction of tensile strength of the joint is shown in Equation 7. The goodness of fit of the regression model is characterized by the coefficient of determination (R^2). The R^2 value of the model is found to be 0.91. The variation between the experimental and predicted responses (strength of the joint) is illustrated in Table 6. Figure 11 indicates that the developed regression model can represent the system under the given experimental domain.

$$\text{Strength of the joint (N)} = -3.5 + 22.9\,A + 2.46\,B + 157.8\,C + 0.064\,AB - 0.925\,BC - 10.4\,AC - 2.61\,A^2 - 0.0151\,B^2 - 25.60\,C^2 - 0.000110\,A^2B^2 + 0.00231\,B^2C^2 + 0.369\,A^2C^2 \quad (7)$$

where A = clamping pressure, B= amplitude of vibration of the sonotrode, C= weld time.

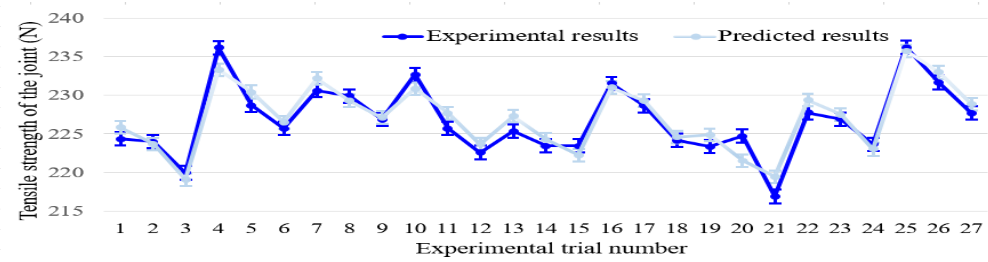

Figure11: Comparison of expermental results and predicted results

Table 6: Results predicted by regression model

Trial No	Experimental values	Predicted values
1	224.331	225.83
2	223.984	223.69
3	219.965	219.08
4	236.140	233.30
5	228.674	230.41
6	225.674	226.51
7	230.567	232.14
8	229.891	229.26
9	226.879	227.08
10	232.630	230.86
11	225.687	227.66
12	222.587	223.66
13	225.348	227.28
14	223.421	224.26
15	223.429	222.27
16	231.520	230.96
17	228.643	229.25
18	224.144	224.56
19	223.321	224.86
20	224.690	221.54
21	216.896	219.44
22	227.710	229.35
23	226.890	227.51
24	223.648	223.00
25	236.190	235.71
26	231.634	232.95
27	227.698	228.87

4. Conclusions

Based on the results obtained from this research work, it can be concluded that:

- The strength of the joint was found to be significantly sensitive to the variations in the levels of process parameters.
- The optimum level of process parameters to achieve maximum strength in the range of 236 N is found to be clamping pressure (2 bar), the amplitude of vibration of the sonotrode (57 µm) and weld time (2.5 seconds).
- The highly effective parameter for achieving maximum strength of the joint was found to be the clamping pressure.
- The results predicted by the developed empirical model were found to be in good agreement with results from experiments.
- The confirmation test validated the process robustness based on the Taguchi method for enhancing the welding performance and optimizing the welding parameters in the ultrasonic metal welding process.
- The electrical contact joints thus made can be further studied for electrical, electronic, magnetic and thermal characterization as future work.

Acknowledgments

This research is funded by the University Grants Commission, New Delhi, Under Major Research Project Scheme (F.No.42-876/2013(SR).The author sincerely thanks his Ph.D. guide Dr, K. Prakasan, Principal of PSG College of Technology, Coimbatore 641 004 for providing necessary support, guidance and facilities to carry out this work.

References

[1] D. Ensminger. Ultrasonics: fundamentals, technology, applications. 3rd ed. New York: CRC Press; 2011.

[2] M. P. Satpathy, B. R. Moharana, S. Dewangan, S. K. Sahoo, “Modeling and optimization of ultrasonic metal welding on dissimilar sheets using fuzzy based genetic algorithm approach”. Engineering Science and Technology, an International Journal. Vol.18, No. 4, 2015, 634-647.

[3] Y. Long, J. Twiefel, J. Wallaschek, “A review on the mechanisms of ultrasonic wedge-wedge bonding”. Journal of Materials Processing Technology. Vol.245, 2017, 241-258.

[4] Panteli, Y. C. Chen, D. Strong, X. Zhang, P. B. Prangnell, “Optimization of aluminium – to - magnesium ultrasonic spot welding”. The Journal of The Mineral, Metals & Materials Society. Vol.64, No. 3, 2012, 414-420.

[5] J. Tsujino, T. Ueoka, E. Sugimoto, “Welding of flat copper braid wire specimens using ultrasonic complex vibration - Direct machining of terminal parts on flat braided wires”. IEEE Ultrasonics Symposium, Conference, Beijing, China, 2008.

[6] Y. Tian, C. Wang, I. Lum, M. Mayer, J. P. Jung, Y. Zhou, “Investigation of ultrasonic copper wire wedge bonding on Au/Ni plated Cu substrates at ambient temperature”. Journal of Materials Processing Technology. Vol.208, 2008, 179-186.

[7] Sarangapani Murali,Narasimalu Srikanth, J. Charles, “Effect of wire diameter on the thermosonic bond reliability”. Microelectronics Reliability. Vol. 46, No.2-4, 2006, 467-475.

[8] J. Tsujino, S. Ihara, Y. Harada, K. Kasahara, N. Sakamaki, “Characteristics of coated copper wire specimens using high frequency ultrasonic complex vibration welding equipment”. Ultrasonics. Vol. 42, 2004, 121-124.

[9] M. Kodama, “Ultrasonic welding of non-ferrous metals”. Welding International, Vol. 3, 1989, 853-860.

[10] Hisashi Imai and Shin-ichi Matsuoka, “Finding the optimum parameters for ultrasonic welding of aluminium alloys”. JSME International Journal. Vol. 48, No. 4, 2005, 311-316.

[11] Zhou, M. D. Thouless, S. M. Ward, “Predicting the failure of ultrasonic spot welds by pull-out from sheet metal”. International Journal of Solids and Structures. Vol. 43, No. 25-26, 2006, 7482-7500.

[12] T. Kuprys, J. Janutėnienė, R. Didžiokas, “Strength of copper wire connections welded by ultrasonic”. Mechanics. Vol. 65, 2007, 30-33.

[13] Pradeep kumar jeyaraj, “Effect of temperature distribution in ultrasonically welded joints of copper wire and sheet used for electrical contacts”. Materials. Vol.11, No.6, 2018, 1-13.

[14] P. J. Ross. Taguchi techniques for quality engineering. 2nd ed. New Delhi: Tata Mcgraw - Hill Publishing Company Limited; 2010.

[15] K. Krishnaiah and P. Shahabudeen.2nd ed. Applied design of experiments and Taguchi methods. New Delhi: PHI Learning Private Limited; 2013.

[16] ASTM D1002-1:2010, “Standard test method for apparent shear strength of single-lap-joint adhesively bonded metal specimens by tension loading (metal-to-metal)”. ASTM international; 2005.

[17] Paul G. Mathews. 3rd ed. Design of Experiments with MINITAB. New Delhi: New Age International (P) Limited; 2005.

[18] J Pradeep Kumar and K Prakasan, “Acoustic horn design for joining metallic wire with flat metallic sheet by ultrasonic vibrations”. Journal of Vibroengineering. Vol. 20, No. 7, 2018, 2758 – 2770.

[19] J Pradeep Kumar, M.S. Arun Kumar, N. Gowsalya Devi, M.Naveen Kumar, S.M. Pavith Raja, “Numerical study on stress distribution in ultrasonically welded electrical contacts

used in automotive". International Journal of Vehicle Structure Systems. Vol. 10, No.4, 2018, 287–290.

[20] J. Pradeep Kumar, "Effect of process parameter characteristics on joint strength during ultrasonic metal welding of electrical contacts". Welding in the World. Vol.64, No.1, 2020, 73-82.

[21] Chihiro Iwamoto, Keisuke Yamauchi, Kazuki Motomura, Yoichi Hashimoto,Kensuke Hamada, "Microstructure of Joint between Stranded Wire and Substrate Welded by Ultrasonic Welding". Applied Sciences. Vol.534, No.9, 2019, 1-10.

[22] Saadat Ali Rizvi, S.P Tewari, "Optimization of welding parameters by using Taguchi method and study fracture mode characterization of SS304H welded by GMA welding". Jordan Journal of Mechanical and Industrial Engineering, Vol. 12, No. 1, 2018, 17-22.

[23] Shashi Dwivedi, Satpal Sharma, "Optimization of resistance spot welding process parameters on shear tensile strength of SAE 1010 steel sheets joint using Box Behnken design". Jordan Journal of Mechanical and Industrial Engineering, Vol. 10, No. 2, 2016, 115-122.

[24] V. RamakoteswaraRao, N. Ramanaiah, M.M.M Sarcar, " Optimization of volumetric wear rate of AA7075 – TiC metal matrix composite by using Taguchi technique". Jordan Journal of Mechanical and Industrial Engineering, Vol. 10, No. 3, 2016, 189-198.

JJMIE

Volume 13, Number 4, December. 2019
ISSN 1995-6665
Pages 243 - 246

Jordan Journal of Mechanical and Industrial Engineering

Study of the Mixer Performance under Different Mixing Conditions

M. Akhondizadeh*[a], M. Khajoei[b]

[a] *Mechanical Engineering Department of Sirjan University of Technology, Sirjan, Iran*
[b]*Department of Mechanical Engineering, Sirjan Branch, Islamic Azad University, Sirjan, Iran*

Received 7 July. 2019

Abstract

In the present work, the performance of a laboratory vertical mixer at different operating conditions has been studied for the mixing of the iron ore concentrate and water. Three discharge valves have been mounted on a mixer wall at different heights.The mixer desired performance occurs when the solid particle contents for three discharge valves are approximately in the same levels. The operating parameters which influence the mixer performance have been studied here including main shaft speed, impeller angle, single or double impeller set and baffle or no-baffle cases.Results show that all mentioned parameters have undeniable role in appropriate mixer performance but the most influencing ones, listed here from most to least, are baffle existence, impeller angle, shaft speed and impeller set.

Keywords: Laboratory mixer, Impeller speed, Impeller angle, Baffle.

1. Introduction

One way of transferring of tiny grains in the mineral industries is by mixing them in water and using vertical cylindrical mixers. The optimum mixing depends on appropriate selection of the mixer performance parameters. These parameters include the impeller rotational speed, impeller dimensions, impeller angle, the position and number of impeller sets and existence or ignoring the baffle in the internal face of cylinder wall. The optimum performance means semi-homogenous slurry to be easily handled and no settlement. The acceptable mixing depends also on the particle properties. The particle cohesiveness, shape, mass, density and etc. may affect the mixer performance. There are complicated relations in computational fluid dynamics (CFD) for prediction of the flow behavior. Commercial CFD software provides the way to have the acceptable solutions for a wide range of engineering problems. However, the experimental observations by laboratory equipment give the reliable data in simple and fast modes in some cases.

Some researches aimed to study the design parameters in order to determine the fluid forces [1, 2]. Hobbs and Muzzio [3] studied the effect on Reynolds number on the laminar mixing. Their results showed that in Reynolds lower than 10 the mixing is independent on Reynolds number. Tanguy et al. [4]investigated experimentally and numerically the mixing performance of a dual impeller mixer and derived a generalized power curve. Effect of the shaft speed and impeller design on the optimum performance of a ribbon mixer was analyzed by discrete element method by Halidan et al. [5]. Gijon and Tecante [6] determined the mixing time which was required to achieve 92% homogeneity. The turbulent flow field generated in a baffled stirred tank was numerically studied by solving the unsteady Navier–Stokes equations by Zamiri and Chung [7]. The Predicted velocity evaluated numerically was compared with experimental measurements. The laminar mixing performance in a cylindrical vessel agitated by a plate impeller was investigated by KC Ng and EYK Ng [8]. They considered several mixing enhancement strategies including the baffling. They observed low radial mixing in an unbaffled vessel. Busciglio et al. [9] provided experimental information by usingthe planar laser induced fluorescence (PLIF) technique on mixing rates in an unbaffled vessel. Torotwa [10] studied the performance of three different types of mixing impeller by Fluent simulation and experimentally. In the present work, the effect of influencing parameters on mixing performance is studied experimentally by a laboratory mixer. The aim is to determine the positive effect of baffle in mixer body and the number of impellers. The optimum impeller angle is determined and the effect of main shaft speed is shown.

2. Laboratory mixer

The present experimental apparatus is a low scale radial-flow mixer which is illustrated in Fig. 1. It is a cylinder with an electrical motor on the upper head. The

* Corresponding author e-mail: m.akhondizadeh@sirjantech.ac.ir

impellers are flat-blade type including three blades on each impeller fixed on a vertical shaft at the specified height (bottom of shaft, 10cm and 20cm from bottom of shaft). The impeller angleθ can be changed from 0^o to 90^o by the screw connection between impeller and shaft. Bafflescanbe mounted on the interior of the vessel body. Baffles are 500×30×10mm Teflon plates. The slurry is a combination of water and iron Pellet-powder whose composition is given in table 1. The mixer body is made of carbon steel and the impellers are cut of Teflon plate same as the baffles. The electrical motor and speed controller are mounted on the top of the main body of mixer. The main shaft end is 10cm above the mixer bottom and the distance between impellers is 15cm. Four baffles mounted around the main body of mixer in 90^o distances.

Table 1. Composition of Pellet- powder

Fe%	Feo%	P%	S%	Sio2%	Cao%	Mgo%	Al2o3%
65.51	1.38	0.04	0.008	3.36	0.745	2.2	0.64

The impellers have end-threads tightened on the main shaft and enables controlling the impeller angle. The impellers can be disassembled to have one, two or three impeller sets. The laboratorymixer dimensions are given in table 2 and test parameters for the present experiments are given in table 3.

Table 2. Dimensions of laboratory mixer

Dimension	Value
Box diameter	410mm
Box length	540mm
Box thickness	2mm
Shaft diameter	12mm
Impeller diameter	350mm
Impeller width	25mm
Impeller thickness	10mm

Table 3. Test parameters

Parameter	Value
Impeller face angle (Deg)	0, 15, 30, 45
Number of impeller sets	1, 2
Number of baffles Without baffle	With baffles,
Impeller speed (Rpm)	90, 120, 150

The governing parameter which guaranties the appropriate mixing is the Reynolds number which is evaluated as follow:

$$R = \frac{ND^2\rho}{\mu} \tag{1}$$

In which N is the main shaft speed in *rev/s*, D is the impeller diameter in meter, ρ is the flow density in kg/m^3 and μ is the viscosity in *Pa.s.*

The slurry physical properties including density and viscosity are evaluated by the following relations: [11].

$$\rho_m = \frac{100}{\frac{C_W}{\rho_S}+\frac{100-C_W}{\rho_L}} \tag{2}$$

Where ρ_m is the density of slurry in kg/m^3, C_w is the solids concentration by weight%, ρ_s is the density of solidin $kg/m^3$and ρ_L is the density of liquid inkg/m^3. The viscosity of slurry is evaluated by the following relation [11]:

$$\mu_m = \mu_L(1 + 2.5\emptyset) \tag{3}$$

In which μ_m is the viscosity of slurry,μ_L is the viscosity of liquid and Φ is the volume fraction of particles. The slurry parameters for the present work are given in table 4.

Table 4. Mixture parameters

C_w	8.3%
ρ_s	4200kg/m^3
ρ_L	1000kg/m^3
$\emptyset$	0.02
μ_L	8.9e-4 Pa.s

According to the given parameters in tables 3 and 4, the slurry density ρ_m and viscosity μ_m are respectively *1075 kg/m^3* and *9.34×10^{-4}Pa.s*

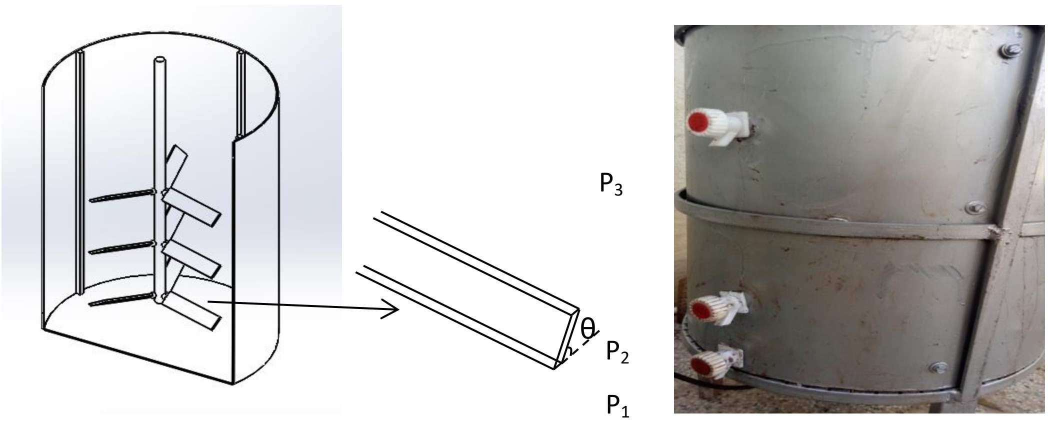

Figure 1. Schematic of the mixer box, baffle and impellers, impeller angle and discharge valve positions

3. Experimental procedure

The main body of mixer is washed completely and dried to be cleaned of particles before each test. The slurry was provided by mixing *2.5kg* magnetite concentrate in *30Liter* of water and the particles were allowed to be settled in 30 minutes. After the particles settled in the bottom of the mixer box, the motor was turned on and experiments start. After *2 minutes*, the discharge valves were opened simultaneously and *250cc* of slurry was taken in glass cups. Discharge valves which their position on mixer body is illustrated in Fig 1., are positioned at the bottom of main box (P_1), *100mm* from the bottom (P_2) and *250mm* from the bottom (P_3). The taken slurry has been dried in laboratory furnace and remained particles have been weighed accurately. The particle content in obtained slurry is considered as the value of the particles at the corresponding position in the main box during the mixing.

4. Results

The particle contents of the taken slurry from 3 discharge valves at three impeller speeds *90, 120* and *150rpm* are illustrated in Fig. 2.The results shown in figure 1 are for impeller angle of 0^o; with two impellers and four baffles mount. The Reynolds number is about *211000, 281000* and *351000* at the impeller speeds of *90, 120* and 150rpm respectively. A tangible difference between the particle content of discharges P_1, $P_2$and P_3 is observed at the shaft speed of *90rpm* which is a sign of non-homogenous slurry in main body of mixer. By increasing the speed to *120rpm* the homogeneity tends to be better and the shaft speed of *150rpm* gives appropriate and homogenous slurry in form of nearlyclose value of particle content from three discharge positions.

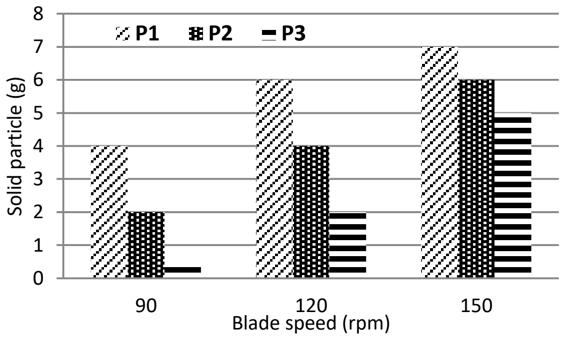

Figure 2. Variation of the solid particle contents at the different positions at three blade speeds

To better illustrate the effect of impeller speed on mixer performance, the variation of particle content by increasing the impeller speed is separately for each valve shown in Fig.3. Vertical axis is the ratio of particle content at the speeds *90, 120* and *150rpm* to the particle content at the speed of *90rpm*. However, as illustrated, by increasing the speed from 90 to 120 rpm the particle content of all three discharge valve increased but there are different graph behaviors. The increment of particle content of P_3 discharge by increasing the impeller speed is evidently higher than the increment for$P_1$and P_2. The particle content of P_3 at the speed of *150rpm* is about *10* times of its content at the speed of *90rpm*.The increment of impeller speed pushes the particles up and increases the particle content from the P_3 discharge valve.

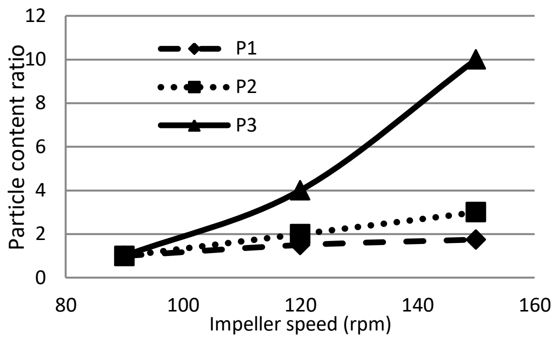

Figure 3. dimensionless Increment of particle content of three discharge positions of mixer by increasing the impeller speed

One of the important parameters which influences the mixer performance is the impeller angle [12]. The effect of impeller angle on the mixing homogeneity can be seen in Fig. 4. The impeller speed is *120rpm* and there are four baffles and two impellers.The zero degree impeller angle behaves like a vertical moving wall pushing the local current which influences the little portion of slurry. Many parts of slurry are not influenced by the impeller-induced current. This means that there will be non-homogeneous current and different particle contents will be achieved from three discharge valves. At the impeller angle of 15^o and 30^o the conditions tend to be better. The impeller angle of 45^o gives the appropriate mixing conditions in form of homogenous slurry in mixer body. The impeller angle of 45^o provides the upward currents in mixer and increases the particle content in P_3 discharge valve.

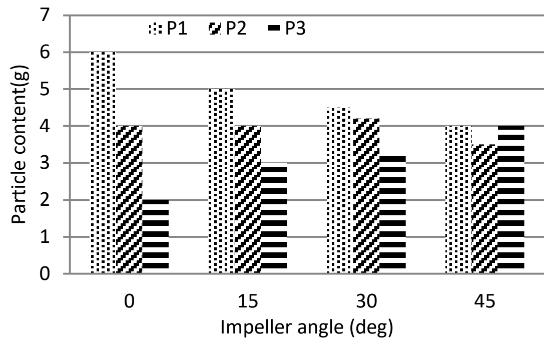

Figure 4. Particle contents at the different impeller angles

Another parameter which has an undeniable influence on the mixer performance is the number of impeller sets on the main shaft. In case of one impeller set at the bottom end of the main shaft, only the slurry around it is influenced. In this case, there is significant content of particles in the P_1 discharge valve and almost no particles inP_2 and P_3. However, by mounting another impeller set *15cm* above the first impeller set on main shaft, a significant improvement in mixing performance is observed as illustrated in Fig. 5. The impeller angle is 30^o, the speed is 120 rpm with four baffles.

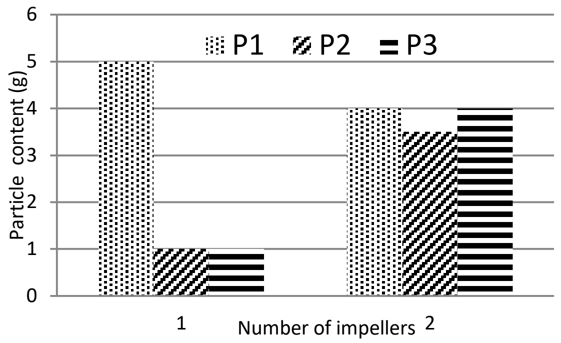

Figure 5. Particle contents discharged from P1, P2 and P3 valves with one and two baffles

Opening the discharge valves at the different times after the start of shaft rotation determines the required time to achieve homogeneity of slurry. It was performed by taking samples from three discharge valves after *60, 120* and *180* seconds after the start of mixer shaft rotation. As illustrated in Fig. 6, the homogeneity observed after 120 seconds.

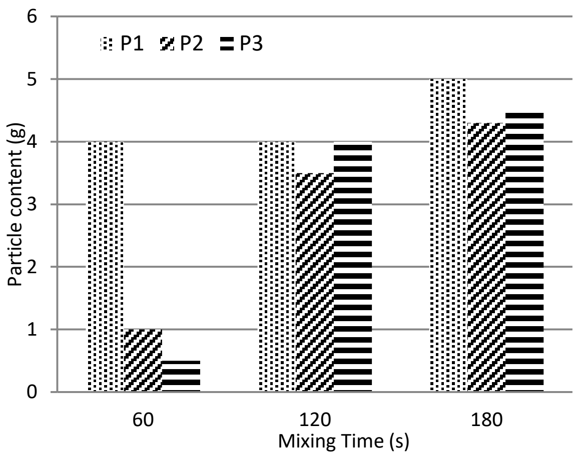

Figure 6. Particle content from discharge valves at the different times after start

The existence of baffle at the interior wall of mixer body has a vital role in mixing performance. As illustrated in Fig. 7, in case of without baffle, the non-homogeneity is clear. By mounting four baffles in mixer wall the significant improvement in mixing performance is observe and clearly homogenous flow is provided in mixer.

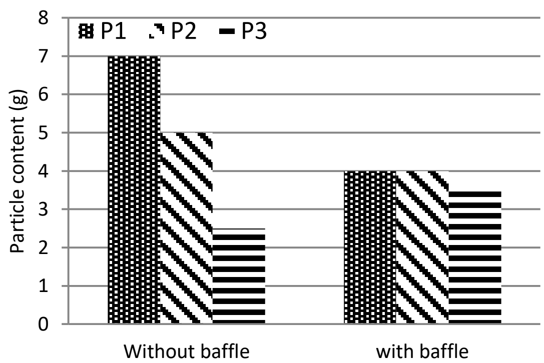

Figure 7. Effect of baffle on mixer performance

5. Conclusions

The mixer performance is important in overall rate of production in mineral complexes. The effect of influencing parameters would help the designers to have appropriate parameter selection for optimal performance. In the present work, a laboratory mixer was designed in which the performance influencing parameters including main shaft speed, number of impeller sets, impeller angle and interior baffles could be altered. Results showed that the low shaft speed provides non-homogenous mixing and by increasing the speed, the improvement was significant however, the more speed increment did not result in higher improvement. The zero impeller angle provided a non-appropriate slurry mix and changing the angle to 30^o or 45^o gavebetter results. The baffles had undeniable positive role in providinghomogenous mixing slurry in mixer. Two impeller sets instead of single impeller set provided turbulent flow in all positions in main body of mixer and helped to provide homogenous flow.

References

[1] Weetman RJ, Gigas B. Mixer mechanical design-fluid forces. InProceedings of the 19th international pump users symposium 2002. Texas A&M University. Turbomachinery Laboratories.

[2] Dickey DS, Fasano JB. Mechanical design of mixing equipment. Handbook of Industrial Mixing: Science and Practice. 2004:1247-332.

[3] Hobbs DM, Muzzio FJ. Reynolds number effects on laminar mixing in the Kenics static mixer. Chemical Engineering Journal. 1998 Jun 1;70(2):93-104.

[4] Tanguy PA, Thibault F, Brito-De La Fuente E, Espinosa-Solares T, Tecante A. Mixing performance induced by coaxial flat blade-helical ribbon impellers rotating at different speeds. Chemical Engineering Science. 1997 Jun 1;52(11):1733-41.

[5] Halidan M, Chandratilleke GR, Dong KJ, Yu AB. Mixing performance of ribbon mixers: Effects of operational parameters. Powder Technology. 2018 Feb 1;325:92-106.

[6] Gijón-Arreortúa I, Tecante A. Mixing time and power consumption during blending of cohesive food powders with a horizontal helical double-ribbon impeller. Journal of Food Engineering. 2015 Mar 1;149:144-52.

[7] Zamiri A, Chung JT. Numerical evaluation of turbulent flow structures in a stirred tank with a Rushton turbine based on scale-adaptive simulation. Computers & Fluids. 2018 Jul 15;170:236-48.

[8] Ng KC, Ng EY. Laminar mixing performances of baffling, shaft eccentricity and unsteady mixing in a cylindrical vessel. Chemical Engineering Science. 2013 Dec 18;104:960-74.

[9] Busciglio A, Grisafi F, Scargiali F, Brucato A. Mixing dynamics in uncovered unbaffled stirred tanks. Chemical Engineering Journal. 2014 Oct 15;254:210-9.

[10] Thomas DG. Heat and momentum transport characteristics of non-Newtonian aqueous thorium oxide suspensions. AIChE Journal. 1960 Dec;6(4):631-9.

[11] Torotwa I, Ji C. A Study of the Mixing Performance of Different Impeller Designs in Stirred Vessels Using Computational Fluid Dynamics. Designs. 2018 Mar 8;2(1):10.

[12] Holm P. Effect of impeller and chopper design on granulation in a high speed mixer. Drug Development and Industrial Pharmacy. 1987 Jan 1;13(9-11):1675-701.

JJMIE

Volume 13, Number 4, December. 2019
ISSN 1995-6665
Pages 247 - 251

Jordan Journal of Mechanical and Industrial Engineering

A New High Accuracy Mathematical Approximation to the Cumulative Normal Density Function

[a]Atif Alkhazali, [b]Mohammad Al-Rabayah, [a]Mohammad M. Hamasha

[a]Department of Industrial Engineering, The Hashemite University, Az Zarqa 13133, Jordan
[b]College of Electrical Engineering, American University of the Middle East, Eqaila, Kuwait

Received 1 July. 2019

Abstract

This paper develops two approximations to the normal cumulative distribution function. Although the literature is rich in approximation functions for the normal distribution, they are not very accurate. This proposed approximation is an enhanced logistic cumulative function approximation to the normal cumulative distribution function. The paper starts with approximating the logistic function to the normal distribution and then introduces a second term to the first approximation to increase the accuracy. Besides the simplicity of the introduced model, it has a maximum error of less than 0.0012 for the entire range. This level of accuracy is superior if compared to other introduced models by other authors. The current can be used to estimate the normal distribution based probabilities and associated statistics. The deviation of the proposed model from the actual normal cumulative distribution with Z score is discussed at the end of this paper.

Keywords: Normal distribution, logistic function, normal cumulative distribution, approximation;

1. Introduction

The normal distribution is one of the most important continuous probability distribution functions used in the field of engineering and science. This is due to the fact that many natural phenomena can be accurately described using this distribution, and that the error measurements follow the normal distribution in theory. Further, the normal distribution is important in predicting solutions in many engineering fields such as heat flow, operations research, mechanics, quality engineering, and reliability engineering.

The normal distribution density function with mean of μ and standard deviation of σ is addressed in equation (1)

$$f(x) = \frac{1}{\sigma\sqrt{2\pi}} e^{-\frac{(x-\mu)^2}{2\sigma^2}} \quad (1)$$

The normal distribution density function with μ=0 and σ=1 is referred by standard normal distribution as addressed in equation (2)

$$\emptyset\,(z) = \frac{1}{\sqrt{2\pi}} e^{-\frac{z^2}{2}} \quad (2)$$

The normal distribution can be transferred into standard normal distribution to be handled by the popular z-table using the transformation formula (i.e., Equation 3).

$$z = \frac{x-\mu}{\sigma} \quad (3)$$

In statistics, the distribution cumulative density function is the probability that the selected random value is equal or less than specific value *c*, or in other words, P(X<c). For the normal distribution, the cumulative distribution function is a complex integral function and usually denoted with the capital Greek letter, Φ as in the Equation (4).

$$\Phi(z) = \frac{1}{\sqrt{2\pi}} \int_{-\infty}^{z} e^{-t^2/2} dt \quad (4)$$

Unfortunately, the above integral cannot be solved into a closed-form formula, and the results of this integral are usually found using calculators, Excel spreadsheets, as well as the popular z- table. One practical problem arises when using such tables, is that those tables only provide the cumulative probabilities for certain discrete values of z. In many scenarios, the required z value will not be available on the table, and therefore, the value will be approximated using adjacent z values.

In order to overcome this practical problem, many researchers have proposed a number of approximate functions for the cumulative normal distribution. However, many proposed approximate functions are either mathematically complicated and lack accuracy, or not valid for the entire range of z values. This paper proposes an enhanced logistic cumulative function approximation to the normal cumulative distribution function. Besides the simplicity of the introduced model, it has a maximum error of less than 0.0012 for the whole range, [-∞:∞].

This paper is organized as follows: In Section 2, a literature review on similar approximate functions with

* Corresponding author e-mail: atif@hu.edu.jo

the introduced one is conducted. Section 3 discusses our proposed model and shows our findings, and finally, section 4 provides a short conclusion on our work.

2. Review of Previous Work

Many proposed approximation functions of normal density are introduced in the literature. However, we can gather these approximations into two main types: approximation based on numerical algorithms and Ad-hoc approximations [1]. This section presents a historical review of different proposed approximations of the cumulative normal distribution function. The results of this review are summarized in Table 1.

Table 1. Summary of approximate functions of the cumulative normal distribution.

Author(s)	Year	Approximate Function
Yerukala and Boiroju [2]	2015	$\Phi(z) \approx 1 - \dfrac{\exp\left(-z^2/2\right)}{\left(\frac{44}{79} + \frac{8}{5}z + \frac{5}{6}\sqrt{z^2+3}\right)}$
Choudhury [3]	2014	$\Phi(z) \approx 1 - \dfrac{1}{\sqrt{2\pi}} \dfrac{e^{\frac{-z^2}{2}}}{0.226 + 0.64z + 0.33\sqrt{z^2+3}}$
Yerukala [4]	2012	$\Phi(z) \approx \begin{cases} 0.46375418 + 0.065687194 H_{11} - 0.602383931 H_{12} & ;0 \le z \le 3.6 \\ 1 & ;z > 3.6 \end{cases}$
Aludaat and Alodat [5]	2008	$\Phi(z) \approx 0.5 + 0.5\sqrt{1 - e^{-\sqrt{\frac{\pi}{8}}z^2}}$
Bryc [6]	2002	$\Phi(z) \approx \dfrac{z^2 + a_1 z + a_2}{\sqrt{2\pi}\, z^3 + b_1 z^2 + b_2 z + 2a_2} e^{\frac{-z^2}{2}}$
Waissi and Rossin [7]	1996	$\Phi(z) \approx \dfrac{1}{1 + \exp\left(-\sqrt{\pi}\left(0.9z + 0.0418198z^3 - 0.0004406z^5\right)\right)}$
Lin [8]	1990	$\Phi(z) \approx 1 - \dfrac{1}{1 + e^{y}}$
Norton [9]	1989	$\Phi(z) \approx \begin{cases} 1 - 0.5e^{-\left(\frac{z^2 + 1.2z^{0.8}}{2}\right)} & ;0 \le z \le 2.7 \\ \frac{1}{\sqrt{2\pi}\, z} e^{-\frac{z^2}{2}} & ;z > 2.7 \end{cases}$
Lin [10]	1989	$\Phi(z) \approx 1 - 0.5\left(e^{-0.717z - 0.416z^2}\right)$
Hammakar [11]	1978	$\Phi(z) \approx 1 - 0.5\left\{1 - \left(1 - e^{-y^2}\right)^{0.5}\right\}$
Hart [12]	1966	$\Phi(z) \approx 1 - \dfrac{e^{\frac{-z^2}{2}}}{\sqrt{2\pi}\, z}\left(1 - \dfrac{\frac{\sqrt{1+bz^2}}{1+az^2}}{P_0 z + \sqrt{P_0^2 z^2 + e^{\frac{-z^2}{2}} \frac{\sqrt{1+bz^2}}{1+az^2}}}\right)$
Zelen and Severo [13]	1964	$\Phi(z) \approx 1 - \left(a_1 t - a_2 t^2 + a_3 t^3\right)\left(\dfrac{e^{\frac{-z^2}{2}}}{\sqrt{2\pi}}\right)$
Tocher [14]	1963	$\Phi(z) \approx \dfrac{e^{2kz}}{1 + e^{2kz}}$, where $k = \sqrt{\dfrac{2}{\pi}}$
Hart [15]	1957	$\Phi(z) \approx \dfrac{1}{\sqrt{2\pi}}\left\{\dfrac{e^{\frac{-z^2}{\pi}}}{z + 0.8e^{-0.4z}}\right\}$
Cadwell [16]	1951	$\Phi(z) = 1/2\left[1 + \left\{1 - \exp\left(\frac{-2z^2}{\pi} - \frac{2(\pi-3)z^4}{3\pi^2}\right)\right\}^{1/2}\right]$
Polya [17]	1945	$\Phi(z) \approx \dfrac{1}{2}\left\{1 + \left(1 - e^{\frac{-2z^2}{\pi}}\right)^{\frac{1}{2}}\right\}$

Most of the above-mentioned models have an accuracy range from 0.01 to 0.001.

3. Proposed Model

The proposed model uses the logistic function to build the first term of our approximation. The logistic function is a continuous probability density function that shares the normal distribution in the shape (i.e., bell shape with symmetry about the mean). However, it has heavier tails (higher kurtosis). Equations (5) and (6) represent the logistic density and cumulative logistic functions, respectively.

$$f(z) = \frac{e^{-\frac{z-\alpha}{\beta}}}{\beta\left(1+e^{-\frac{z-\alpha}{\beta}}\right)^2}, -\infty < z < \infty \quad (5)$$

$$F(z) = \frac{1}{1+e^{-\frac{z-\alpha}{\beta}}}, -\infty < z < \infty \quad (6)$$

The best cumulative logistic approximation to the cumulative normal distribution can be achieved with using the ratio α/β of 1.702. See Equation (7). Figure 1 shows the deviation between the logistic cumulative function and the cumulative normal distribution of at α/β = 1.702. In spite of the best approximation we achieved, the error is significant and cannot be used as a good approximate without modification. The best logistic approximation to the normal distribution is shown in Equation (8). These introduced approximations are very simple compared with any other approximations, and the accuracy level is very acceptable for most engineering and science applications.

$$\Phi_1(z) \approx \frac{1}{1+e^{-1.702z}}, -\infty < z < \infty \quad (7)$$

$$\emptyset(z) \approx \frac{1.702e^{-1.702z}}{(1+e^{-1.702z})^2}, -\infty < z < \infty \quad (8)$$

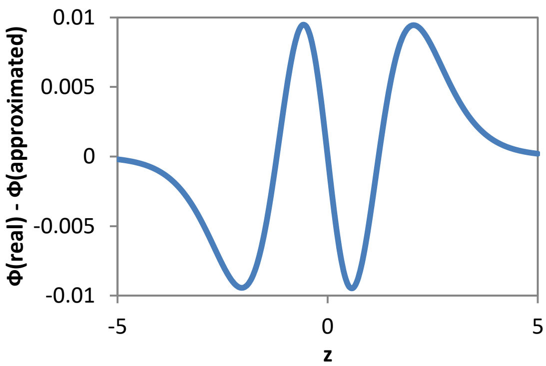

Figure 1. The deviation of best fit logistic cumulative function to the cumulative normal distribution.

The previous approximation can be enhanced to be a more accurate approximation. We noticed that the shape of deviation vs. z curve can be approximated in the middle with a damped negative sign wave. with discarding the value of sign wave (deviation) over the range of -2 to 2, we significantly reduce, as addressed in Equation (9).

$$\Phi_2(z) = \frac{1}{1+e^{-1.702z}} - 0.0095\sin(2.5z)\, e^{-0.01z^2} \quad -\infty \le z \le \infty \quad (9)$$

Although the approximation is very good at -2<z<2, the deviation is high outside of this region, as shown in Figure 2. Therefore, we developed a separate second term to be discarded from the best-fit logistic function for the region (-∞<z<-2 and 2<z<∞). The final approximation is addressed in Equation (10).

$$\Phi_3(z) \cong \begin{cases} \dfrac{1}{1+e^{-1.702z}} - 0.0095\sin(2.5z)\, e^{-0.01z^2}, |z| \le 2 \\ \dfrac{1}{1+e^{-1.702z}} + 10^{-3}(0.2656|z|^5 - 5.197|z|^4 + 39.81|z|^3 - 147.6|z|^2 + 258.64|z| - 163.3), |z| \ge 2 \end{cases} \quad (10)$$

The deviation between the introduced model results and real standard normal cumulative distribution results with Z score is shown in Figure3. The maximum absolute deviation is 0.0012 at z=1.1 and z=-1.1.

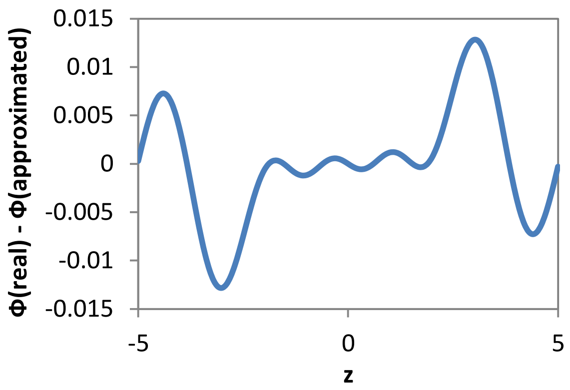

Figure 2. The deviation of Equation (9) cumulative density function approximation from the actual values.

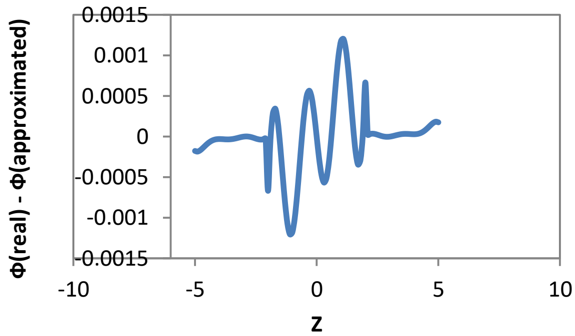

Figure 3. The deviation of Equation (10) cumulative density function approximation from the actual values.

The proposed approximate function is competitive compared to the cumulative logistic approximation function, as well as to other different proposed approximation functions. Such comparison is shown in Table 2.

Table 2. Illustration of the proposed model accuracy compared to cumulative logistic function and other approximation functions accuracies in term of the deviation approximation from the actual values.

Z	Φ(Introduced)	Logistic	Cadwell	Lin 1988	Lin 1989	Lin 1990	Bryc
-4	2.96098E-05	0.00107201	3.08567E-05	3.06079E-05	4.86714E-06	5.62865E-06	1.03553E-05
-3.8	3.24454E-05	0.001478192	6.8885E-05	6.84348E-05	8.35073E-06	7.42694E-06	2.77357E-05
-3.6	3.37333E-05	0.002018822	0.000146014	0.000145852	1.3289E-05	7.86377E-06	6.97113E-05
-3.4	2.65647E-05	0.002721472	0.000292592	0.000295512	1.93103E-05	5.26687E-06	0.000164983
-3.2	1.24453E-05	0.00360615	0.000551839	0.000567549	2.48944E-05	1.69102E-06	0.000368331
-3	7.1871E-08	0.004673872	0.000975503	0.001030156	2.66901E-05	1.22292E-05	0.000776305
-2.8	4.28237E-07	0.005890706	0.001610124	0.001761942	1.91451E-05	2.09886E-05	0.001544627
-2.6	1.39324E-05	0.007169	0.002473075	0.002831687	4.7625E-06	1.61284E-05	0.002899789
-2.4	3.23402E-05	0.008350522	0.003524086	0.004265179	5.05495E-05	1.93149E-05	0.005131209
-2.2	3.38921E-05	0.009199975	0.004645573	0.006006956	0.000115869	9.90841E-05	0.00854618
-2	0.000667975	0.009420556	0.005647979	0.007893744	0.000180436	0.000215536	0.013373235
-1.8	0.000286853	0.008703622	0.006309427	0.009659229	0.000193979	0.000313553	0.019615519
-1.6	0.000189019	0.006818886	0.006442876	0.010981261	6.73163E-05	0.000267983	0.026884312
-1.4	0.000469301	0.003737062	0.005967099	0.011564025	0.000324296	0.000112152	0.034274623
-1.2	0.001074377	0.000247096	0.004950418	0.011228747	0.001113512	0.001024159	0.040363059
-1	0.001177894	0.00445102	0.003603905	0.009978327	0.00237755	0.002543438	0.04339849
-0.8	0.000708202	0.007875015	0.002220613	0.008009102	0.004034403	0.004457013	0.041718158
-0.6	1.72474E-05	0.009459397	0.001080216	0.005663014	0.005707264	0.006146993	0.03437842
-0.4	0.00051429	0.008495484	0.000354031	0.003336229	0.006583897	0.006635908	0.021986536
-0.2	0.000475254	0.005027975	4.69985E-05	0.001375983	0.005314561	0.004846699	0.007844134
0	0	0	0	0	0	0	9.39381E-09
Maximum Absolute error	0.001177894	0.009459397	0.006442876	0.011564025	0.006583897	0.006635908	0.04339849

4. Potential Application of the Model

The normal distribution can describe the probability (uncertainty) of many surrounding of engineering measurements. It, for example, describes the uncertainty of barometric pressure. If the engineer has not the proper device to measure the pressure, he/she can guess center of a normal distribution from the previous data and he/she would know estimate the pressure. With the current model, he/she can approximate the result mathematically with a very close result. The deviation of the model result approximation from the actual values is not noticeable for all engineering application. Furthermore, the normal distribution fits many human performance variations. For example, the commonly IQ is normally distributed and can estimated using the current model. The central limit theorem puts the normal curve as most important continuous distribution. This is besides the fact that many data are very accurately described with normal distribution.

The normal distribution is very popular in the research. In this regard, we find more than 6.5 million published papers on google scholar dealing with normal distribution in various fields. Further, there are 13 papers in Jordan journal of mechanical and industrial engineering handling the normal distribution [18-30].

As practical example, our model will be applied on a selected case study from Jordan Journal of Mechanical and Industrial Engineering. Aljebory and Alshebeb [19] discussed a case study of statistical process control of a chemical product. Figure 4 is a snap shot of $\bar{X}$ control chart for the pH of that product. Assuming a shift happen in the Phase II from $\bar{X} = 9.26$ to $\bar{X} = 10$, we can expect the average run length to detect the shift or, in other words, the number of subgroups required to detect the shift, as follows.

$$3\sigma_{\bar{X}} = 10.278 - 9.26 = 1.018$$

$$\sigma_{\bar{X}} = 0.339$$

$$Shift = 10 - 9.26 = 0.74$$

$$Shift\ in\ term\ of\ \sigma_{\bar{X}} = \frac{0.74}{0.339} = 2.18$$

$$\beta = \Phi(\mathrm{L} - \mathrm{K}) - \Phi(-\mathrm{L} - \mathrm{k}) \cong \Phi(0.82)$$

By using our model, Φ(0.82)=0.79312, which is very close to the actual number 0.7938

Furthermore, the average run length to detect the shift (ARL_1) equals to1/(1- β)=0.79 using the model and it is almost the same actual value.

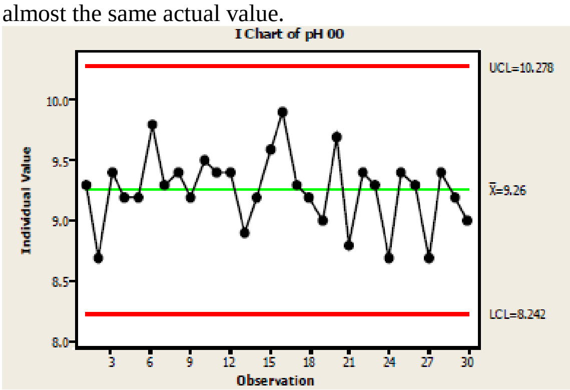

Figure 4. $\bar{X}$ control chart for a chemical product discussed in [19]

The normal distribution occupied a wide area of probability and statistics science. As well known, the probability and statistics is a major area in the industrial and systems engineering, and indeed, it is the background of other major areas of industrial and systems engineering.

5. Conclusion

In this paper, an approximation to the cumulative distribution function is proposed. The best approximation of logistic function to the normal distribution CDF is found. Then, a second part is added to the logistic function approximation to increase the accuracy to reach better accuracy level compared with other introduced models. A numerical comparison shows that our approximation is very accurate with a maximum absolute error of 0.0012 for the entire region.

References

[1] Matic, R. Radoici, D.“Stefanica, A sharp Pólya-based approximation to the normal cumulative distribution function”, Applied Mathematics and Computation,Vol. 322, 2018, 111–122.

[2] R. Yerukala, N. Boiroju,“Approximation to standard normal distribution function, International journal of Scientific and engineering research”, International Journal of Scientific and Engineering Research, Vol. 6, 2015, 515-518.

[3] Choudhury,“A simple approximation to the area under standard normal curve”, Mathematical statistics,Vol. 2, 2014, 147-149.

[4] R. Yerukala, “Functional approximation using neural networks”, Thesis, Department of Statistics. Osmania University, Hyderabad, Telangana, India.2012.

[5] K.M. Aludaat, M.T. Alodat,“A note on approximating the normal distribution function”, Applied Mathematical Science,Vol. 2, 2008, 425-429.

[6] W. Bryc, “A uniform approximation to the right normal tail integral”, Applied Mathematics and Computation,Vol. 127, 2002, 365-374.

[7] G.R. Waissi, D.F. Rossin, “A sigmoid approximation of the standard normal integral”,Applied Mathematics and Computation,Vol. 7, 1996, 91-95.

[8] J.T. Lin,“A simpler logistic approximation to the normal tail probability and its inverse”,Journal of the Royal Statistical Society, Series C,Vol. 39, 1990, 255-257.

[9] R.M. Norton,“Pocket-calculator approximation for area under the standard normal curve”, American Statistician,Vol. 43, 1989, 0-1.

[10] J.T. Lin,“Approximating the normal tail probability and its inverse for use on a pocket-calculator”,Journal of the Royal Statistical Society, Series C, 38, 1989, 69-70.

[11] H.C. Hammakar,“Approximating the cumulative normal distribution and its inverse”,Applied Statistics, Vol. 27, 1978, 76-77.

[12] R.G. Hart,“A close approximation related to the error function (in Technical Notes and Short Paper)”, Mathematical Computation, Vol. 20, 1966, 600-602.

[13] M. Zelen, N.C. Severo,“Probability function in handbook of mathematical functions”,Dover, New York, pp. 925-995, 1981.

[14] K.D. Tocher,“The art of simulation”. English University Press. London. 1963.

[15] R.G. Hart,“A formula for the approximation of definite integrals of the normal distribution function”, Tables and other Aids to Computation, Vol. 11, 1957, 265-265.

[16] J.H. Cadwell“The Bivariate Normal Integral”, Biometrika, 38, 1951, 475-479.

[17] G. Polya,“Remarks on computing the probability integral in one and two dimensions”, 1st Berkeley Symposium on Mathematical Statistics and Probability, 1945,63-78.

[18] B.C. M. Reddya, K. H. Reddyb , C. N. Muni Reddy, K.V. K. Reddy,“Quota Allocation to Distributors of the Supply Chain under Distributors' Uncertainty and Demand Uncertainty by Using Fuzzy Goal Programming”, Jordan Journal of Mechanical and Industrial Engineering,Vol. 2, No. 4, 2008, 215 -226.

[19] K. M. Aljeborya, M. Alshebeb, “Integration of Statistical and Engineering Process Control for Quality Improvement (A Case Study: Chemical Industry - National Chlorine Industries)”, Jordan Journal of Mechanical and Industrial Engineering,Vol. 8, No., 4, 2014, 243 – 256.

[20] P..S. Raoa, C..Ratnam, “Damage Identification of Welded Structures Using Time Series Models and Exponentially Weighted Moving Average Control Charts”, Vol. 4, No.6, 2010, 701 – 710.

[21] M. Alata, W. Masarweh, S. Kamal, “A Fuzzy Monitoring System for an Extrusion Line”,Jordan Journal of Mechanical and Industrial Engineering, Vol. 1, No 1, 2007, 17 – 21.

[22] F. Abdul Moneim, “Expected Delays in Completing Projects under Uncertainty”, Jordan Journal of Mechanical and Industrial Engineering, Vol. 2, No 1, 2008, 65 – 69.

[23] M. Al-Marsumi, “Total Quality Management in the Top Rank of the Dairy Industry in Jordan”, Jordan Journal of Mechanical and Industrial Engineering Mechanical and Industrial Engineering, Vol. 3, No 1, 2009, 47- 58.

[24] M. Al-Ghandoor, M. Samhouri, “Electricity Consumption in the Industrial Sector of Jordan: Application of Multivariate Linear Regression and Adaptive Neuro-Fuzzy Techniques”, Jordan Journal of Mechanical and Industrial Engineering, Vol. 3, No 1, 2009, 69- 76.

[25] V. Raviprakash, A. P. Sidharth, B. Prabu, N. Alagumurthi,“Structural Reliability of Thin Plates with Random Geometrical Imperfections Subjected to Uniform Axial Compression”, Jordan Journal of Mechanical and Industrial Engineering Vol. 4, No 2, 2010, 270- 279.

[26] Neelufur, K. S. Rao, K. V. Subbaiah, “Studies On $\bar{X}$- Control Chart With Pareto In-Control Times for Non Normal Variates”,Jordan Journal of Mechanical and Industrial Engineering, Vol. 4, No 3, 2010, 364 – 371.

[27] P. S. Rao, C. Ratnam, “Damage Identification of Welded Structures Using Time Series Models and Exponentially Weighted Moving Average Control Charts”,Jordan Journal of Mechanical and Industrial Engineering, Vol 4, No 6, 2010, 701 – 710.

[28] S. Prasad, M. M. Sarcar, “Analysis of Face Milling Operation Using Acousto Optic Emission and 3D Surface Topography of Machined Surfaces for In-Process Tool Condition Monitoring”, Jordan Journal of Mechanical and Industrial Engineering, Vol 5, No 6, 2011, 509 – 519.

[29] O. Alsaed , I. S. Jalham, “Polyvinyl Butyral (PVB) and Ethyl Vinyl Acetate (EVA) as a Binding Material for Laminated Glass”,Jordan Journal of Mechanical and Industrial Engineering, Vol 6, No 2, 2012, 127 – 133.

[30] Luo , S. Jing, Xi. Han, Y. Liu, C. Du, “Load Characteristics of Pick Cutting Coal Seams with Coal and Rock Interface”,Jordan Journal of Mechanical and Industrial Engineering,Vol. 10 No 3,2016, 205-210.

JJMIE

Volume 13, Number 4, December. 2019
ISSN 1995-6665
Pages 253 - 264

Jordan Journal of Mechanical and Industrial Engineering

Three-Material Beam: Experimental Setup and Theoretical Calculations

Mohammad A. Gharaibeh[a], Adel A. Ismail, Ahmad F. Al-Shammary, Omar A. Ali

Mechanical Engineering Department, The Hashemite University, Az Zarqa 13133, Jordan

Received 19 August. 2019

Abstract

This paper presents an experimental setup for the evaluation of the lateral deflection of a three-material composite beam subjected to a concentrated force. The three materials used in this setup are steel, aluminum and wood. In this experiment, two layer-bonding methods were considered: glued and bolted. In the glued configurations, the three stacked up layers were attached to each other using glue commercial along the beam length. For the bolted system, the layers were connected using four symmetrically-distributed bolts and nuts. The experimental results of the beam lateral deflections, for both bonding methods, were compared to theoretical computations. Comparison results showed that the glued system deflection data were in better agreement with theory. Also in this paper, the equivalent section method was implemented to solve for the composite beam bending stresses. Finally, the effect of the key geometric and material parameters of the composite beam on the beam bending stress is thoroughly investigated with the emphasis on the structural analysis of electronic assemblies subjected to mechanical bending loading.

Keywords: Three-Material Beams, Electronic Packaging, Experiments, Theory.

1. Introduction

The problem of a beam composed of two or more materials appears in several real-life engineering applications such as the composite beams used in highway and building constructions [1] as well as in electronic packaging industry [2]. For building constructions, composite beams are usually made of concrete slabs that are re-enforced by steel bars joined by mechanical connectors or epoxy resins [3, 4]. In electronics, a typical electronic system consists of a printed circuit board (PCB), an integrated circuit (IC) component both are connected by solder interconnects. The three-material beam problem has been successfully used to model this electronic structure [5]. For this problem, several elasticity solutions were presented and related to the electronic packaging application [6-8]. For experimental work, only a few papers were published in the area of the experimental evaluation of composite beam structures [9-11].

A larger scale problem that has been widely studied in the electronic packaging application, is the multi-layer plates. In 2015, Gharaibeh et al. [12] provided an analytical solution based on Ritz method to solve for the natural frequencies, mode shapes and the dynamic response of an elastically-coupled plates system. This analytical model was validated with finite element simulations and with experiments. Hence, this solution was employed to study the effect of the various geometric and material parameters of the electronic system on the stresses, i.e. fatigue performance, of the assembly. This assembly was further expanded to solve for the transient and random vibration responses of electronic structures [13-17].

In addition to electronics application, the composite beam structure is widely used in the microelectromechanical systems (MEMS). Ghadiri et al. [18] investigated the effect of the non-ideal supports on the free vibration of composite beams with spring-mass-damper attachments analytically. The study results showed that the arrangements of the layers of the composite beams as well as the support uncertainty could significantly affect the natural frequencies and the out-of-plane deformations of the composite beam structure. Sari et al. [19] studied the non-linear dynamic response of a composite beam with initial imperfections between the beam layers using the nonlocal elasticity theory. They proved that such type of imperfections have a non-negligible effect on the beam linear as well as nonlinear behaviors.

The objective of this paper is to provide an experimental setup for the evaluation of the lateral deflections of a three-material composite beam subjected to a concentrated point force. In this setup, two methods were used to bond the three layers of the composite structure. The experimentally measured beam deflections were validated with theory. In addition, this paper

* Corresponding author e-mail: mohammada_fa@hu.edu.jo

presented a thorough discussion, based on mechanics of materials analytical solution, on the effect of the key parameters of the composite beam on the structural analysis of electronic assemblies under mechanical bending.

2. Description of the Problem

The three-material beam structure can be defined as a beam consisting of three material layers stacked up and joined together, as shown in Figure 1(a). Specifically, this beam is made of the top layer (layer 1), the middle layer (layer 2) and the bottom layer (layer 3). In the present analysis, the three layers are considered to have identical lengths (L) and widths (b). The top, middle and bottom layers are selected to be ST37 Steel, T6061 Aluminum and commercial wood, respectively. The geometric details and material properties of this structure are listed in Table 1.The beam of the present analysis is considered to beam simply supported at both ends and loaded by a concentrated point force (P) at a distance x from the left end, as shown in Figure 1(b).

Table 1. Geometric and material properties of the three-material beam.

Beam layer #	**Material**	**Thickness**	**Width**	**Length**	**Elastic Modulus**
Top (1)	ST37 Steel	$h_1 = 10\ mm$			$E_1 = 200\ GPa$
Middle (2)	T6061 Aluminum	$h_2 = 10\ mm$	$b = 300\ mm$	$L = 1\ m$	$E_2 = 70\ GPa$
Bottom (3)	Wood	$h_3 = 10\ mm$			$E_3 = 13\ GPa$

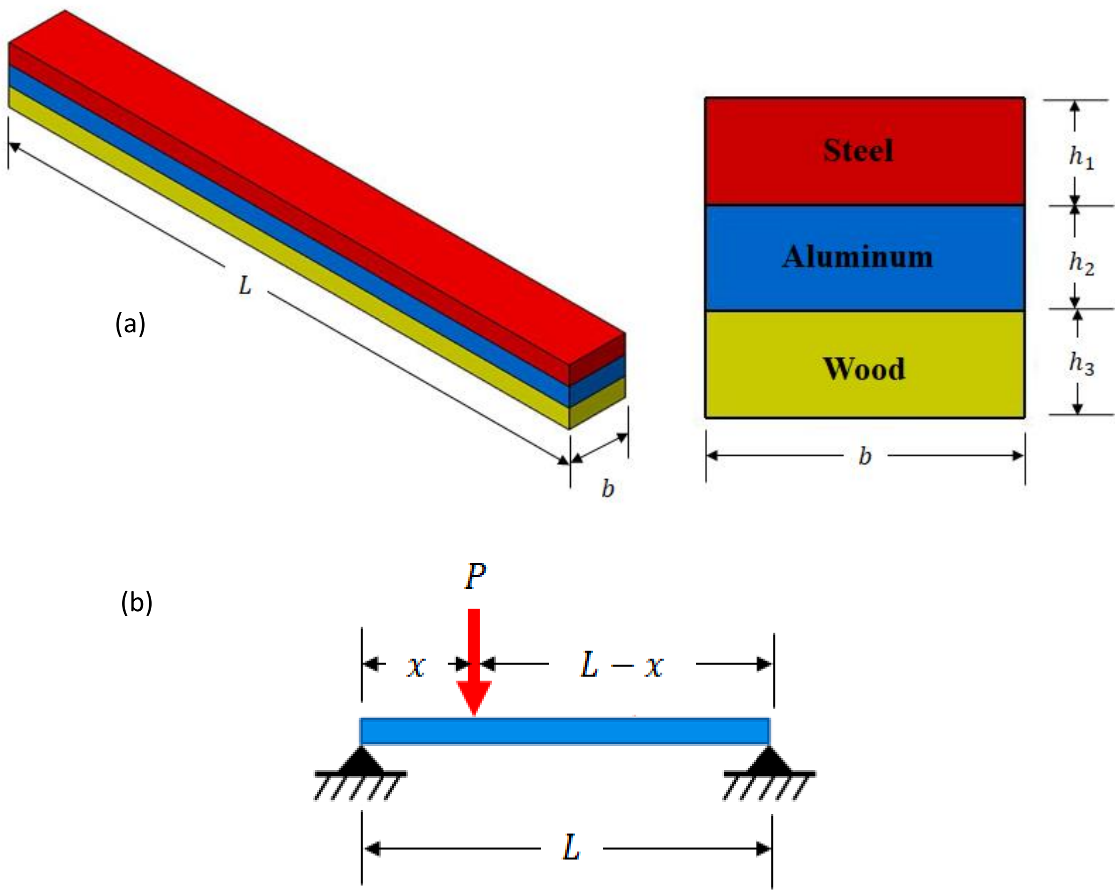

Figure 1. (a) Three-material beam configuration (b) Simply supported beam with point force.

3. Mathematical Modeling

Equivalent section method is a common solution approach used to solve for the bending deflections, strains and stresses of composite beams. The chief assumption of this method is that the axial strain is linearly proportional throughout the beam cross section, irrespective of material. For a three-material composite beam, this method aims to transform an existing two materials to one material with an equivalent cross section. Generally, the width of the stiffer material is increased by the ratio of the elastic moduli to calculate the transformed section moment of inertia. Conversely, the width of the softer material is reduced to provide the equivalent section. In both cases, the thickness of each layer remains unchained due to the previously mentioned assumption. In this paper, the steel and aluminum layers are mathematically transformed to wood. Thus, the ratio between steel and wood (n_1) and aluminum to wood (n_2) elastic moduli are given by

$$n_1 = \frac{E_1}{E_3} \quad (1.a)$$

$$n_2 = \frac{E_2}{E_3} \quad (1.b)$$

Therefore, the width of steel (b_s) and aluminum (b_a) in the transformed section would be

$$b_s = bn_1 \quad (2.a)$$

$$b_s = bn_2 \quad (2.b)$$

Thus, the centroidal axis location measured from the beam bottom ($\bar{y}$) and the moment of inertia about the centroidal axis (I) are given by

$$\bar{y} = \frac{n_1 h_1(0.5h1 + h_2 + h_3) + n_2 h_2(0.5h_2 + h_3) +}{n_1 h_1 + n_2 h_2 + h_3} \quad (3)$$

$$I = b\left(\frac{1}{12} n_1 h_1^3 + n_1 h_1(0.5h_1 + h_2 + h_3 - \bar{y})^2 + \frac{1}{12} n_2 h_2^3 + n_2 h_2(0.5h_2 + h_3 - \bar{y})^2 + \frac{1}{12} h_3^2 + h_3(0.5h_3 - \bar{y})^2\right) \quad (4)$$

Now, the lateral deflection of the beam at the force location $y(x)$ can be easily calculated as

$$y(x) = -\frac{PL^3}{48E_3 I}(3L^2 - 4x^2) \quad (5)$$

Where $0 \le x \le L/2$.

The results of the experimentally measured deflections for different beam configurations will be validated with Eq. (5) above.

4. Experimental Setup

The experimental setup used to measure the composite beam lateral deflection in this work is shown in Figure 2. This setup includes test fixture, beam supports and load application handle as well as the composite beam test piece. The beam lateral deflection was measured using a high accuracy dial gage with a precision of $0.001mm$. Also, the concentrated force was applied by placing masses on the load application handle. Masses (M) of 1, 2, 3 5, 6 and 8 kilograms were used in this experiment. The point force was then calculated using simple equation $\mathrm{P = Mg}$ where g is the gravity acceleration and equal to $9.81\ \mathrm{m/s^2}$. To eliminate the handle effect, the dial gage was zeroed after placing the load application handle on the beam body. The beam deflection was measured at three different locations $x = 200, 300$ and $500\ mm$ while the load is applied on the beam center point ($L/2$). For each test run, three trials were made and then the mean value of the three trials was used as a final data point.

Two beam joining methods were tested in this work; glued and bolted beam configurations. For the glued configuration, the three layers were joined together using a thin layer of ALTECO110 high strength Cyanoacrylate adhesive. Care was taken to ensure equal glue deposition along the beam length. For the bolted system, the beam layers were attached by four symmetrically-distributed bolts and held by washers and nuts.

5. Results and Discussions

5.1. Experimental Results

The experimental results of the previously discussed loading conditions from both beam configurations were collected and compared to theoretical calculations of Eq. (5). The results of this comparison are listed in Table 2 and Table 3.

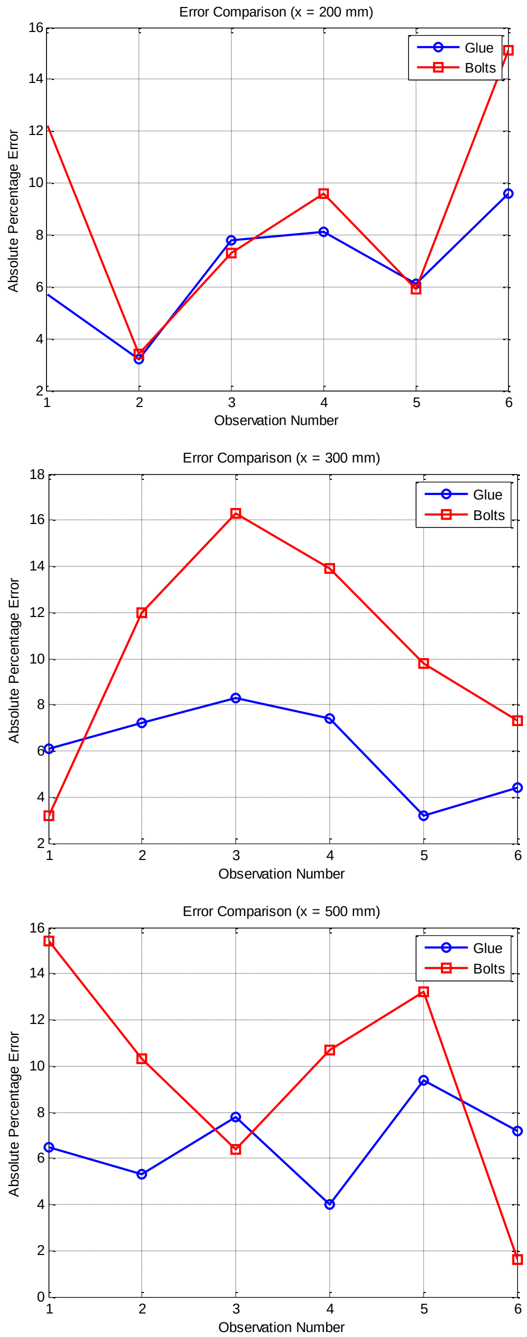

Figure 3. Error comparison between glued and bolted beam configurations for different loading locations.

Table 2. Lateral deflection results for the glued beam configuration.

Observation #	**M (kg)**	**P (N)**	**Experiment (mm)**	**Theory (mm)**	**% Error**
$x = 200mm$					
1	1	9.81	0.032	0.034	5.7
2	2	19.62	0.066	0.068	3.2
3	3	29.43	0.110	0.102	-7.8
4	5	49.05	0.156	0.169	8.1
5	6	58.86	0.216	0.203	-6.1
6	8	78.48	0.245	0.271	9.6
$x = 300mm$					
1	1	9.81	0.044	0.047	6.1
2	2	19.62	0.101	0.094	-7.2
3	3	29.43	0.153	0.142	-8.3
4	5	49.05	0.219	0.236	7.4
5	6	58.86	0.274	0.283	3.2
6	8	78.48	0.361	0.378	4.4
$x = 500mm$					
1	1	9.81	0.056	0.060	6.5
2	2	19.62	0.113	0.119	5.3
3	3	29.43	0.197	0.179	-10.2
4	5	49.05	0.310	0.298	-4
5	6	58.86	0.324	0.358	9.4
6	8	78.48	0.443	0.477	7.2

From both tables, it can be seen that both beam configurations experimental results are in well agreement with theoretical calculations with a percentage error of less than 11% in the glued configuration and less than 17% in the bolted system. However, the errors in the bolted configuration are observed to be higher than those of the glued system. This observation is confirmed in **Figure 3**. This means that the glued system models this problem experimentally better than the bolted system and that is due to the fact that the glue provides very low stiffness along the beam length unlike the high local stiffness at bolts locations in the bolted system.

Figure 2. Experimental setup (a) main frame (b) dial gage.

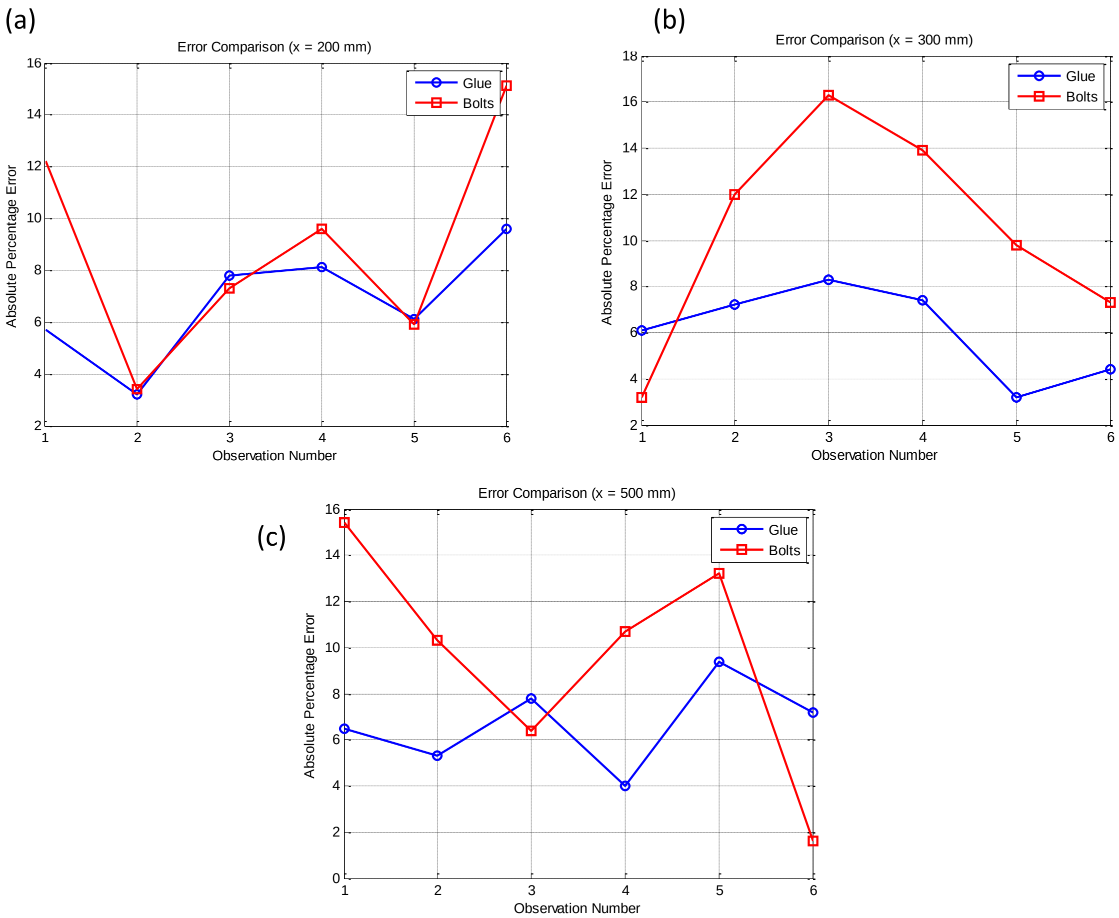

Figure 3. Error comparison between glued and bolted beam configurations for different loading locations.

Table 2. Lateral deflection results for the glued beam configuration.

Observation #	M (kg)	P (N)	Experiment (mm)	Theory (mm)	% Error
$x = 200mm$					
1	1	9.81	0.032	0.034	5.7
2	2	19.62	0.066	0.068	3.2
3	3	29.43	0.110	0.102	-7.8
4	5	49.05	0.156	0.169	8.1
5	6	58.86	0.216	0.203	-6.1
6	8	78.48	0.245	0.271	9.6
$x = 300mm$					
1	1	9.81	0.044	0.047	6.1
2	2	19.62	0.101	0.094	-7.2
3	3	29.43	0.153	0.142	-8.3
4	5	49.05	0.219	0.236	7.4
5	6	58.86	0.274	0.283	3.2
6	8	78.48	0.361	0.378	4.4
$x = 500mm$					
1	1	9.81	0.056	0.060	6.5
2	2	19.62	0.113	0.119	5.3
3	3	29.43	0.197	0.179	-10.2
4	5	49.05	0.310	0.298	-4
5	6	58.86	0.324	0.358	9.4
6	8	78.48	0.443	0.477	7.2

Table 3. Lateral deflection results for the bolted beam configuration.

Observation #	M (kg)	P (N)	Experiment (mm)	Theory (mm)	% Error
$x = 200mm$					
1	1	9.81	0.030	0.034	12.2
2	2	19.62	0.065	0.068	3.4
3	3	29.43	0.109	0.102	-7.3
4	5	49.05	0.153	0.169	9.6
5	6	58.86	0.215	0.203	-5.9
6	8	78.48	0.230	0.271	15.1
$x = 300mm$					
1	1	9.81	0.046	0.047	3.2
2	2	19.62	0.106	0.094	-12.0
3	3	29.43	0.119	0.142	16.3
4	5	49.05	0.269	0.236	-13.9
5	6	58.86	0.256	0.283	9.8
6	8	78.48	0.350	0.378	7.3
$x = 500mm$					
1	1	9.81	0.069	0.060	-15.4
2	2	19.62	0.107	0.119	10.3
3	3	29.43	0.177	0.179	1.3
4	5	49.05	0.330	0.298	-10.7
5	6	58.86	0.405	0.358	-13.2
6	8	78.48	0.470	0.477	1.6

5.2. Stress Analysis

The problem of three-material beam was extensively raised by engineers in electronic packaging industry. Typically, an electronic package consists of three common parts: The printed circuit board (PCB), solder interconnects area array and the integrated circuit (IC) component. Researchers in electronic packaging field, modeled this electronic structure using the three-material beam considering that the PCB is the bottom beam, the solder interconnects layer is the middle and finally the IC component is the top beam. Numerous research studies using elasticity solutions investigated the effect of the geometric and material characteristics of the electronic assembly on solder stresses as they are the most critical design factor. In the case of solder failure, it has been seen that the solder cracks are initiated at the top or the bottom (component and PCB sides, respectively) of the solder. Therefore, it is very important to investigate stress distributions at the both sides of the solder. In this paper, the previously presented method of equivalent section was used to compute the bending-induced solder stresses. Here, the stresses at the interface between the bottom and middle beams (PCB side) as well as between the top and the middle beams (component side) were investigated. Thus, the common bending stress in beams (σ) equation is expressed as:

$$\sigma = \frac{\mathrm{Mc}}{\mathrm{I}} \tag{6}$$

Where M is the bending moment, c is the vertical distance from the equivalent section centroidal axis and I is the moment of inertial of the equivalent section.

In the present analysis, the effect of the ratio between the thickness of the top beam and the thickness of the middle beam (h_1/h_2) and the ratio between the thickness of the bottom beam and the thickness of the middle beam

(h_3/h_2) on the middle beam stresses at interfaces with the top and bottom beams was studies and fully presented. Besides, this work examines the effect of the ratio between the elastic moduli of the top and middle beams (E_1/E_2) as well as the ratio elastic moduli of the bottom and middle beams (E_3/E_2). In electronic packaging words, ratios h_1/h_2 and h_3/h_2 represent the ratios of the thickness of the IC component and PCB to the solder joint standoff height. Also, ratios E_1/E_2 and E_3/E_2 represent the ratios of the elastic moduli of the IC component and PCB to the solder joint elastic modulus.

In the present analysis, Eq. (6) was used to evaluate middle beam interface stresses assuming a unity positive bending moment load $(M = 1)$ and a beam width $(b = 1)$. In this equation, the distance from the centroidal axis to the middle beam top surface is $c = h_2 + h_3 - \bar{y}$ and the distance from the centroidal axis to the middle beam bottom surface is $c = \bar{y} - h_3$. As the equivalent section in the present paper was created to be wood, the resultant stress of Eq. (6) was multiplied by the ratio between the middle beam and bottom beam elastic moduli ratio (n_2).

Figure 4shows the effect of E_1/E_2 on the middle layer top and bottom stresses. For the top surface stresses, the middle layer stresses to be very high for stiff middle layer $(E_1/E_2 \leq 1$). However, for softer layers $(E_1/E_2 \geq 1$), the top surface stress becomes lower and approaches to zero for very high E_1/E_2 ratios. For bottom surface stress, tensile stresses tend to increase as E_1/E_2 increase in the range of $0 \leq E_1/E_2 \leq 2$ at the case of equal elastic moduli of bottom and middle layers $(E_3/E_2 = 1$). For higher E_3/E_2 values, the bottom surface stresses start to be compressive then they transfer to be tensile stress for higher E_1/E_2 ratios. Therefore, it is highly recommended to design an electronic assembly with component to solder elastic moduli ratio between zero and 2 combined with PCB to solder elastic moduli ratio higher than 3.

Figure 5 and Figure 6 represent the effect of E_1/E_2 on the middle layer top and bottom stresses at different h_1/h_2 and h_3/h_2 ratios, respectively. in both cases, middle beam top stresses are observed to be higher for small E_1/E_2 values while they eventually dying out for high ratios. Additionally, bottom surface stresses are very high for a unity h_1/h_2 and h_3/h_2 ratios. Besides, bottom surface stresses are higher in the range of $E_1/E_2 \leq 2$ while much lower stresses appear for high E_1/E_2 configurations. Therefore, this paper recommends the use of electronic packages with component to solder elastic moduli ratio higher than 2 maintained with high component to solder and PCB to solder elastic thickness ratio for lowest bending-induced stresses.

Figure 7- 9 represent the effect of E_3/E_2 on the middle layer top and bottom stresses. From all figures, middle layer top stresses are the highest for E_3/E_2 values between 0 and 2 especially for unity E_3/E_2, h_1/h_2 and h_3/h_2 ratios. Also, top surface stresses are reduced for higher elastic moduli and thickness ratios. For E_3/E_2 values less than 2, bottom surface stress are observed to be very high while they vanish for higher ratiosE_3/E_2. For these reasons, electronic packages with very high component to solder and PCB to solder elastic moduli as well as thickness ratios are highly recommended.

Figure 10 – 15depict the effect of h_1/h_2 and h_3/h_2 ratios on middle beam layer stresses. From Figure 10 - 12, it can be clearly seen that top and bottom surfaces of the middle layer stresses vanish for $h_1/h_2 > 2$ and $h_3/h_2 > 5$ respectively. In contradiction, stress of the middle layer at the top and bottom interfaces vanish for $h_1/h_2 > 5$ and $h_3/h_2 > 2$, respectively, as presented in Figure 13 - 15. Therefore, it is highly recommended to build electronic structures with high component to solder and PCB to solder thickness ratios to ensure lowest mechanical stresses.

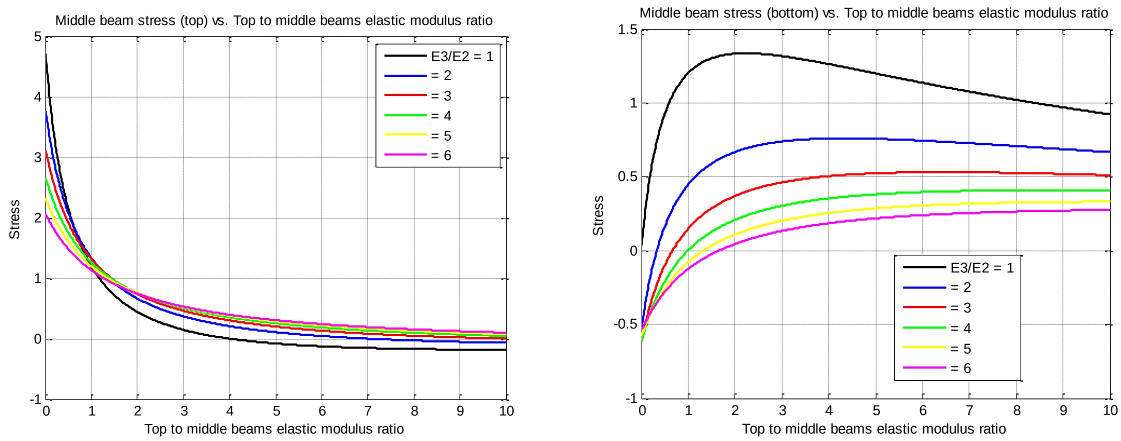

Figure 4. Middle beam stresses at the (left) top and (right) bottom surfaces as a function of top to middle beams elastic moduli ratios (E_1/E_2) at different bottom to middle beams elastic moduli ratios (E_3/E_2).

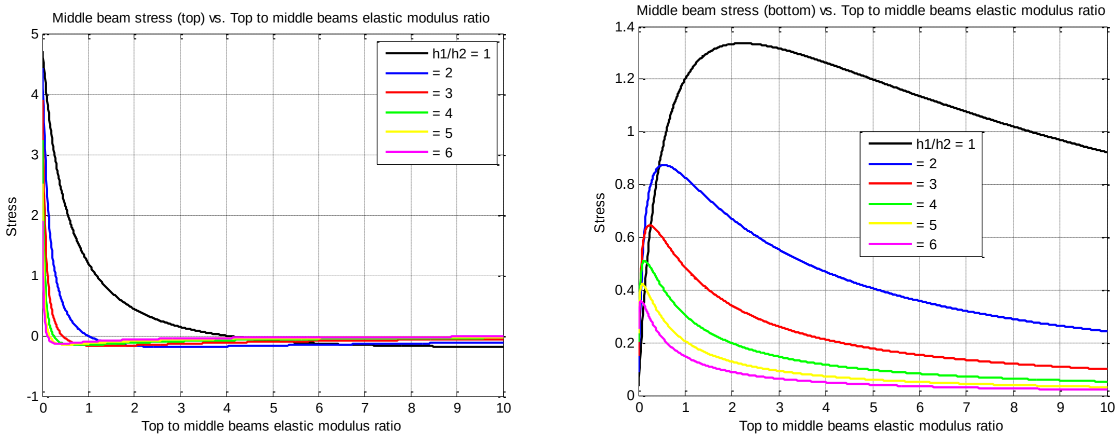

Figure 5. Middle beam stresses at the (left) top and (right) bottom surfaces as a function of top to middle beams elastic moduli ratios (E_1/E_2) at different top to middle beams thickness ratios (h_1/h_2).

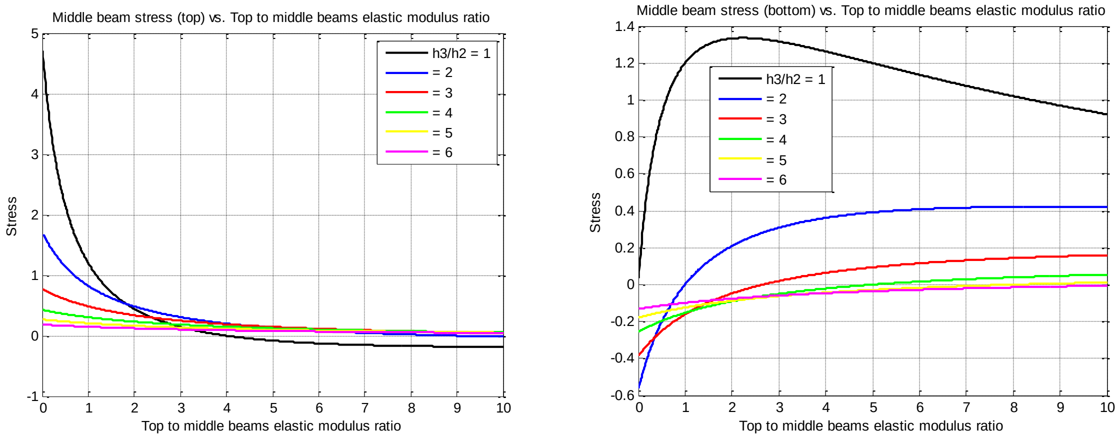

Figure 6. Middle beam stresses at the (left) top and (right) bottom surfaces as a function of top to middle beams elastic moduli ratios (E_1/E_2) at different bottom to middle beams thickness ratios (h_3/h_2).

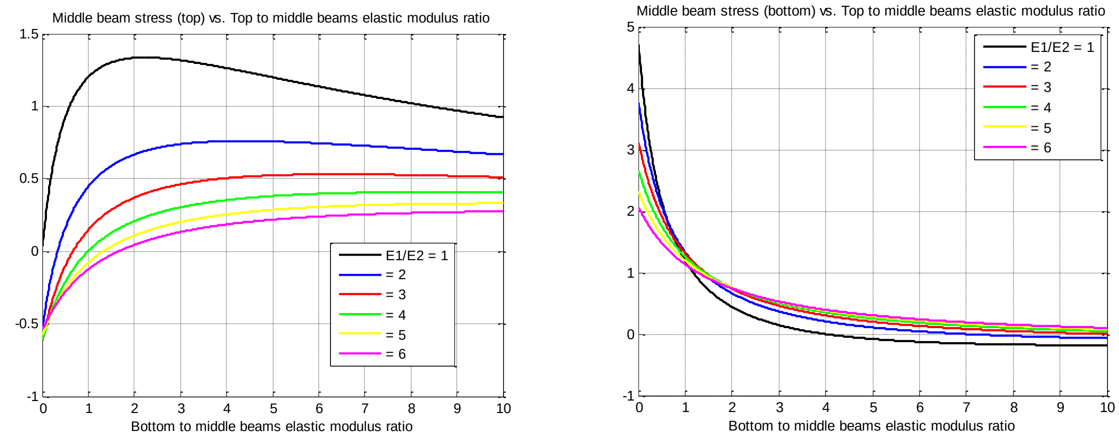

Figure 7. Middle beam stresses at the (left) top and (right) bottom surfaces as a function of bottom to middle beams elastic moduli ratios (E_3/E_2) at different top to middle beams elastic moduli ratios (E_1/E_2).

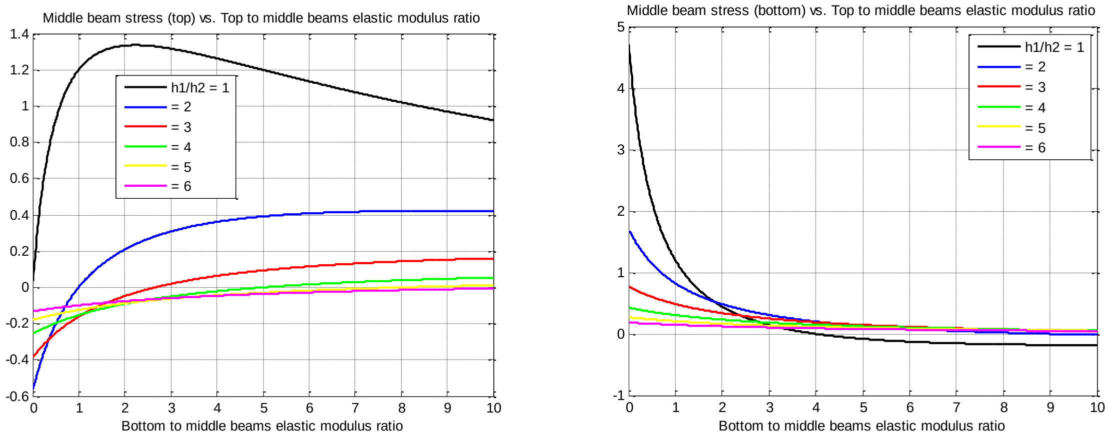

Figure 8. Middle beam stresses at the (left) top and (right) bottom surfaces as a function of bottom to middle beams elastic moduli ratios (E_3/E_2) at different top to middle beams thickness ratios (h_1/h_2).

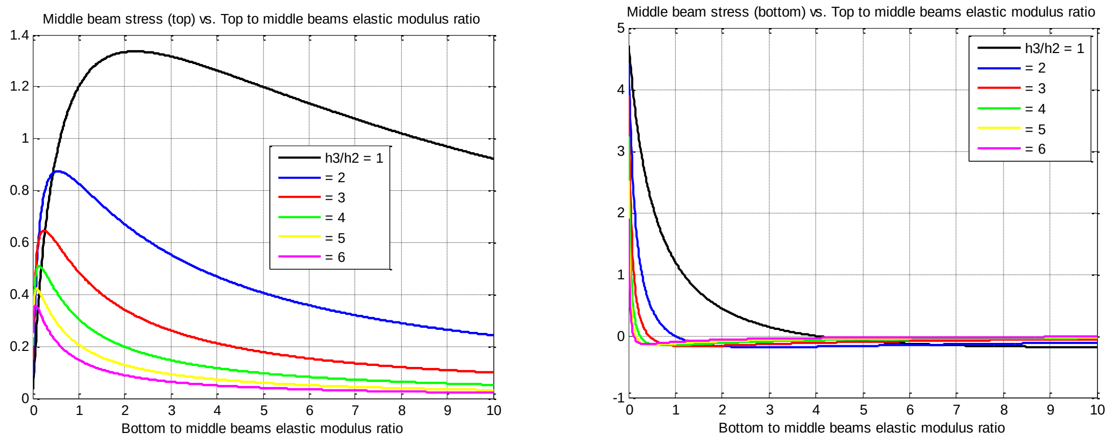

Figure 9. Middle beam stresses at the (left) top and (right) bottom surfaces as a function of bottom to middle beams elastic moduli ratios (E_3/E_2) at different bottom to middle beams thickness ratios (h_3/h_2).

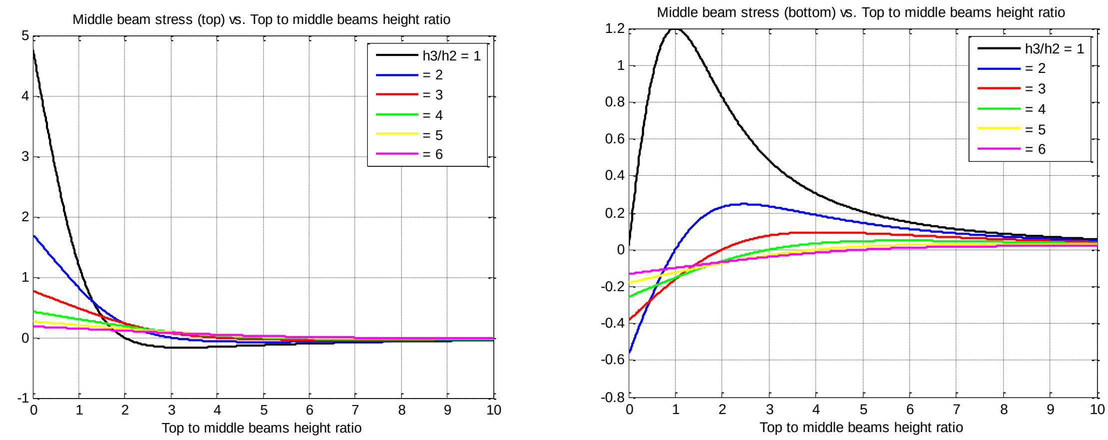

Figure 10. Middle beam stresses at the (left) top and (right) bottom surfaces as a function of top to middle beams height ratios (h_1/h_2) at different bottom to middle beams thickness ratios (h_3/h_2).

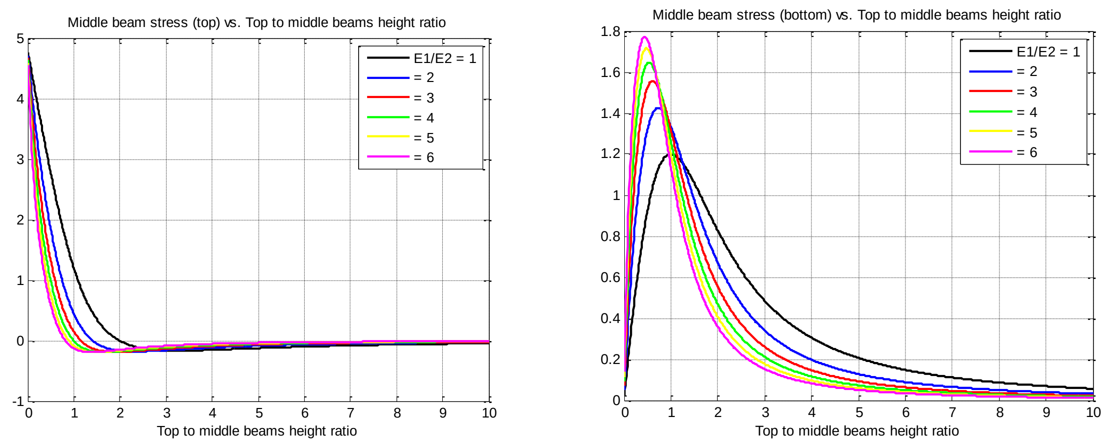

Figure 11. Middle beam stresses at the (left) top and (right) bottom surfaces as a function of top to middle beams height ratios (h_1/h_2) at different top to middle beams elastic moduli ratios (E_1/E_2).

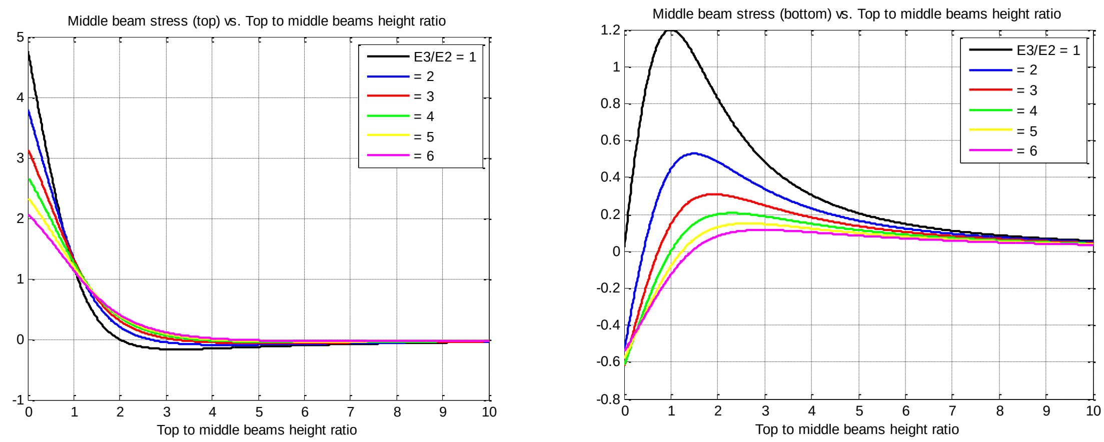

Figure 12. Middle beam stresses at the (left) top and (right) bottom surfaces as a function of top to middle beams height ratios (h_1/h_2) at different bottom to middle beams elastic moduli ratios (E_3/E_2).

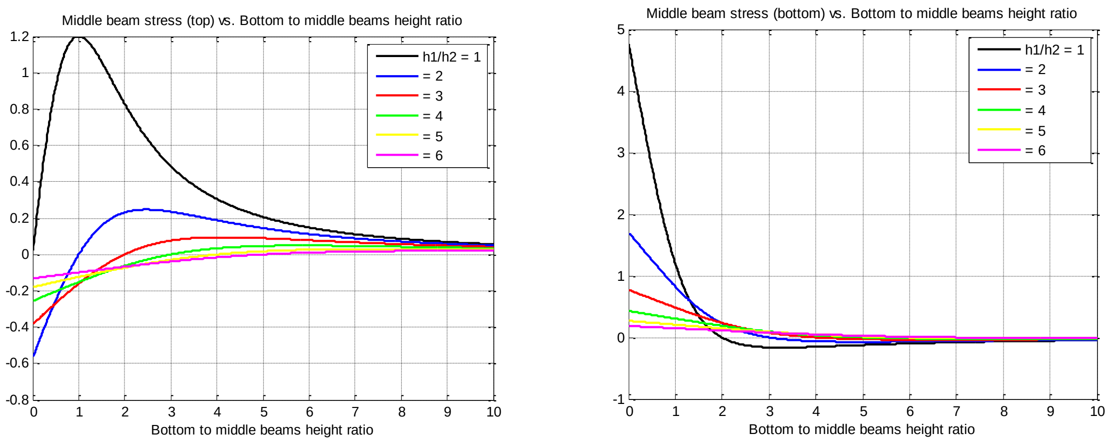

Figure 13. Middle beam stresses at the (left) top and (right) bottom surfaces as a function of bottom to middle beams height ratios (h_3/h_2) at different bottom to middle beams thickness ratios (h_3/h_2).

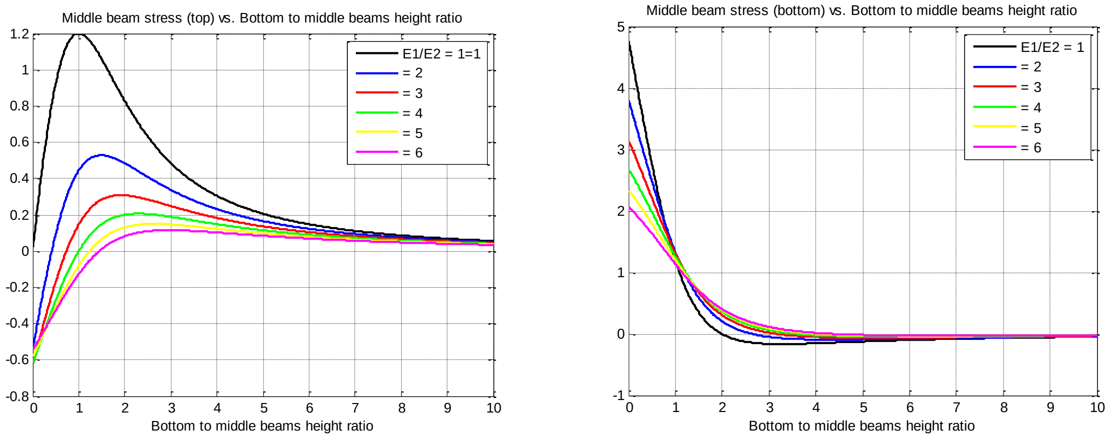

Figure 14. Middle beam stresses at the (left) top and (right) bottom surfaces as a function of bottom to middle beams height ratios (h_3/h_2) at different top to middle beams elastic moduli ratios (E_1/E_2).

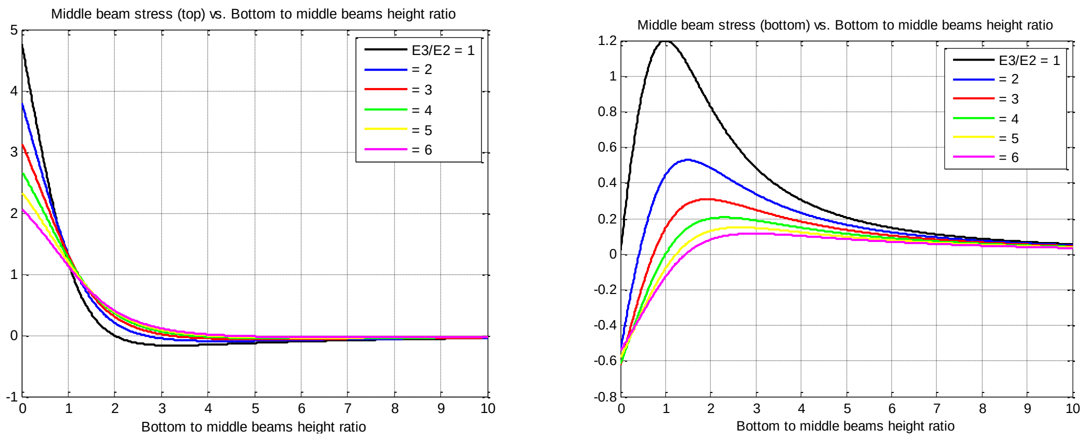

Figure 15. Middle beam stresses at the (left) top and (right) bottom surfaces as a function of bottom to middle beams height ratios (h_3/h_2) at different bottom to middle beams elastic moduli ratios (E_3/E_2).

6. Conclusions

This paper presented an experimental setup for the evaluation of a three-material composite beam lateral deflection. The materials of this beam were selected to be steel, aluminum and wood. Two bonding configurations were considered, glued and bolted. The experimentally measured lateral deflections of the composite beam were compared to theoretical calculations. The comparison showed that glued beam system is in a better agreement with theory than bolted configuration. In addition, the analytical solution of the three-material beam was extended to solve for the middle layer stresses. Finally, the effect of the key parameters of the composite beam on beam stresses is discussed in detail with emphasis on the application of structural analysis of electronic assemblies subjected to mechanical bending.

Acknowledgment

The authors wish to thank the deanship of scientific research at the Hashemite University for providing the necessary tools and funds. In addition, we would like to acknowledge Mr. Ahmad Al-Shorman of the mechanical engineering department of the Hashemite University for his good help throughout this work.

References

[1] Viest, I. M. (1960). Review of research on composite steel-concrete beams. Journal of the Structural Division, 86(6), 1-22.

[2] Suhir, E. (1988). On a paradoxical phenomenon related to beams on elastic foundation: Could external compliant leads reduce the strength of a surface-mounted device?. Journal of applied mechanics, 55(4), 818-821.

[3] Miklofsky, H. A., Brown, M. R., & Gonsior, M. J. (1962). Epoxy bonding compounds as shear connectors in composite beams. Engineering Research Series, 62-2.

[4] Kriegh, J. D., & Endebrock, E. G. (1963). THE USE OF EPOXY RESINS IN REINFORCED CONCRETE--STATIC LOAD TESTS: PART II (No. Final Report No. 2).

[5] Pitarresi, J. M., & Ceurter, J. (1999). Elasticly coupled beams loaded by a point force. In 13th Engineering Mechanics Conference, Baltimore, MD, June (pp. 13-16).

[6] Gharaibeh, M. A., Liu, D., & Pitarresi, J. M. (2017). A pair of partially coupled beams subjected to concentrated force. IEEE Transactions on Components, Packaging and Manufacturing Technology, 7(8), 1293-1304.

[7] Wong, E. H., Mai, Y. W., Seah, S. K., Lim, K. M., & Lim, T. B. (2007). Analytical solutions for interconnect stress in board level drop impact. IEEE transactions on advanced packaging, 30(4), 654-664.

[8] Wong, E. H., & Wong, C. K. (2009). Approximate solutions for the stresses in the solder joints of a printed circuit board

subjected to mechanical bending. International Journal of Mechanical Sciences, 51(2), 152-158.

[9] Stüssi F., Zusammengesetzte Vollwandträger (Composed Beams), International Association for Bridge and Structural Engineering (IABSE), 1947, 8, 249-269

[10] Newmark, N. M. (1951). Test and analysis of composite beams with incomplete interaction. Proceedings of society for experimental stress analysis, 9(1), 75-92.

[11] Lee, P. G., Shim, C. S., & Chang, S. P. (2005). Static and fatigue behavior of large stud shear connectors for steel–concrete composite bridges. Journal of constructional steel research, 61(9), 1270-1285.

[12] Gharaibeh, M. A., Su, Q. T., & Pitarresi, J. M. (2016). Analytical solution for electronic assemblies under vibration. Journal of Electronic Packaging, 138(1).

[13] Gharaibeh, M. A. (2018). Reliability analysis of vibrating electronic assemblies using analytical solutions and response surface methodology. Microelectronics Reliability, 84, 238-247.

[14] Gharaibeh, M. (2018). Reliability assessment of electronic assemblies under vibration by statistical factorial analysis approach. Soldering & Surface Mount Technology.

[15] Gharaibeh, M. A., Su, Q. T., & Pitarresi, J. M. (2018). Analytical model for the transient analysis of electronic assemblies subjected to impact loading. Microelectronics Reliability, 91, 112-119.

[16] Gharaibeh, M. A., & Pitarresi, J. M. (2019). Random vibration fatigue life analysis of electronic packages by analytical solutions and Taguchi method. Microelectronics Reliability, 102, 113475.

[17] Gharaibeh, M. A. (2020). Analytical solutions for electronic assemblies subjected to shock and vibration loadings. In Handbook of Materials Failure Analysis (pp. 179-203). Butterworth-Heinemann.

[18] Ghadiri, M., Malekzadeh, K., & Ghasemi, F. A. (2015). Free Vibration of an Axially Preloaded Laminated Composite Beam Carrying a Spring-Mass-Damper System with a Non-Ideal Support. Jordan Journal of Mechanical & Industrial Engineering, 9(3).

[19] Sari, M. E. S., & Al-Qaisia, A. (2016). Nonlinear Natural Frequencies and Primary Resonance of Euler-Bernoulli Beam with Initial Deflection using Nonlocal Elasticity Theory. Jordan Journal of Mechanical & Industrial Engineering, 10(3).

JJMIE

Volume 13, Number 4, December. 2019
ISSN 1995-6665
Pages 265 - 269

Jordan Journal of Mechanical and Industrial Engineering

The Effect of Temperature on the Stresses Analysis of Composites Laminate Plate

Louay S. Yousuf

Department of Mechanical Engineering, San Diego State University, 5500 Campanile Drive, San Diego, California, 92182-1323, USA

Received 21 August. 2019

Abstract

In this paper, the derivation of analytic formulation of stresses analysis has been done using the theory of classical laminate plate. The method of Navier solution is used in the calculation. The composite laminate plate is exposed to out-off plane temperature. The temperature gradient of thermal shock is varied between (60 C^o and -15 C^o). The analytic results of normal stresses are checked and verified using ANSYS software. The normal stress and strain values are decreased sinusoidal and exponentially with the increasing of aspect ratio and fiber volume fraction respectively under the effect of temperature (60 C^o) along x and y directions. For (-15 C^o), the value of normal strain is decreased with the increasing of fiber volume fraction along x and y directions.

Keywords: Classical Plate Theory, Composite Laminate Plate, Temperature Effect, Stresses Analysis;

Nomenclature

σ_{xx}, σ_{yy}: Lamina Stresses Vector, N/m^2.

$\varepsilon_{xx}^{(0)}, \varepsilon_{yy}^{(0)}$: Extensional strain vector.

$\varepsilon_{xx}^{(1)}, \varepsilon_{yy}^{(1)}$: Bending strain vector.

a,b: Length of large and small span of the rectangular plate respectively, m.

N: Total number of layers.

Q_{ij}: Reduced stiffness elements, N/m^2.

B_{ij}: Extension coupling stiffness elements, N.

D_{ij}: Bending stiffness elements, N.m.

M_{xx}, M_{yy}, M_{xy}: Bending and twisting moments, N.m.

ΔT: Gradient uniform temperature, C^o.

A_1, A_2: Bending moment due to temperature, N.m/C^o.

m,n: Double trigonometric of Furrier series.

u_o, v_o: Mid plane in-plane displacement along x and y directions, m.

w_o : Mid plane deflection along z-direction.

x,y,z: Cartesian coordinate system, m.

z_k, z_{k+1}: Upper and lower lamina surfaces coordinates along z direction, m.

α_1, α_2: Thermal expansion coefficient in longitudinal and lateral directions, 1/C^o.

1. Introduction

The effect of temperature on the thermal stress distribution of composites laminate plate are one of the primary life limiting factors of machinery components. The main contribution of this work is the mismatch of the resin and fiber due to thermal loading through a plate thickness. The mismatch of the composite laminate plate occurs since the matrix shear stress around the fiber could exceed the allowable matrix shear stress or the bond between the fiber and the matrix might be broken, [1]. The application of this work is in reusable launch vehicle, satellite, and rocket engine. Thangaratnam R.K. et al. presented the thermal stresses in cross-ply and angle-ply of laminated plates and shells under the effect of thermal gradients a cross the thickness, [2]. They used semiloof finite element formulation to extend the thermal stress analysis for different boundary conditions taking into consideration the temperature dependence of the material properties. An exact closed-form solutions are presented by Carrera E. et al. using the applications of Ritz method and Finite element method, [3]. Sen F. et al. used ANSYS finite element software to evaluate the thermal stress analysis of symmetric angle-ply laminated thermoplastic composite plates with different square hole dimensions. They selected a uniform temperature such as (50 C^o, 60C^o, 70 C^o, 80 C^o, 90 C^o, and 100 C^o) and examined the effect of increasing uniform temperature on the value of thermal stresses, [4]. Sit M. et al. analyzed laminated composite plates in which is subjected to a constant temperature using third order shear deformation theory. The results of deflection and stresses are validated using ANSYS Ver. 14 based on the first order shear deformation theory. Finite element modeling has been generated using an eight nodes isoperimetric element with seven degrees of freedom per node, [5,6]. Rohwer K. et al. used first order shear

* Corresponding author e-mail: lalroomi@sdsu.edu

deformation theory to determine the transverse shear and normal stresses for any plate under a sinusoidal temperature distribution, [7]. Vnuec Z. performed a numerical analysis of stress and strain values of angle-ply with four symmetric layered of laminated plate, [8]. Moreover EL Moufari and Meryem proposed a several numerical simulation to describe the interaction between thermal and mechanical stresses, [9,10]. In this paper, the effect of temperature on the stresses analysis of composites laminate plate is studied.

2. Equations of Motion In Terms of Displacement

In this paper, classical laminate plate theory represents the three dimensional of experimental stress analysis in two dimensional form using the state of plane stress. For especially orthotropic (that the material axes coincide with respect to laminates coordinates), the stress-strain relation is as below, [11]:

$$\begin{Bmatrix}\sigma_{xx}\\ \sigma_{yy}\\ \sigma_{xy}\end{Bmatrix}^{k} = \begin{bmatrix}Q_{11} & Q_{12} & 0\\ Q_{12} & Q_{22} & 0\\ 0 & 0 & Q_{66}\end{bmatrix} * \left(\begin{Bmatrix}\varepsilon_{xx}\\ \varepsilon_{yy}\\ \gamma_{xy}\end{Bmatrix} - \begin{Bmatrix}\alpha_1\\ \alpha_2\\ 0\end{Bmatrix} * \Delta T\right) \quad (1a)$$

$$\begin{Bmatrix}\varepsilon_{xx}\\ \varepsilon_{yy}\\ \gamma_{xy}\end{Bmatrix} = \begin{Bmatrix}\varepsilon_{xx}^{(0)}\\ \varepsilon_{yy}^{(0)}\\ \gamma_{xy}^{(0)}\end{Bmatrix} + z * \begin{Bmatrix}\varepsilon_{xx}^{(1)}\\ \varepsilon_{yy}^{(1)}\\ \gamma_{xy}^{(1)}\end{Bmatrix} \quad (1b)$$

Where:

$$\{\varepsilon^{(0)}\} = \begin{Bmatrix}\varepsilon_{xx}^{(0)}\\ \varepsilon_{yy}^{(0)}\\ \gamma_{xy}^{(0)}\end{Bmatrix} = \begin{Bmatrix}\dfrac{\partial u_o}{\partial x}\\ \dfrac{\partial v_o}{\partial y}\\ \dfrac{\partial u_o}{\partial y} + \dfrac{\partial v_o}{\partial x}\end{Bmatrix}$$

And;

$$\{\varepsilon^{(1)}\} = \begin{Bmatrix}\varepsilon_{xx}^{(1)}\\ \varepsilon_{yy}^{(1)}\\ \gamma_{xy}^{(1)}\end{Bmatrix} = \begin{Bmatrix}-\dfrac{\partial^2 w_o}{\partial x^2}\\ -\dfrac{\partial^2 w_o}{\partial y^2}\\ -2 * \dfrac{\partial^2 w_o}{\partial x\,\partial y}\end{Bmatrix}$$

The differential laplacian equation of motion for an isotropic thin rectangular plate is as follows:

$$\frac{\partial^2 M_{xx}}{\partial x^2} + 2 * \frac{\partial^2 M_{xy}}{\partial x\,\partial y} + \frac{\partial^2 M_{yy}}{\partial y^2} = 0 \quad (2)$$

The resultant moment including the temperature effects are:

$$\begin{Bmatrix}M_{xx}\\ M_{yy}\\ M_{xy}\end{Bmatrix} = \begin{Bmatrix}M_{xx}^{Mech.}\\ M_{yy}^{Mech.}\\ M_{xy}^{Mech.}\end{Bmatrix} - \begin{Bmatrix}M_{xx}^{Ther.}\\ M_{yy}^{Ther.}\\ M_{xy}^{Ther.}\end{Bmatrix} \quad (3)$$

Where:

$$\begin{Bmatrix}M_{xx}^{Mech.}\\ M_{yy}^{Mech.}\end{Bmatrix} = \begin{bmatrix}B_{11} & B_{12} & 0\\ B_{12} & B_{22} & 0\\ 0 & 0 & B_{66}\end{bmatrix} * \begin{Bmatrix}\dfrac{\partial u_o}{\partial x}\\ \dfrac{\partial v_o}{\partial y}\\ \dfrac{\partial u_o}{\partial y} + \dfrac{\partial v_o}{\partial x}\end{Bmatrix} - \begin{bmatrix}D_{11} & D_{12} & 0\\ D_{12} & D_{22} & 0\\ 0 & 0 & D_{66}\end{bmatrix} * \begin{Bmatrix}\dfrac{\partial^2 w_o}{\partial x^2}\\ \dfrac{\partial^2 w_o}{\partial y^2}\\ 2 * \dfrac{\partial^2 w_o}{\partial x\,\partial y}\end{Bmatrix}$$

And;

$$\begin{Bmatrix}M_{xx}^{Ther.}\\ M_{yy}^{Ther.}\end{Bmatrix} = \sum_{k=1}^{N} \begin{bmatrix}Q_{11} & Q_{12}\\ Q_{12} & Q_{22}\end{bmatrix}^{(k)} * \begin{Bmatrix}\alpha_1\\ \alpha_2\end{Bmatrix}^{(k)} * \int_{z_k}^{z_{k+1}} \Delta T * z \; dz$$

It can be assumed that all layers have the same orientation (Θ =0), and the same thickness in which (B_{ij} = 0). Substitute Eqn.(3) into Eqn. (2) it can be obtained the equation of motion in terms of stiffness bending:

$$D_{11} * \left(\frac{\partial^4 w_o}{\partial x^4}\right) + 2 * (D_{12} + 2 * D_{66}) * \left(\frac{\partial^4 w_o}{\partial x^2\,\partial y^2}\right) + D_{22} * \left(\frac{\partial^4 w_o}{\partial y^4}\right) = -\left(\frac{\partial^2 M_{xx}^{Ther.}}{\partial x^2} + \frac{\partial^2 M_{yy}^{Ther.}}{\partial y^2}\right) \quad (4)$$

3. Calculation of Thermal Stress by Using Navier Solution

The thermal stress is derived based on the solution of classical laminate plate theory using Navier equation taking into consideration the simply supported boundary condition from all edges. It can be assumed that the temperature is varied linearly through the plate thickness, is as below:

$$\Delta T(x, y, z) = z * T_1(x, y) \quad (5)$$

Where:

T_1 is the out-off plane uniform temperature when the heater is in the out-off plane direction.

$$\Delta T(x, y, z) = \sum_{m=1}^{\infty} \sum_{n=1}^{\infty} T_{mn}(z) * \sin(\alpha_m * x) * \sin(\beta_n * y) \quad (6)$$

Equation (6) can be written in another form,is as below:

$$T_{mn}(z) = \frac{4}{a*b} * \int_0^a \int_0^b \Delta T(x, y, z) * \sin(\alpha_m * x) * \sin(\beta_n * y)\,dxdy \quad (7)$$

Where:

$$\alpha_m = \frac{m * \pi}{a}, m = 1,3,5, \dots, \infty$$

$$\beta_n = \frac{n * \pi}{b}, n = 1,3,5, \dots, \infty$$

Substitute Eqn.(5) into Eqn.(7):

$$T_{mn}(z) = \frac{16*T_1*z}{m*n*\pi^2} \quad (8)$$

The thermal loading is defined as follows:

$$\begin{Bmatrix} M_{xx}^{Ther.} \\ M_{yy}^{Ther.} \end{Bmatrix} = \sum_{m=1}^{\infty}\sum_{n=1}^{\infty} \begin{Bmatrix} M_{mn}^{(1)} \\ M_{mn}^{(2)} \end{Bmatrix} * \sin(\alpha_m * x) * \sin(\beta_n * y) \quad (9)$$

Where:

$$M_{mn}^{(1)} = \sum_{k=1}^{N} \int_{z_k}^{z_{k+1}} (Q_{11} * \alpha_1 + Q_{12} * \alpha_2) * T_{mn}(z) * z\, dz$$

$$M_{mn}^{(2)} = \sum_{k=1}^{N} \int_{z_k}^{z_{k+1}} (Q_{12} * \alpha_1 + Q_{22} * \alpha_2) * T_{mn}(z) * z\, dz$$

After simplify Eqn.(9), the thermal loading is as below:

$$\text{thermal loading} = \frac{\partial^2 M_{xx}^{Ther.}}{\partial x^2} + \frac{\partial^2 M_{yy}^{Ther.}}{\partial y^2} = \frac{-16 * T_1}{3 * \pi^2} \sum_{m=1}^{\infty}\sum_{n=1}^{\infty} \frac{(A_1 * \alpha_m^2 + A_2 * \beta_n^2)}{m * n} * \sin(\alpha_m * x) * \sin(\beta_n * y)$$

The solution of normal deflection is as below:

$$w_o = \sum_{m=1}^{\infty}\sum_{n=1}^{\infty} w_{mn} * \sin(\alpha_m * x) * \sin(\beta_n * y) \quad (10)$$

Substitute Eqn.(9) and Eqn.(10) into Eqn.(4):

$$w_{mn} = \frac{\frac{16*T_1}{3*\pi^2*m*n}*(A_1*\alpha_m^2+A_2*\beta_n^2)}{D_{11}*\alpha_m^4+2*(D_{12}+2*D_{66})*\alpha_m^2*\beta_n^2+D_{22}*\beta_n^4} \quad (11a)$$

Then:

$$w_o(x,y) = \frac{16*T_1}{3*\pi^2} * \sum_{m=1}^{\infty}\sum_{n=1}^{\infty} \frac{(A_1*\alpha_m^2+A_2*\beta_n^2)*\sin(\alpha_m*x)*\sin(\beta_n*y)}{m*n*[D_{11}*\alpha_m^4+2*(D_{12}+2*D_{66})*\alpha_m^2*\beta_n^2+D_{22}*\beta_n^4]} \quad (11b)$$

Where:

$$A_1 = \sum_{k=1}^{N} (Q_{11} * \alpha_1 + Q_{12} * \alpha_2) * (z_{k+1}^3 - z_k^3)$$

$$A_2 = \sum_{k=1}^{N} (Q_{12} * \alpha_1 + Q_{22} * \alpha_2) * (z_{k+1}^3 - z_k^3)$$

Derive eqn.(11b) once and twice to obtain the thermal stresses analysis:

$$\sigma_{xx}^{(k)}(x,y,z) = -z * [-\sum_{m=1}^{\infty}\sum_{n=1}^{\infty}(Q_{11} * \alpha_m^2 + Q_{12} * \beta_n^2) * w_{mn} * \sin(\alpha_m * x) * \sin(\beta_n * y)] \quad (12a)$$

$$\sigma_{yy}^{(k)}(x,y,z) = -z * [-\sum_{m=1}^{\infty}\sum_{n=1}^{\infty}(Q_{12} * \alpha_m^2 + Q_{22} * \beta_n^2) * w_{mn} * \sin(\alpha_m * x) * \sin(\beta_n * y)] \quad (12b)$$

4. Numerical Simulation

In this paper, finite element discretization is carried out using ANSYS Ver. 19.2. (SHELL 132) element is used to mesh the composite laminate plate, [12]. SHELL 132 is defined by eight nodes having six degrees of freedom at each node to calculate the normal stress-strain analysis. The maximum value of stress and strain of the middle point has been selected in which it has maximum normal bending deflection. In numerical simulation, the effect of temperature is considered. Fiber volume fraction (25.076%) has been selected from the experimental results. The simply supported boundary condition from all edges is used to compare the value of thermal stress of Navier solution. The out-off plane temperature is constant and distributed along the length and the width of the composite laminate plate. The loading condition are shown in Figure 1.

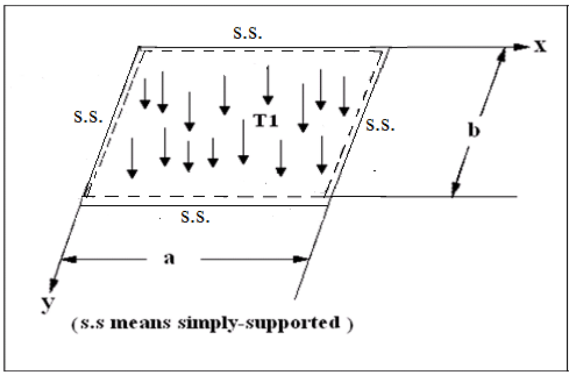

Figure 1. Loading condition on composite laminate plate.

5. Results and Discussions

Figure 2 and 3 show the verification of normal stress versus the aspect ratio along x and y directions. Navier method and ANSYS Ver. 19.2 are verified and checked for thermal stress analysis under the effect of temperature which is varied between (60 C^o) and (-15 C^o). The normal stress value is decreased sinusoidal with the increasing of aspect ratio for (60 C^o) along x and y directions, as illustrated in Figures 2 and 3, while it is decreasing for (-15 C^o) along x direction, as shown in Figure 2. The value of stress is increased with the increasing of aspect ratio for (-15 C^o) in which the normal stress settlesat aspect ratio between (1.8-2.3) along y direction, as depicted in Figure 3. In general, the value of normal stress at (60 C^o) along x and y directions is bigger than the value of normal stress at (-15 C^o).

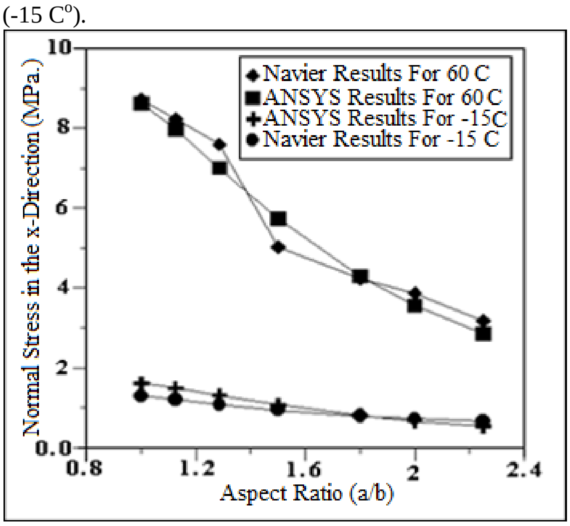

Figure 2. Verification of normal stress in the x-direction for (60 C^o) and (-15 C^o).

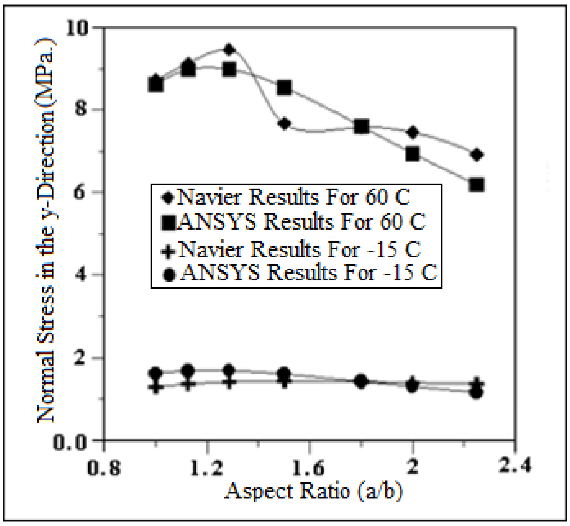

Figure 3. Verification of normal stress in the y-direction for (60 C^o) and (-15 C^o).

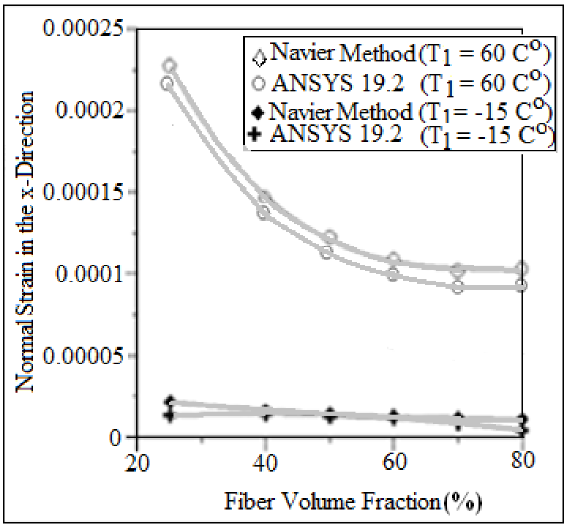

Figure 4. Verification of normal strain in the x-direction for (60 C^o) and (-15 C^o).

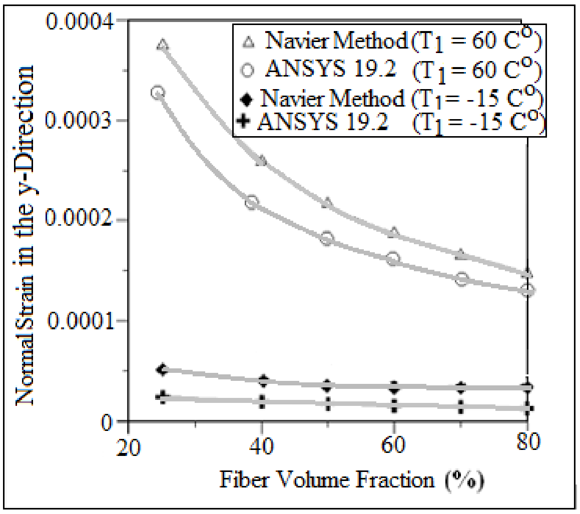

Figure 5. Verification of normal strain in the y-direction for (60 C^o) and (-15 C^o).

Figures 4 and 5 show the verification of normal strain against the percent of fiber volume fraction along x and y directions. Navier method and ANSYS Ver. 19.2 are verified and checked for normal strain under the effect of temperature which is varied between (60 C^o) and (-15 C^o). The normal strain is decreased exponentially with the increasing of fiber volume fraction for (60 C^o), as illustrated in Figures 4 and 5, while it is decreasing for (-15 C^o) along x and y directions, as shown in Figures 4 and 5 respectively. The value of normal strain settlesat the volume ratio between (50-70 %) for (-15 C^o). In general, the value of normal strain at (60 C^o) along x and y directions is bigger than the value of normal strain at (-15 C^o).

Figures 6 and 7 show the verification of normal bending deflection using Navier solution taking into consideration ANSYS 19.2 results in the comparison. The normal bending deflection decreased with the increasing of plate aspect ratio because of the increasing in plate bending stiffness at (60 C^o) and (-15 C^o) for fiber volume fraction (25.075%). The bending deflection value when (60 C^o) is higher than the value of bending deflection when (-15 C^o).

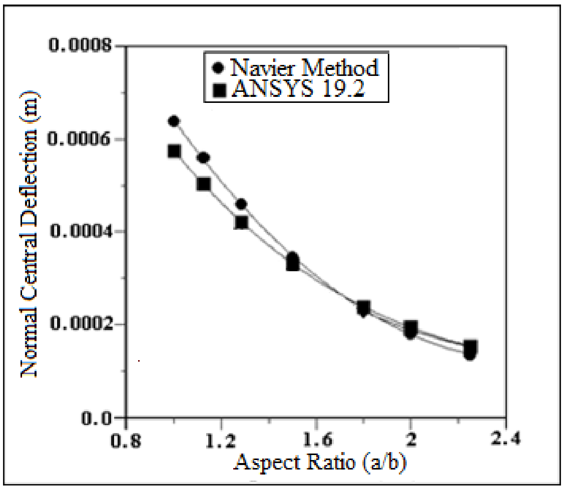

Figure 6. Normal bending deflection versus with laminate plate aspect ratio at (60 C^o).

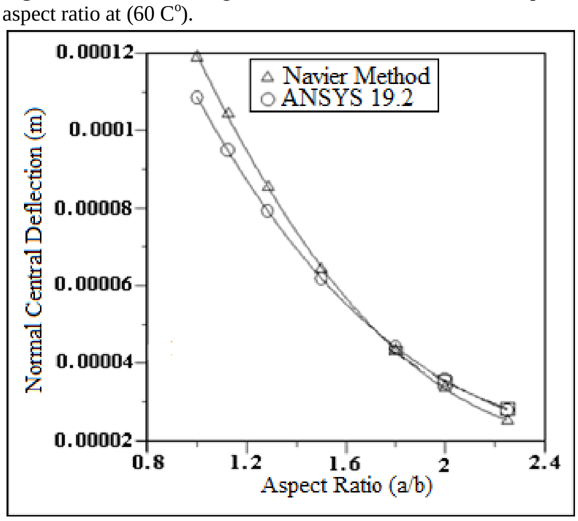

Figure 7. Normal bending deflection versus with laminate plate aspect ratio at (-15 C^o).

6. Conclusions

In this paper, the derivation of analytic formulation of thermal stress analysis has been done using the theory of classical laminate plate. The method of Navier solution is used in the calculation. ANSYS software is used in the verification. The normal stress-strain values are decreased sinusoidal and exponentially with the increasing of aspect ratio and fiber volume fraction respectively under the effect of temperature (60 C^o) along x and y directions. For (-15 C^o), the value of normal strain is decreased with the increasing of fiber volume fraction along x and y directions.

Acknowledgments

I want to first thank the reviewers and the editor for reviewing my paper.

References

[1] Al-Hamdan Ali, Y.L. Nimir, and R.J. Mustafa,"Ballistic Impact Fracture Behavior of Continuous Fiber Reinforced Al-Matrix Composites", Jordan Journal of Mechanical and Industrial Engineering, Vol.104, Issue 5, pp.605-614, 2010.

[2]R.K. Thangaratnam, Palaninathan, and J.Ramachandran,"ThermalStress Analysis of Laminated Composite Plates and Shells", Journal of Computers and Structures, Vol.30, Issue6, pp.1403-1411,1988.

[3] E. Carrera, M. Cinefra, and F.A. Fazzolari,"Some Results on Thermal Stress of Layered Plates and Shells by Using Unified Formulation", 10th International Congress on Thermal Stresses, Nanjing, China, Tayler Francis, Vol. 36, Issue 6, pp. 589-625, 2013.

[4] F. Sen, M. Toparli, and N.S. Koksal,"The Evaluation of Thermal Stresses in Thermoplastic Laminated Composites with Different Square Holes", Journal of Mathematical and Computational Applications, Vol. 12, Issue 1, pp.59-68, 2007.

[5]M. Sit, C. Ray, and D. Biswas," Thermal Stress Analysis of Laminated Composite Plates Using Third Order Shear Deformation Theory", Journal Advances in Structural Engineering, pp. 149-156, 2015.

[6] B.S. Redddy, J.S. Kumar, C.E. Reddy, and K.V.K. Reddy,"Static Bending Behavior of Functionally Graded Plates Subjected to Mechanical Loading", Jordan Journal of Mechanical and Industrial Engineering, Vol.8, Issue 4, pp.1995-6665, 2014.

[7] K. Rohwer, R. Rolfes, and H. Sparr"Higher-Order Theories for Thermal Stresses in Layered Plates", International Journal of Solids and Structures, Vol. 38, Issue 21, pp. 3673-3687, 2001.

[8] Z. Vnučec, "Analysis of the laminated composite plate under combined loads",5th International Scientific Conference on Production Engineering, 2005.

[9] El Moufari, and Meryem,"Interaction of Thermal Loading on the Damage Evolution of Composite Materials", 22th French Mechanics Congress, 2015.

[10] M. Ali,"Synthesis and Characterization of Epoxy Matrix Composites Reinforced withVarious Ratios of TiC",Jordan Journal of Mechanical and Industrial Engineering, Vol.10, Issue 4, pp.231-237, 2016.

[11] J.N. Reddy,"Mechanics of Laminated Composite Plates and Shells: theory and analysis", 2ndEdition, CRC Press, 2004.

[12]M. K. Thompson and J. M. Thompson," ANSYS mechanical APDL for finite element analysis", Butterworth-Heinemann, 2017.

JJMIE

Volume 13, Number 4, December. 2019
ISSN 1995-6665
Pages 271 - 275

Jordan Journal of Mechanical and Industrial Engineering

Thermo-acoustic Engine Pressure Wave: Analysis of Working Fluid Effect

Somayya Esmat Elshabrawy, Mohammed Noorul Hussain, Isam Janajreh*

Mechanical Engineering Department, Khalifa University of Science and Technology, Masdar Institute, PO Box 54224, Abu Dhabi, United Arab Emirates

Received 3 October. 2019

Abstract

Thermo-acoustic Engines (TAE) utilize the production of acoustic waves to generate mechanical power when a thermal gradient is applied to a stack placed in the resonator of TAE. Owing to non-existence of moving parts that a conventional engine has, TAEs are typically mechanically more efficient and reliable, hence are an important area of research. The thermos-acoustic phenomenon for TAEs is only driven by temperature gradient that induces fluid flow. However, in the previous works related to numerical study of standing wave TAEs, an initial disturbance in the form of pressure gradient has been imposed to generate fluid flow. In this paper, a 2D numerical analysis of a standing wave TAE is performed using computational fluid dynamics (CFD) modeling to capture the pressure fluctuations (without any initial disturbance) with time in the resonator channel in order to assess its thermo-acoustic performance. The results are obtained for pressure variation at specific points and the development of temperature profiles within the resonator. Using the pressure variations, FFT analysis was performed to identify sound pressure levels and resonant frequencies. Also, a sensitivity study has been carried out. The objective is to analyze the pressure wave development under different fluid properties. In this study, equivalent properties of a certain mixture of gases are prescribed to represent a composite working fluid. Two cases are considered i.e. mixture of air and helium and mixture of air and carbon dioxide. The compositions are varied in each case. It is noticed that in He mixtures the onset of pressure wave is quicker than in only air or CO2 mixtures, this due to the higher thermal conductivities. However, when only He is considered there is no pressure wave unlike only air or only CO2 cases due to low molecular weight. Frequency in He mixtures rises as He composition is increased, and the contrary is seen in CO2 mixtures. This is due to the collective consequence of the Cp, thermal conductivity and molecular weight. The study shows how important the thermal properties of the working fluid are for the pressure wave.

Keywords: Thermos-acoustic engine, Stirling cycle, refrigeration;

Nonmenclature

Abbreviations

TAE	Thermo-acoustic Engines
COP	Coefficient of Performance
CFD	Computational Fluid Dynamics
CFL	Friedrichs Lewy number
Symbols	
ρ	Density
μ	Dynamic viscosity
ν	Kinematicviscosity
δ_κ	Thermal penetration length
δ_ν	Viscous penetration length
c_p	Specific Heat
ω	Angular frequency
κ	Thermal diffusivity
k	Thermal conductivity

1.

Introduction

Thermo-acoustic heat engines (TAE) are devices that convert thermal energy to acoustic energy with the advantage of the absence of moving parts [1] and using the Stirling engine cycle principle. This gives them the potential to be more reliable, low cost as they can operate without exotic materials and precision machining or tight tolerance. Decays of developments have pushed the efficiency of today's Internal combustion engines to 30% and as high as 40% for large diesel engine. The Coefficient of Performance (COP) of the vapor-compression refrigeration systems can also reach 50% of Carnot's COP. Although the potential exists for thermo-acoustic engine, these efficiencies are still unattained and pose some technical challenges.

In the Stirling cycle, a working gas is compressed in a piston cylinder arrangement, while a heat sink is actively absorbing the excess heat to keep the temperature of the gas constant. Tgas is then flowing through a

* Corresponding author e-mailisam.janajreh@ku.ac.ae

regenerator/stack where it absorbs heat at constant volume. It is further heated at the heat source where it expands to deliver power to a piston [2]. Researchers like Ceperley[3]worked on replacing the pistons in a Stirling engine with sound waves and created the very first thermo-acoustic heat engine technology. As the Stirling engine experiences similar pressure-velocity dephasing as those occurs in a travelling acoustic wave, the development of standing wave thermo-acoustic engines and refrigerators are evolved by Los Alamos group. These are the two types of the thermo-acoustic engines, the moving/travelling -wave and the standing wave. In both systems the main component is the regenerator or stack, which is a porous solid medium that consists of heating plates, placed between two heat exchangers to transfer heat to/from the external thermal reservoirs and the working fluid.

Moreover, the thermal (δ_κ) and viscous (δ_v)penetration depths are indicative of the boundary effect beyond which unnoticeable diffusion of heat or momentum can be felt within the oscillating period. This puts a limit to stack spacing and is defined as:

$$\boldsymbol{\delta_\kappa = \sqrt{2\kappa/\omega}}, \text{ where } \boldsymbol{\kappa = k/\rho c_p} \quad (1)$$

$$\boldsymbol{\delta_v = \sqrt{2v/\omega}}, \text{ where } \boldsymbol{v = \mu/\rho} \quad (2)$$

Where κ is the thermal diffusivity and k is the thermal conductivity of the working gas, ρ is the density, μand νare the dynamic and kinematic viscosities and c_p is the specific heat. Successful operation of a standing wave engine requires deliberately imperfect thermal contact between the gas and the stack, which is obtained when the spacing between the plates is roughly a few δ_k. The ratio of $\mathbf{\delta_k/\delta_v = \pi c_p/k}$ is identified as the square root of Prandtl number, which is near unity for common gases and vindicating an equal order of thermal and viscous penetration. It is worth noting that in thermos-acoustic engine these penetration lengths are at much smaller length than the displacement amplitude, which is smaller than the acoustic wave length.

In literature thermoacoustic engines have been investigated and designed both experimentally and with computational fluid dynamics. Nijeholt et al[5] simulated a travelling wave thermoacoustic engine via a 2D CFD model. The authors reported that effects like streaming mass flows and vortices formation can be visualized, which was otherwise impossible when linear theory is used. Designs of thermoacoustic engines with looped tubes has been presented by Yazaki et al[6]. The design was built and tested experimentally. Results showed that looped tubes acted as wave power amplifiers and the onset temperature ratios were smaller in the loop. Biwa et al [7] experimentally investigated the lowest critical temperature ratio necessary to run a thermoacousticstirling engine. They showed a 32% decrease in critical temperature ratio by using up to 5 differentially heated generators. Other works have shown the application of thermoacoustic engines as electric generators and refrigerators[8][9].

In previous work by the authors [4]physical parameters like effect of length and temperature gradient have been studied. In this work, the focus is on the fluid dynamic aspect that is characteristic to the working fluid since it is not well investigated. Mixture of air with helium and air with carbon dioxide are studied as cases, where the equivalent viscosity, thermal conductivity and specific heat with varying compositions are represent new working fluids.

2. Methodology

An axisymmetric cylindrical TAE is modeled in Ansys Fluent. The geometry is similar to that in the previous work by the authors [4]and is shown in Fig. 1. It shows the asymmetrical geometry of the discretized model mesh representing a stack of horizontal plates modeled at plate thickness of 5mm and a gap of 5 mm between each plate.

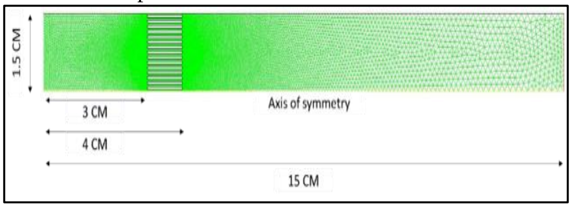

Figure 1. Modeled TAE baseline geometry in Fluent

The numerical model is based on the transient, non-isothermal and 2D cylindrical Navier-Stokes flow. The ideal gas model is assumed to govern the fluid state, as the developed pressure wave is relatively small. Turbulence is accounted for following the averaging of these equations where the resulted Reynolds stresses are modeled via the common eddy viscosity$(-\rho V_i'V_j' = \mu_t(\partial V_i/\partial V_j + \partial V_j/\partial V_i)$and k-ε transport model. Eq. 3-8 describe the overall governing equations (Eq. 3 the continuity, Eqs. 4, 5, and 6 the momentums, Eq. 8 is the general transport equation for any of the scalar quantity like those that govern the turbulence-k and -ε following the common eddy viscosity model. Eq. 9 governs the energy equation).

The continuity equation is as follows for axisymmetric geometries:

$$\frac{\partial\rho}{\partial t} + \frac{\partial(\rho V_x)}{\partial x} + \frac{\partial(\rho V_r)}{\partial r} + \frac{\rho V_r}{r} = 0 \quad (3)$$

Where x is the axial coordinate, r is the radial coordinate, V_x is the axial velocity, and V_r is the radial velocity. The momentum equation is written as:

$$\frac{\partial(\rho\vec{V})}{\partial t} + \nabla.(\rho\vec{V}\vec{V}) = -\nabla p + \nabla.\mu[(\nabla\vec{V} + \nabla\vec{V}^T) - \frac{2}{3}\nabla.\vec{V}I] + \rho\vec{g} \quad (4)$$

Where ρ is the static pressure, μ is the molecular viscosity, and I is the unit tensor and itsterm accounts tothe effect of volume dilation/expansion.The ρg term is the gravitational body forces vector. In 2D axisymmetric geometries the axial and radial conservation of momentum equations are written as:

$$\frac{\partial\rho V_x}{\partial t} + \frac{1}{r}\frac{\partial}{\partial x}(r\rho V_x V_x) + \frac{1}{r}\frac{\partial}{\partial r}(r\rho V_r V_x) = -\frac{\partial p}{\partial x} + \frac{1}{r}\frac{\partial}{\partial x}[r\mu(2\frac{\partial V_x}{\partial x} - \frac{2}{3}(\nabla.\vec{V})] + \frac{1}{r}\frac{\partial}{\partial r}[r\mu(\frac{\partial V_x}{\partial r} - \frac{\partial V_r}{\partial x})] + \rho g_x \quad (5)$$

$$\frac{\partial \rho V_r}{\partial t} + \frac{1}{r}\frac{\partial}{\partial x}(r\rho V_x V_r) + \frac{1}{r}\frac{\partial}{\partial r}(r\rho V_r V_r) = -\frac{\partial p}{\partial r} + \frac{1}{r}\frac{\partial}{\partial x}\left[r\mu\left(\frac{\partial V_r}{\partial x} + \frac{\partial V_x}{\partial r}\right)\right] + \frac{1}{r}\frac{\partial}{\partial r}\left[r\mu\left(2\frac{\partial V_r}{\partial r} - \frac{2}{3}(\nabla.\vec{V})\right)\right] - 2\mu\frac{V_r}{r^2} + \frac{2\mu}{3r}(\nabla.\vec{V}) + \rho g_r \qquad (6)$$

Divergence in axisymmetric geometrics is as:

$$\nabla.\vec{V} = \frac{\partial V_x}{\partial x} + \frac{\partial V_r}{\partial r} + \frac{V_r}{r} \qquad (7)$$

The transport equation in terms of ϕ dependent variable and in particular for each of the two turbulence scalars iswritten following the common four term formulation, i.e. temporal, adjective, diffusive and anyadditional sources as:

$$\frac{\partial(\rho\phi)}{\partial t} + \nabla.(\rho\vec{V}\phi - \Gamma\nabla\phi)) = S_{\phi_k} \qquad (8)$$

Where ϕ corresponds once to turbulent kinetic energy (k) and second to itsdissipation rate (ε); Γ is the diffusion coefficient and S is the source term corresponding to each of the scalar equations. The k and ε equations are related by the eddy viscosity term such that $\mu_T = C_{e2}\rho\frac{\varepsilon^2}{k}$ where μ_T the turbulent viscosity. The internal energy (E) equation is written as:

$$\frac{\partial(\rho E)}{\partial t} + \nabla.(\rho\vec{V}(\rho E + p)) = -\nabla.[K\nabla T + (\mu(\nabla\vec{V} + \nabla\vec{V}^T) - \frac{2}{3}\nabla.\vec{V}I).\vec{V}] \qquad (9)$$

Where ρ is the density, V represents the velocity field, p is the flow pressure, μ is the dynamic viscosity, μ_T is the turbulent viscosity. The internal system energy (E) can be described as:

$$E = H - p/\rho + \frac{1}{2}\vec{V}.\vec{V} \qquad (10)$$

Where H is the system enthalpy, which related to internal energy by the static pressure and density term per Eq. 10. Equations 3-10 are solved numerically in computing the physical quantities. First the geometry or the computation domain is discretized. Then, these differential equations are integrated over the finite volume of a computational cell and over a finite time where a second-order central difference scheme is used in the discretization of the convective and diffusive terms while first-order fully implicit scheme used for time. With respect to boundary conditions, all walls except the outlet are prescribed no slip. A free pressure outflow is prescribed at the outlet. The temperature at the stack walls is crucial, for the horizontal walls of each stack a decreasing temperature gradient profile is prescribed from 1000K to 300 K. The vertical walls of the stack are prescribed a 50 $Wm^{-2}K^{-1}$ heat transfer coefficient. The model is initially computed with a steady state, with a prescribed pressure (10 Pa. [4]) at the left closed wall, to create a minute velocity in the system, as is the practical case. Further on transient computation follows with a time step of 1E-5s, in accordance with the Courant Friedrichs Lewy number (CFL) principal. The pressure wave development, frequency and amplitude are analyzed.

3. Results and Discussion

3.1. Mesh sensitivity

In line with the authors' previous work, four levels of mesh were used to assess the solution independence, i.e. fine, baseline, and coarse-1 as well as coarse-2. Results are captured in the stack temperature at upstream and downstream, and the absolute relative errors are evaluatedand summarized inTable 1. A compromise between accuracy and computation time was sought particularly when soliciting long unsteady solution. Therefore, a baseline mesh at an absolute temperature error values of 0.7% compared to the 1.5% and 10.7%, for coarse 1 and 2,respectively. A very strict residual of 10E-11 wastargetedfor all the considered levels.

Table 1. Mesh sensitivity results

Mesh level	Numb.of Cells	Up Temp (°C)	Down Temp (°C)	Temp Diff, (°C)	Rel. Err (%)
Fine	76,262	405.35	322.73	82.62	-----
Baseline	30,003	405.93	322.72	83.21	0.71
Coarse-1	21,293	406.58	322.70	83.88	1.52
Coarse-2	17,617	414.24	322.74	91.50	10.7

Table 2 summarizes the properties of the selected working fluids and it lists the theoretical and the obtained numerical values of the acoustic speeds. Accordingly, as the obtained numerical values are in agreement with the anticipated values, it provides further validity to the undertaking model.

Table 2. Calculated equivalent properties for different cases at the wavelength of soundλ=30cm

Case Study	C_p (J/kg.K)	C_v (J/kg.K)	γ Cp/Cv	Thermal Cond. (W/m.K)	Viscosity (Pa.s)	MolecularWeight (g)
W1 – He 100%	5193	3120	1.66	0.1520	1.99E-5	4.00
W2 – (25% He, 75% Air)	2053	1318	1.56	0.0562	1.84E-5	22.72
W3 – (50% He, 50% Air)	3099	1919	1.62	0.0881	1.90E-5	16.49
W4 – (70% He, 30% Air)	3937	2399	1.64	0.1137	1.92E-5	11.49
W5 – CO_2 100%	840.4	655.0	1.28	0.0145	1.4E-5	44.00
W6 – (25% CO_2, 75% Air)	964.9	702.3	1.37	0.0218	1.7E-5	32.77
W7 –(50% CO_2, 50% Air)	923.4	686.5	1.35	0.0194	1.6E-5	36.48
W8 – (70% CO_2, 30% Air)	890.2	673.9	1.32	0.0174	1.5E-5	39.49
W9- Air 100%	1006.4	718.0	1.40	0.0242	1.8E-5	28.97

3.2. Working Fluid Study

The working fluid sensitivity was conducted using the temperature gradient from 1,000 K to 300 K. This sensitivity was carried out initially for four compositions for each gas mixture, i.e. Helium – air and CO_2 - air. The first case (W1) was with using Helium gas as single working fluid, and the second (W2) was using the mixture ratio (25:75) of Helium with air gas.The third (W3) case was using the mixture ratio (50:50) of Helium with air gas, whereas the fourth case (W4) was using the mixture ratio (70:30) of Helium with air gas. The corresponding cases for the CO_2 – air mixture are denoted as W5, W6, W7 and W8. The W9, however represents the case ofusing air gas only.

Results for the pressure monitor placed at 14 cm downstream are analyzed. The results are compared with a single case of 'Air only' working fluid for better understanding. In cases W2, W3, W4, W5, W6, W7, W8, and W9 it was noticedthat there is clear formation of a standing wave in the resonator. For W1 with the Helium gas, there is a bleak pressure fluctuation in first few time steps, which quickly dies out. Fig. 2 shows these results.

One can clearly notice that the onset of the standing wave is quickest for the Helium mixture, followed by 'Air only' cases then finally the CO_2 – air mixtures. To understand this behavior, it is important to study the equivalent properties which are shown in Table 2. In case of He –air mixture the thermal conductivity seems to increase as the share of air increases. It is a trivial fact that it is the thermal interaction between the thermal stack and the working fluid is what allows the development of a standing wave. With increase in conductivity the working fluids heats up faster, andthereby it initiates the pressure fluctuation much quicker. Comparing the compositions of He and CO_2 cases, it is evident that Helium mixtureshave much higher thermal conductivity than CO_2 mixtures. This explains why the onset of the pressure wave is quicker for He mixtures compared to CO_2 mixtures. Even more evidence for this correlation can be found in the analysis of the wave for different CO_2 mixtures. In this case, with increasing air fraction the thermal conductivity decreases and the response is a clear delay in the pressure wave development. It must also be noticed that the c_p is also increasing in the He mixture cases, however it seems that the high temperature gradient prescribed at the stack provides sufficient energy to counter a delay in pressure wave onset. The viscosity variation is miniscule in these cases; therefore, it would not be appropriate to correlate the results with this property.

When anyof the gases, i.e. He, CO_2 and air are individually considered as working fluids, it is seen that there is a pressure wave formation in the case of air and CO_2, but not in the case of He. Upon analysis of the properties, it appears that the molecular weight and the thermal conductivity, or rather, the tradeoff between these two properties is the controlling factor. In the case of He, the low molecular weight, resulting in less mass and added to that the high c_p seems to restrict the pressure wave development. Air, having a median molecular weight and median thermal conductivity that develops a pressure wave quicker than CO_2. Although CO_2 does show a standing wave, the onset is delayed due to low thermal conductivity.

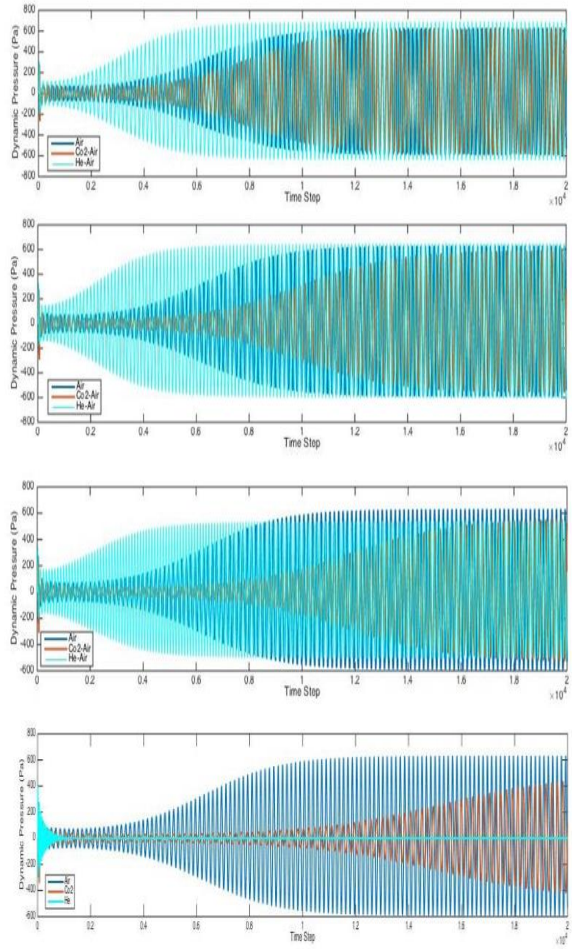

Figure 2. Static pressure wave development in the resonator for the Helium Gas cases (Top-Down: 25% Gas + 75%Air, 50%Gas + 50%Air, 70% Gas + 30%Air, Individual working fluids)

3.3. Frequency and Acoustic Speed Analysis

Fig. 3 shows the analysis of different frequencies obtained in the different cases. A particular but opposite trend is seen in cases of He and CO_2 mixtures. With increase in He in the system, the frequency increases, while increase in CO_2 reduces the frequency.

Peculiarly the molecular weight in the system decreases in the He mixtures, while it increases in the CO_2 mixtures. One expects that the speed of sound to be higher in denser mixtures and in turn reporting a higher frequency, but rather the case seems to be quite contrary. The explanation lies again in the thermal properties of gases. It is a common phenomenon that in hotter gases the speed of sound is higher compared to colder gases, although one expects the colder gases to be denser and by principle the speed of sound to be higher. Nevertheless, hotter gases have higher kinetic energy and thus there will be more potential for vibrations to occur. This leads to an increase in the speed of sound in the hotter gases. In this system the effect on frequency is likely a combined consequence of c_p, thermal conductivity and molecular weight. In He mixtures with increase in He the increasing c_p is balanced by the reducing mass while the thermal conductivity increases, thus potentially causing higher temperatures and in turn higher frequencies. Whereas in CO_2 mixtures, the decreasing $c_p$is balanced with increasing molecular weight while the thermal conductivity decreases. This can potentially cause lower temperatures and thus lower frequencies.

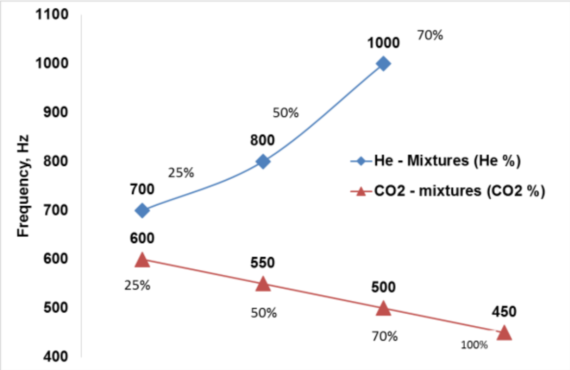

Figure 3. Analyzed frequencies for different working fluid cases

Further validation of this work is pertained to the evaluation and assessment of both thermal and viscous penetration lengths. These values are summarized in Table 3 for each of the successful runs.It is also in agreements with Swift recommendation. On one hand their ratio is near the value of the Prandtl number which close to unity for these near ideal gases. On the other hand, their values are only several folds of the distance between the stacks as indicated by Swift et al.

4. Conclusion

In this work numerical simulation of a Thermo-acoustic heat engine was carried out. The pressure wave in the resonator wasanalyzed for its time inception and the resulted frequency. The study aimed to understand the effect of working fluid in the thermo-acoustic engine and study the crucial properties affecting the pressure wave. Gas mixtures of He – air and CO_2 – air was assumed and the compositions were varied. The equivalent properties were prescribed in the system.

It is noticed that in He mixtures the onset of pressure wave is quicker than in only air or CO_2 mixtures. This was attributed to the He higher thermal conductivities. However, when only He was considered there was no pressure wave development. It was unlike the single gas of air or CO_2 cases. This was attributed to the low molecular weight of the He. Frequency in He mixtures rises as He composition is increased, whilethe contrary wasobservedin CO_2 mixtures. This is due to the collective consequence of the c_p, thermal conductivity and molecular weight. The study shows how important the thermal properties of the working fluid are for the pressure wave. The variation in viscosity was miniscule, and therefore no conclusions were drawn to thisrespect. It must also be acknowledged that a perfectly mixed system is assumed whereas in real cases diffusion characteristics of gases may play a role.

Table 3. Evaluated properties corresponding to the 9 different cases

Case	Frequency	δk	δv	δk/ δv
W1 - He 100 %	-	-	-	-
W2 - (25% He, 75% Air)	700	1.14E-4	9.32E-5	1.22
W3 - (50% He, 50% Air)	800	1.27E-4	1.03E-4	1.23
W4 - (70% He, 30% Air)	1000	1.37E-4	1.12E-4	1.22
W5 - CO2 100%	450	7.85E-5	7.00E-5	1.12
W6 - (25% CO2, 75% Air)	600	1.76E-4	7.95E-5	2.22
W7 - (50% CO2, 50% Air)	550	1.84E-4	7.55E-5	2.44
W8 - (70% CO2, 30% Air)	500	1.93E-4	7.37E-5	2.62
W9 - Air 100%	650	9.80E-5	8.46E-5	1.16

References

[1] Guoyao Y, Dai W, Ercang L. CFD simulation of a 300 Hz thermoacoustic standing wave engine. Cryogenics 2010; vol. 50, pp. 615-622.

[2] U. S. D. of. Energy Information, Stirling Engine with Air Working Fluid, 1985.

[3] Ceperley P. Gain and efficiency of a short traveling wave heat engine. J. Acoust. Soc. Am. 1985 vol. 77, no. 3, pp. 1239-1244.

[4] Swift, G. W., & Engines, S. (n.d.). Gregory W. Swift.

[5] Nijeholt, J. A. L., Tijani, M. E. H., & Spoelstra, S. (2005). Simulation Ofa Traveling-Wave Thermoacoustic Engine Using Computational Fluid Dynamics. J. Acoust. Soc. Am. vol. 118, pp. 2265-2270.

[6] Yazaki, T., Iwata, A., Maekawa, T., &Tominaga, A. (1998). Traveling Wave Thermoacoustic Engine in a Looped Tube. Phsical Review Letters. vol. 81, pp. 3128 – 3131.

[7] Biwa, T., Hasegawa, D., &Yazaki, T. (2010). Low Temperature Differential ThermoacousticStirling Engine. Applied Physics Letters. vol 97, pp. 1-3.

[8] Backhaus, S., Tward, E., &Petach, M. (2004). Traveling Wave Thermoacoustic Generator. Applied Physics Letters. vol 85, pp. 1085-1087.

[9] Russell, D. A., & Weibull, P. (2002). Tabletop Thermoacoustic Refrigerator for Demonstrations. Am. J. Phys. vol 70, no. 12, pp. 1231-1233.

[10] Hussain, M. N., & Janajreh, I. (2017). Analysis of Pressure WaveDevelopment in a Thermo-acoustic Engine and Sensitivity Study.Energy Procedia, 142, 1488–1495. https://doi.org/10.1016/j.egypro.2017.12.597.

JJMIE

Volume 13, Number 4, December. 2019
ISSN 1995-6665
Pages 277 - 290

Jordan Journal of Mechanical and Industrial Engineering

Sustainable Dyads in Supply Chain Management: A Qualitative Perspective

Mohannad Jreissat [a], Luai Jraisat [b]

[a] *Faculty of Engineering, Industrial Engineering, The Hashemite University, Zarqa 13133, Jordan*
[b] *Faculty of Business and Law, University of Northampton, Northampton, NN1 5PH, UK*

Received 10 October. 2019

Abstract

The study seeks to explore themes concerning collaboration for sustainable buyer-seller relationships involving information sharing along supply chains. Two case studies of ten dyadic sustainable relationships and a literature review are used to examine these themes. The case studies allow this undefined area to be clarified and existing theories to be empirically examined regarding fresh fruit and vegetables (FFV) industry. The study identifies five types of themes influencing information sharing in collaboration for sustainable relationships: two external themes at the chain level, namely information flow strategy and product flow strategy, and three internal themes at the dyad level, namely contracting strategy, price strategy and revenue strategy. The case studies reveal that top management plays a pivotal role in improving collaboration involving information sharing for better sustainability performance. There appears to be an established connection between the levels of collaboration between chain actors and dyadic actors in information sharing for their sustainable relationships. This study contends that chain actors involved in information sharing need to partner dyadic actors rather than do transactional processes. The multi-case studies that support the development of the framework provide real-life perspectives whose insights are a valuable practical reference for similar supply chain contexts.

Keywords: information sharing, collaboration, sustainable chain relationship, fresh fruit and vegetables;

1. Introduction

Witnessing a value transformation is needed in which supply chain actors are inextricably bonded through collaboration that links supply with demand, forming a competitive industrial supply chain [1, 2]. An understanding of collaborations based on information sharing between actors in agricultural supply chains is still highly underexplored. These attempts at ensuring that information sharing between such actors for the benefit of the total performance are referred to as collaboration in sustainable buyer-seller relationships. From a relationship marketing perspective, information has taken on its own reality, which can be detached from the movement of products [1, 3].

Relatively little attention has been paid to information sharing in their relationship marketing along the supply chain [4]. Yet this interface exhibits one of the most contentious flows for dyadic actors and their relationships and it attracts an increased attention from both policy makers and academics. Prior research considering the cross-functional relationship for information sharing has suggested that this interface exhibits many unclear characteristics [e.g. 5, 6, 7, 8]. There is often an undefined association between information sharing and collaboration, particularly in supply planning, pricing, revenue and market demand along the chain actors [5]. These tensions have created the need to examine sustainable buyer-seller relationships from a multidimensional perspective [9]. To allow practitioners and academics to identify how the association between information sharing and collaboration in a supply chain can be improved, it is necessary to identify the contextual factors that can be utilized to influence this interface. Although there have been several recent papers conceptualizing this association, they have been based purely on literature reviews or limited empirical results [e.g. 10, 11, 12, 13].

This study will use existing literature as well as case studies to examine the information sharing and collaboration interface along dyadic actors in a supply chain. This could be by identifying the possible high-order themes of sustainable relationships that can provide benefits in terms of sustainability chain performance [12]. The study poses the following research questions:

- RQ1: How can key themes of information sharing be associated for collaboration in sustainable relationships?
- RQ2: How and why are these key themes effectively linked to collaboration in sustainable relationships to improve supply chain performance in practice?

* Corresponding author e-mail: Luai.Jraisat@northampton.ac.uk

This paper provides relevant views from the dyadic perspective of fresh fruit and vegetables (FFV) actors in supply chains. The article starts with a theoretical background on sustainable relationships, collaboration and information sharing. Next, the research methodology is presented. Then key findings and discussion are presented. Lastly, conclusions are provided with managerial implications.

2. Literature Review

2.1. Sustainable Buyer-Seller Relationships

The growing interest in sustainable relationships has led to the development of underpinning concepts to explain this term. Traditionally, a sustainable supply chain has been a set of various activities, with links to production, flow management of information and products, supply and demand, relationship management, logistics, contracting, risk, marketing, pricing, revenue, consumption, as well as value added activities along the supply chain [14, 9]. There is a focus on key outcomes of these activities in order to encourage actors to collaborate and improve their overall performance [12, 8]. An analysis of studies shows that sustainable relationships are defined as links being put into long-term collaboration between dyadic actors along the FFV supply chain [14, 15]. Based on the analysis of the studies, the key characteristics underpinning concepts of sustainable relationships may thus be identified as: product flow, information flow, information sharing, collaboration, and performance. The underlying rationale is to expand the body of knowledge in the field of sustainable relationships.

In this scenario, authors argued that it is important to identify a well-established approach to both information sharing and collaboration, thus leading to improved performance for a set of actors (e.g. number of buyers and sellers along the supply chain) rather than a single actor (e.g. a seller) [14]. Although these authors do not ignore the importance of the business buyer in collaboration, they do not focus fully on the involvement of the business buyer in the mechanism of information sharing, and especially in strategic issues, such as pricing and revenue. Recently, an emerged approach for examining both information sharing and collaboration in sustainable relationships has been established from the perspective of supply chain management [16, 17, 18]. Here the new approach is to consider how both buyers and sellers can focus on a mutually beneficial approach [15, 9]. In a more detailed scenario, this mutual approach focuses on pricing strategy between buyers and sellers from inside the supply chain and on revenue strategy between them from outside the supply chain [19]. This is also linked to an orientation towards the potential for collaborative activities based on information sharing in order to improve sustainable performance (e.g. economic, environmental and social themes) [12, 8, 18]. The present research suggests that there is a need to understand this more complex scenario of collaboration for dyadic SBSRs (Sustainable Buyer-Seller Relationships), and in particular, to examine the association between information sharing (e.g. sharing strategies of pricing and revenue), collaboration, and sustainable performance.

In summary, this shift has created an opportunity for more logical pricing strategies and the extraction of better revenues among the supply chain actors in their SBSRs [16, 17, 18]. Thus, in this research information sharing could be this opportunity that should be highlighted as a value creation for SBSRs to be involved in supply chain collaboration. Motivated by this issue, SBSRs is defined as a dyad that includes collaboration between a buyer and a seller aimed at creating value by information sharing along the supply chain actors for better sustainable performance.

2.2. Collaboration in Sustainable Buyer-Seller Relationships

Collaboration is an active process between actors where cooperation and coordination are achieved with key mutual segments between buyers and sellers [20]. The movement from coordination to collaboration requires high levels of commitment and information sources that lead to stronger dyadic sustainable relationships with other actors to reach that next step of integration whereby future design and product performance, and long-term strategic relationships, are formed. In fact, buying and selling actors are interdependent and become conduits of information between the business focal actors and their preferred suppliers, customers or service providers to create value better than before [15]. Experiences have shown that collaboration between chain actors may be enhanced through joint planning and joint problem solving at both pricing strategy and revenue levels. The FFV business with sustainable value chains has grown dramatically over the last two decades [9]. However, improvements in production and marketing activities along the agricultural value chain, especially enabled by unsustainable mechanizations and unplanned collaboration in resource use and consumer added value, have led to negative environmental, social and economic impacts [13]. These impacts are related to various pollutants (e.g. water resources, machinery usage, soil mineralization) as well as short-term social (e.g. job security and family business) and economic (e.g. income and profitability) benefits [18].

Drawing from the above, a supply chain needs to press for collaboration to serve the needs of both buyers and sellers in their SBSRs [13, 20]. Hence, this research has a focus on how actors need to foster a climate of mutual respect when collaborations are established, particularly when the business actors rely on the support strategies from the other dyadic side in both information flow and product flow.

2.3. Information Sharing in Sustainable Buyer-Seller Relationships

Information sharing is a key to the dissemination of information across all actors along the value chain, aiding interaction and sustainable collaboration [5]. Aggarwal and Srivastava [3] noted that frequent meetings to discuss joint involvement and to increase the sharing of information aided in the establishment of dyadic collaboration and its consequences. The inclusion of information flow into interaction collection and dissemination processes is also essential to developing collaboration [21]. One of the key issues among dyadic SBSRs is pricing strategies and revenue approaches. Indeed, a new collaboration is needed based on pricing processes from a dyadic supply chain perspective for a joint outcome from production to consumption points. More importantly, this brings information as a collaborative tool to enhance the joint revenue along the dyadic sustainable relationships and ensure efficient information flow and product flow, where contracting between buyers and sellers is existing within the supply chain [19]. Such contracting collaborations in supply chains can define sustainability and codified information shared for better procedures and value creation [22, 18].

The leading evaluation of the role of information sharing on pricing and revenue strategies for collaboration in SBSRs was done, on pricing strategy, and on revenue strategy [19] (See Figure 1).

Therefore, when considering the active role performed by buyers and suppliers along the supply chain to manage information sharing on both pricing and revenue for collaboration, there is a need for a win-win approach in FFV values-based supply chains [9, 23]. In this research, this should have s focus on SBSRs, where involved actors interact in price setting across the entire supply chain in order to ensure the welfare of all strategic partners, including appropriate profit margins and agreements of an appropriate duration.

3. Research Methodology

3.1. Research design

The research is based on a qualitative methodology, which is applied by considering various underlying concepts and clarifying the associations between these conceptual themes [24]. This research has two questions highlighted as follows:

RQ1: How can key themes of information sharing be associated for collaboration in sustainable relationships?

RQ2: How and why are these key themes effectively linked to collaboration in sustainable relationships to improve supply chain performance in practice?

RQ1 is derived deductively from the literature and RQ2 is derived inductively after data collection. The present research reflects relevant views from the perspective of dyadic SBSRs in the context of the FFV supply chain in Jordan. Both secondary and primary data are used [24], generally with an inductive nature to provide knowledge about this specific context. Secondary data is analyzed following an extensive review of books and peer-reviewed journals. For primary data, a multi-case study method is a rich source for exploration and explanation of complex emergent phenomena. A triangulation approach is applied by the use of existing research studies (e.g. Journal articles) and case studies (e.g. multiple-case studies) to ensure construct validity. In previous research, the case study method has been instrumental in generating rich theoretical and practical insights, especially in the field of collaboration in sustainable FFV supply chains [e.g. 8, 23].

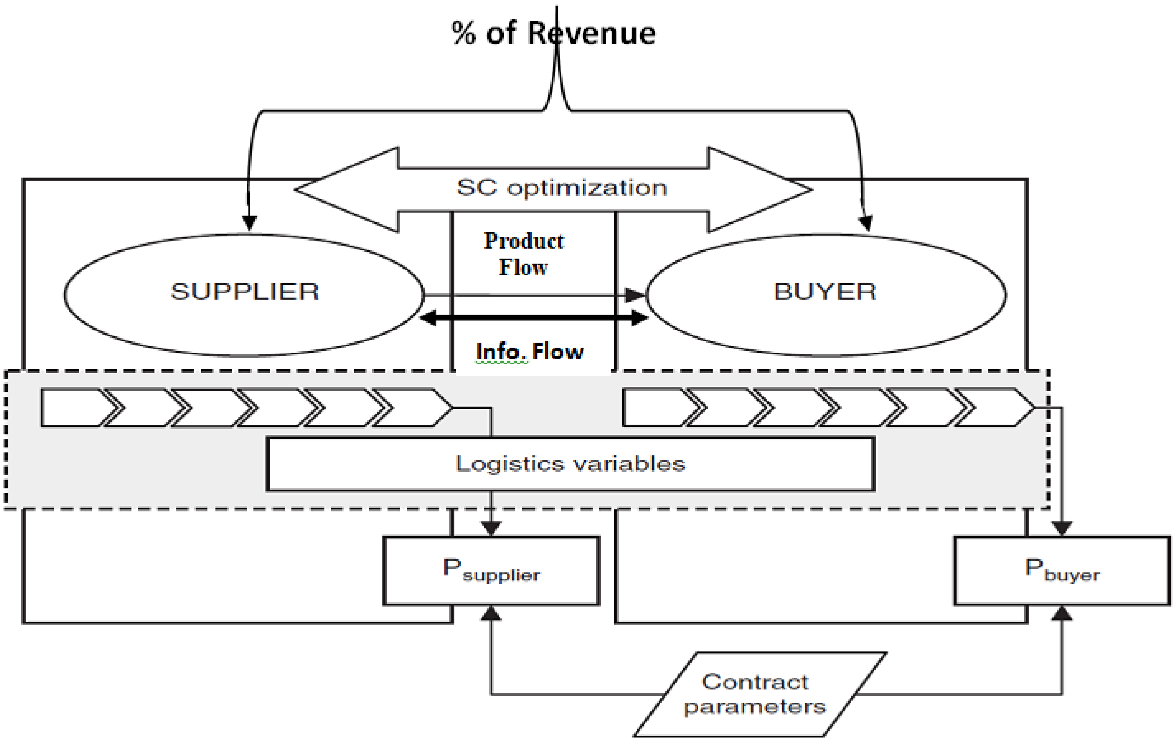

Figure 1. Pricing process and revenue in a dyadic SBSR [Source: Adopted from Van der Rhee et al. [19]

There are two case studies, including ten SBSRs, which have been selected based on theoretical sampling in order to provide new insights into an emergent theory. These cases are identified as sustainable collaborative relationships by certified bodies and each actor should have information sharing and collaboration functions in FFV supply chains. This sampling selection is based on advanced research of the online directory of sustainable firms in Jordan and it included firms that have been working for at least five years with various dyadic firms in FFV supply chains. This led to a list of 80 firms, which were then shortlisted to 10 firms based on three steps: satisfactory achievement records, positive email responses and an initial interview. Then, each firm was asked to identify a dyadic collaborative firm to form the unit of analysis as a dyadic sustainable relationship. This is where two different FFV supply chains (SCs) (Case: SC 1 and SC2) of similar 10 dyads (unit of analysis) of two different actors (sub-unit of analysis) are examined. Each FFV supply chain is formed of a type1-retailer-importer (for dyads A1, A2), type 2-importer-exporter (for dyads B1, B2), type 3-retailer-distrubutor (for dyads C1, C2), type 4-distributor-wholesaler (for dyads D1, D2), type 5-wholesaler-importer (for dyads E1, E2) (Table 1).

The basis for these studies was semi-structured interviews with four managers at each dyadic sustainable relationship. Managers as key informants were selected because they provide an overview of the information sharing and collaboration. Jordan is one of the developing countries which has agreements and contracts across FFV chain actors, including collaborative sustainable relationships [15]. The FFV supply chains is characterized by key features: sector structure of vertical and horizontal collaborations, product features as these are perishable products and sometimes seasonal products, actor types as this chain includes a variety of collaborative firms (importer, retailer, etc.) and dealing with international actors (e.g. supplying exporter). Hence a collaborative sustainable relationship approach is vital for the Jordanian FFV supply chain.

3.2. Data Collection

Primary data were collected from 40 semi-structured interviews as a key source and 10 observation days on different supply chain sites were applied within each actor for triangulation purposes. Each interview (ranging from one to two hours) was obtained from the managers involved in collaborative sustainable relationships in May-July 2017. The aim was to gain answers on how far collaboration in information sharing goes, what the roles of information sharing in the price process and revenue approach are within the FFV supply chain, how top management regard this collaboration in linking supply with demand with better information and product flows, and how collaborations affect sustainability performance.

Two managers at each actor of a dyad were selected for the data collection stage. Both literal replication and theoretical replication are followed by applying both multiple cases for the same dyad type and cases of different dyad types, both multiple level of managers for the same dyadic actor, same manager type for different dyad types, and same FFV supply chain type for different dyad types [25]. A case study protocol was applied for all cases for better research reliability. In total, 40 managers were interviewed for the two cases (10 dyadic sustainable relationships). To obtain reflective practitioner inputs, there were several contacts with those managers with specific clarifications involving emails, phone calls and document exchanges, which created mutual benefits. Interviews were conducted and recorded by the author in person, who were asked the same questions. The interviews were also transcribed and then sent to the managers for revisions. The approved interviews were used to develop the case studies, which were analyzed through cross-case analyses [24]. At the same time, research assistants as silent observers attended one meeting at each sustainable relationship.

Table 1. Case Study in the Context of FFV Supply Chains.

Case	Relationships	Age	Dyadic Industry	Establishment Year	Employees No.	Interviewee Type
Case 1 FFV (SC1)	A1	5	Retailer1-Importer1	1991-2000	100-200	Operation Manager; Relationship Manager-Operation Manager; Relationship Manager
	B1	7	Importer1-Exporter1	1991-2003	100-300	Marketing Manager; Contracting Manager - Operation Manager; Relationship Manager.
	C1	7	Retailer2-Distrubutor1	2000-2000	150-200	Marketing Manager; Contracting Manger - Operation Manager; Relationship Manager.
	D1	10	Distributor2-Wholesaler1	1980-2000	150-1000	Marketing Manager; Contracting Manager – IT Manager; Trade Union Manager.
	E1	5	Wholesaler2-Importer2	1980-1991	100-1000	Market Manger; Trader – IT manager; Service Manager
Case 2 FFV (SC2)	A2	6	Retailer3-Importer3	2000-2005	200-500	Operation Manager; Relationship Manager-Operation Manager; Relationship Manager
	B2	10	Importer4-Exporter2	2000-2010	200-400	Marketing Manager; Contracting Manager - Operation Manager; Relationship Manager.
	C2	12	Retailer4-Distrubutor3	1999-2005	200-500	Marketing Manager; Contracting Manger - Operation Manager; Relationship Manager.
	D2	12	Distributor4-Wholesaler3	1980-1999	200-1000	Marketing Manager; Contracting Manager – IT Manager; Trade Union Manager.
	E2	5	Wholesaler4-Importer4	1980-2000	200-1000	Market Manger; Trader – IT manager; Service Manager

3.3. Data Analysis

Several stages have been applied in data analysis as follows: **the first** was a coding (an analytical process in which data are indexed to facilitate analysis; concept-driven approach linking of data to the research idea), followed by initial codes that were generated from themes amongst the literature review, for data reduction and display for each case by using the interview transcripts and other sources (observations). **The second** was refinement for the selected key themes to be more focused as non-repetitive themes [24]. This is where each case of the five SBSRs was presented based on the key themes and related key quotes to support forming each proposition with the literature evidence. **The third** was a cross-case comparison for data exploration to enhance replication logic amongst the 10 dyads, providing the actor, dyad, and supply chain level-focused themes.

In summary, data analysis mainly followed two approaches: the first approach (coding and key themes) is the nested approach to analyze data gathered from each case [25]. This approach examines multiple sources from two managers for each actor as opposed to a single case (each SC: 20 managers, 10 actors, 5 sustainable relationships), providing a better opportunity to examine the cases. The second approach (cross-case comparison) is the cross-case approach to analyze the commonalities between the two cases. The process was iterative, moving backward and forward in time, exploring what their supply chain was like before the sustainable collaboration, how and why they started to change. The benefit of this analysis method was to allow the development of insights into the information sharing and collaboration association from the empirical findings. This research has achieved quality validity and reliability (Table 2).

4. Findings and Discussion

4.1. Case Study Level

At the case study level, the selection of variables for the initial conceptual association was guided by the existing literature review [e.g. 26, 18], which identified several initial themes as influencing the collaboration for SBSRs associated with information sharing. This is an exploratory level, where the findings of the two case studies of supply chains (SC1 and SC2) are presented and discussed based on the key themes identified by the literature and the sub-themes that emerged from the data analysis from both cases. This analysis resulted in 22 first-order themes for a sustainable relationship, which were then coded as 15 second-order themes that turned into five aggregate dimensions. These aggregate dimensions are associated to one overarching theme, "information sharing for collaboration in a dyadic sustainable relationship", in order to establish the theoretical association for the current research (Table 3). The key themes matched to analyze the data from the exploratory case studies are: external key themes: product flow and information flow, and internal key themes: pricing strategy, revenue strategy and contracting in relation to information sharing in collaboration for SBSR in the FFV supply chains (overall aggregate dimension) as shown in the table 3(. This is to explore how key themes about information sharing can be associated for collaboration in sustainable relationship. Thus, the research provides an attempt to answer RQ1 at this level.

Table 2. Research Quality

Validity and Reliability	Research design	More related stage
Construct Validity	-Building trust with interviewees. -Multiple source of evidence at data collection: interviews; observation (meetings) -Chain of evidence at data collection: two relationships for each case and use the same case protocol. -Transcripts are refined by the interviewees	Research design Data collection
Internal Validity	-Explanatory approach: develop a theoretical association between information sharing and collaboration. [at both Case level/ Cross case level] -Chain of evidence at data analysis: key theme matching and coding via support of key literature and key interview quotations. [at Case level] -Chain of evidence at data analysis: key proposition development. [at Cross-Case level] -Data triangulation: comparing quotes from interviews with observations. [at Cross Case level]	Data analysis
External Validity	-Multiple cases: replication logic among the 10 relationships for two cases. -Analytical generalization: building a new framework.	Research design
Reliability	-Case study protocol is the same for all cases -Case database: interview quotes and meetings -Key themes guided propositions and discussions -External review: final case report was validated by uninvolved experts (Policy makers).	Data collection

Table 3. A summary for Interviews Data Structure: Key theme of Information Sharing in Collaboration for sustainable relationships from SC1 and SC2.

First-order concepts	Second-order themes	Aggregate dimensions
External-focused key themes "Chain Level"		
-Human asset specificity such as training and experience (SC1 and SC2) *-Physical specificity such as production to market equipment (SC1 and SC2)*	Asset specificity in the SC (L.R)	Product flow strategy
-Bonds and leadership in the SC network (SC1 and SC2)	Actors' (buyer's and seller's) SC position (NT)	
-Selecting the right dyadic actors and also working with the same dyadic actors (SC1 and SC2)	Transaction frequency between the dyadic actors in the SC. (L.R)	
-Flexible and able to link actors with visibility (SC1 and SC2) *-Joint planning between the dyadic actors (SC1 and SC2)*	Cooperation between the dyadic actors in the SC (L.R)	Information flow strategy
-Perform training programmes for the dyadic actors (SC1 and SC2) *-Emphasis on sustainable relationships for the dyadic actors (SC1 and SC2)*	Coordination between the dyadic actors in the SC (L.R)	
-Interaction between the dyadic actors in social events, exhibitions and study tours. (SC1 and SC2)	Communication between the dyadic actors In the SC (L.R)	
Internal-focused key themes "Dyadic Level"		
-Exchange activities in dyads (SC1 and SC2) *-Business planning with dyadic actors in the supply chain. (SC1 and SC2)*	Activities between the dyadic actors and other firms in the SC (L.R)	Contacting strategy
-Tapping into the chain's physical resources (SC1 and SC2) *-Tapping into the chain's human resources (SC1 and SC2)*	Resources gained by the two actors from their SC (L.R)	
-Problems with contracts (SC1 and SC2) *-Changes in policies and standards (SC1 and SC2)*	Uncertainty in the dyad (NT)	
-Cost analysis between the two actors in relationships *(SC1 and SC2)*	Cost analysis (L.R)	Price strategy
-Price setting across the entire supply chain relations (SC1 and SC2)	Pricing process (L.R)	
-Selfish behavior between the partners and misleading behavior in the SC. (SC1 and SC2)	Opportunism Between the dyadic actors in the SC (NT)	
-Costs distribution between the two dyadic actors (SC1 and SC2)	Sharing costs (L.R)	Revenue strategy
-Profits distribution between the two dyadic actors (SC1 and SC2)	Sharing profits (L.R)	
-Equal benefits of profits and sustainable aspects are between the dyadic actors (SC1 and SC2)	Equal benefits (L.R)	

Evidence is shown in FFV Supply chain 1 (SC1), FFV Supply chain 2 (SC2), Literature Review (LR) and New Theme (NT)

At the FFV supply chain level (see Figure 2), there was strong evidence in the literature that sustainable relationships cannot be formed without the link between demand and supply where products flow from the main supplier to the end-customer [27, 28]. This is important for all dyadic relationships in the supply chain. A manager SC1 said: "*The product flow is the movement of products which is managed and communicated on both assets investment and human resources from a supplier to a customer for good information […]."* Another manager SC2 said: "*In fact, we discuss the product flow with our chain actors to develop frequent collaboration […]."* Although information flow and systems may be an antecedent to the interaction of collaborative chain actors, the case studies found that all dyadic actors recognized the importance of developing strong information flow links, which include the collaboration themes. A manager SC1 explained: "*We all take it as a responsibility to try, where we can, to pick up competitive information based on cooperation and coordination […] frequently get it and bring it back in."* A manager SC2 explained that: "*He or she can get feedback from the communication with customers, end users, from the sales and marketing team, from his own team. It comes from a variety of points based on actor position [...] the market information is then disseminated back through regular, functional meetings and also systems."*

At the dyadic relationship level, the two actors in a dyadic sustainable relationship can share tactical information (e.g. operations and logistics) and strategic information (e.g. marketing and customer information) in order to incorporate more benefits [4]. Those actors can be motivated to share information when they are aware of the benefits and revenue control that information sharing can bring. A manager SC1 said: "*The companies ask us to provide them with information and we also do the same […] this helped us to sign contracts to collaborate with them all the time especially to have accurate, various and valuable information from our sustainable actors for better equal revenue and profits […]".* A manager SC2 explained: "*Yes, collaborations make the solid sustainable relationships. There are various methods of exchange through contracts, social networks, social events, workshops, mail, face-to-face meetings, telephone, internet, and faxes […] in addition we regularly plan together and form budgets and pricing strategy for our advanced collaboration."* Information sharing is enhanced by an efficient information flow in order to establish better sustainable value relationships for better decision making along the product flow [10]. It is this process of disseminating and sharing information between chain actors which is believed to underpin dyadic relationships between the two actors based on the sharing of pricing strategy and revenue strategy and on forming a contracting approach for both in order to enhance a sustainable FFV supply chain.

The dyadic actors in both supply chains realize the benefits of developing solid ties with each other. The findings suggest that dyadic actors have a key motivation behind developing information sharing for their collaboration. Therefore, from table 3, the overall aggregate theme of information sharing is linked to five aggregate dimensions: product flow strategy of asset specificity, actor position and transaction frequency; and information flow strategy of cooperation, coordination and communication at the supply chain level and contracting strategy of activities, resources and uncertainty; price strategy of cost analysis, pricing process and opportunism; and revenue strategy of sharing costs, sharing profits and equal benefits at the dyad level. Amongst these themes, actor position, uncertainty and opportunism are concepts that have newly emerged from the stage of exploring the two case studies. Therefore, the research attempts to further understand the key theme of information sharing for collaboration in SBSRs in the FFV context with a focus on these five dimensions, their themes and the newly emerged themes in the explanation stage of cross-case analysis below.

4.2. Cross-Case Study Level

Academic researchers have proposed definitions, frameworks and key findings to carry out development in sustainable supply chains [e.g. 14, 9]. Their research studies are formed based on key underpinning concepts that can be termed the building blocks of assumptions and frameworks. However, a wider body of knowledge about SBSRs is needed to overcome overlapping concepts in order to generate consistent findings [9]. Thus, the intention of the present research is to contribute to the body of knowledge by providing new propositions for collaboration for SBSRs attached to information sharing between the dyadic actors in FFV supply chains.

At the cross-case level, to answer RQ2, we explain how and why the key themes of information sharing are effectively linked to collaboration in SBSRs to improve value chain performance in practice. The exploratory case studies have indicated that the key themes should be categorized into two themes: theme 1- external-focused key themes between all dyadic actors at the supply chain level: information flow of cooperation, coordination and communication; product flow of assets investment, actor position and frequency. Theme 2- internal-focused key themes between dyadic actors in their dyadic sustainable relationships: pricing strategy of cost analysis, pricing process and opportunism; revenue strategy of sharing costs, sharing profits and equal revenue; contracting strategy of activities, joint planning and opportunism. Amongst these, information sharing has become the central theme, which is formed by themes 1 and 2 as antecedences for information sharing. The cross-case analysis has provided more explanations for these key themes, where the dyadic actors of sustainable relationship are the key sustainable actors that find the right framework for collaboration to create sustainable value along the FFV supply chain. Table 4 illustrates the key themes, their definitions and key supporting authors.

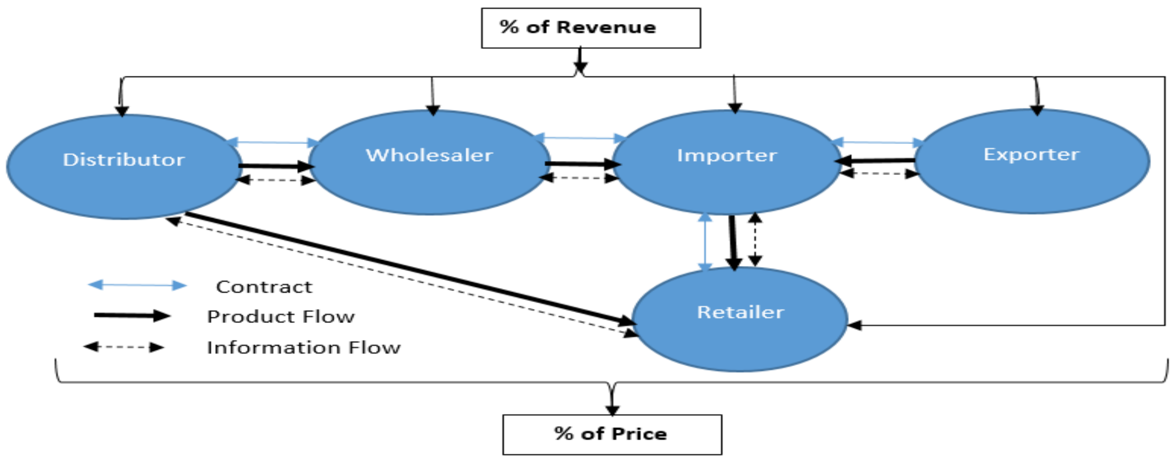

Figure 2. FFV supply chain.

Table 5 shows data triangulation, including representative quotes from interviews and observations. The interviewed managers in all cases among the ten relationships indicated the importance of pricing strategy, revenue strategy and contracting strategy as three key themes for internal-focused information sharing drivers [14, 29] and the concepts of product flow and information flow as two key themes for external-focused information sharing drivers [26, 18]. This is also supported by evidence from meetings between the dyadic actors at each sustainable relationship.

Table 4. Key themes of information sharing for collaboration in sustainable relationships, their definitions and key supporting author.

Key theme	Definition (Present research)	Key supporting author
Information flow Strategy	Both effective formal and informal interactions for information management (cooperation, coordination and communication) where chain actors working at cross-purposes with a dyadic actor to develop cohesive strategy and systems for information sharing, which is essential for collaboration.	Porter and Millar (1985); Burritt and Tingey-Holyoak, (2012).
Product flow Strategy	Both direct and indirect interactions for relationship management (asset investment, actor position and transaction frequency) where chain actors working at cross-purposes with a dyadic actor to exchange products along the supply chain forming a link between demand and supply for collaboration.	Horvath (2001); Flynn et al. (2010).
Contracting Strategy	An arrangement that can be as a set of rules of between dyadic actors in their collaborative supply chain for optimization and what roles they may perform based on their information sharing.	Williamson (1979)
Price Strategy	An approach that involves price setting and processes across dyadic actors in the entire supply chain in order to link strategic partner to better business agreements of appropriate duration.	Voeth and Herbst (2006) Formentini and Romano (2016)
Revenue Strategy	An approach that involves sharing costs and profits across dyadic actors in the entire supply chain in order to link strategic partner to better profit margins of appropriate duration.	Van der Rhee et al. (2010); Formentini and Romano (2016)
Information Sharing	A set of exchanges of data, knowledge and experience between the dyadic actors for collaboration in their SBSR in the entire supply chain.	Porter and Millar (1985). Kembro, et al. (2014)
Collaboration	A business relationship between dyadic actors based on information sharing that yields in a competitive advantage resulting in a greater sustainability business performance.	Spekman et al. (1998); Luzzini, et al. (2015).

Table 5. Data triangulation: interview quotes and observations.

Case	Relationship	Representative Quotation	Observation
Case 1	Relationship A1	"*We are looking for a win-win solution, where we can, to work cooperatively with our importer […] to develop a sustainable relationship of coordination, good communication, trust and agree on beneficial options for competitive resource agenda and training programs[...].*"	A meeting between the retailer and the importer, June 2018.
	Relationship B1	"*Our sustainable importer always ask about how we can help in managing their product flow with other transactional actors […] we do that in different ways such as providing a holistic support for quality systems at chain level, negotiate with the government to solve their leading approach along the supply chain […].*"	A meeting between the importer and the exporter , June 2018.
	Relationship C1	"*Our contracts are for setting sharing many things together[…] actually we share activities, resources and uncertainty for the success of our dyad, leading to shar information in a way of sharing costs, price setting and also positive financial benefits with them […]*".	A meeting between the retailer and the distributor, June 2018.
	Relationship D1	*"We also support jointly our regular and old suppliers in a dyad for tax flexibility, sharing our market facilities, providing a membership for market information, but still this is not effective […]".*	A meeting between the distributor and the wholesaler, July 2018.
	Relationship E1	"*Our relationship with importers is for setting together and putting joint planning together for our costs and then profits […] It is a way of sharing information for gaining better performance with our actors in the chain […]*".	A meeting between the wholesaler and the importer, July 2018.
Case 2	Relationship A2	*"[…] we do want to support our retailer to develop our coordinated transportation and equipment and there is frequent meetings for this cooperation."*	A meeting between the retailer and the importer, June2018.
	Relationship B2	"*Yes, we do want to support exporters to develop their logistics (e.g. transportation and equipment) in the future transactions and there is a number of sharing for frequent meetings, plans, cost, profits and training for this sustainable purpose.*"	A meeting between the importer and the exporter , June 2018.
	Relationship C2	"*Our sustainable retailer ask about how we can manage their product flow with other transactional actors […] we do that in different ways such as providing a holistic support for quality systems at chain level, negotiate with the government to solve leading approaches along the supply chain […].*"	A meeting between the retailer and the distributor, June 2018.
	Relationship D2	*"Our dyadic actor is fully aware about our pricing strategy on raw material, packaging, customer service and even our damaged inventories […].*	A meeting between the distributor and the wholesaler, July 2018.
	Relationship E2	*"Pricing together is the way we share information […] we always try to avoid any misleading by analysis costs together and putting prices scenarios together."*	A meeting between the wholesaler and the importer, July 2018.

Both the literature review and cross-case findings support the suggestion that information sharing is the main key for collaboration between dyadic actors that affect their sustainable relationship, and this is also based on good information sources from both actors and demand-side [6, 30]. Findings from cross cases highlighted how dyadic actors at both levels, chain and dyad, share information for a long-term collaboration, and this reflects a positive sustainable relationship approach. The key findings have highlighted the fact that both dyadic actors in all relationships for dyads (A1, A2), (B1, B2), (C1, C2), (D1, D2), (E1, E2) generally identify high effects of the antecedents in forming information sharing for collaboration in SBSRs. The relationships of cases (E1, E2) show low to medium effects of the antecedents in forming information sharing in sustainable relationships. Overall, the most significant antecedents are information flow, pricing strategy, revenue strategy towards information sharing as can be seen in the overall scores of cross cases that reflect medium to high effects of the antecedents. On the other hand, the rest of the antecedents, product flow and contracting strategy, reflect medium effects of the antecedents in forming information sharing in collaboration between the dyadic actors for better sustainable relationships in FFV supply chains (Table 6).

This research finds that there is strong support for the emergent propositions from the two cases, where dyadic actors function to build their sustainable relationships of collaboration based on the information sharing between them, where information flow and product flow also affect these dyads at the FFV supply chain level. In these cases, the dyadic actors are mainly local organizations which form strong collaborations in their sustainable relationships along the FFV supply chains. This includes training and workshops as coordination activities, equipment and technology for production development as resource allocations, quality control as joint planning, cost analysis for their shared products, and reasonable sharing costs for input purchasing and various business tours. These findings are consistent with works by Fearne [14], Mikkola [31], Bailey and Francis [10] and Porter and Kramer [16], who have indicated that many of these themes drive information sharing in collaboration for sustainable relationships. However, in both cases the dyads E1 in SC1 and E2 in SC2 offer weak support for these propositions. In both dyadic sustainable relationships, actors are part of a wholesaler-importer dyad which provides very limited support for information sharing between them along the supply chain. For example, there is a membership body at the wholesaler site for the importer and this is not effective and has very limited activities. There is also a limited number of coordinated training sessions and workshops within specific projects. Quality control programmes are also very few as a joint planning, certification body as cooperation is available for cooperation in a short time, and both have low sharing costs for exhibitions and tour visits for local and export markets. This finding gives a similar framing to those developed by Jraisat and Sawalha [32] and MacMillan, et al. [33].

Table 6. Antecedents of Information Sharing in collaboration for sustainable relationships: Cross-Case Comparison based on chain level /dyad level-focused themes

Case Study		**External-focused Key theme (Chain level-focused)**						**Internal-focused Key theme (Dyad level-focused)**								
		Information Flow			**Product Flow**			**Pricing Strategy**			**Revenue Strategy**			**Contracting Strategy**		
		Cooperation	Coordination	Communication	Assets investment	Actor position	Frequency	Cost Analysis	Opportunism	Pricing Process	Sharing Costs	Sharing Profits	Equal Revenue	Activities	Resources	Uncertainty
Case 1 (SC1)	Relationship A1	H	H	H	H	M	H	H	M	H	H	M	H	H	M	H
	Relationship B1	H	H	H	H	H	H	H	H	H	H	H	H	H	H	H
	Relationship C1	H	H	H	H	H	M	H	M	H	H	H	H	H	H	H
	Relationship D1	H	H	H	H	H	H	H	H	H	H	M	H	H	H	H
	Relationship E1	M	M	L	L	L	L	L	L	M	L	L	L	M	L	L
Case 2 (SC2)	Relationship A2	H	H	H	H	H	H	H	M	H	H	H	H	H	M	H
	Relationship B2	H	H	H	H	M	H	M	L	H	M	M	M	M	M	H
	Relationship C2	H	H	H	M	H	M	H	L	H	M	M	H	M	M	H
	Relationship D2	M	H	H	L	L	H	M	L	M	M	M	M	M	M	M
	Relationship E2	M	L	L	L	L	L	L	M	M	L	L	M	M	L	L
	Overall Score	H	H	H	M	M	M	H	M	H	H	M	H	M	M	M

Level of scoring from the perspective of dyadic actors: High (H), Medium (M), Low (L).

The key findings have highlighted how information flow promotes collaboration, and that effective internal formal interaction (meetings and conferences), and informal interaction (casual contacts) may be used to develop a cohesive strategy at a dyad level. Cooperation has become the starting point for information flow as a necessity [20]. Coordination and communication between partners takes various forms, such as the use of information technology and/or other traditional ways such as current plan sharing and exchange of resources and experts, possibly between chain members and service providers [31]. The case studies found that all ten relationships recognized the importance of developing cooperation, coordination and a communication approach, including the process of an interest base for information sharing. Most of the managers in all dyads displayed evidence of these themes between the dyadic actors through the development of collaborative SBSRs. There was negotiation in many relationships about what is jointly possible and desirable. A few relationships showed little evidence of good information flow and cooperation in exchange information, and these relationships were the least effective in collaboration. It is proposed that:

P1. Information flow of cooperation, coordination and communication between dyadic actors at the chain level will have good effects on information sharing between them in their collaboration for a sustainable relationship.

Product flow was added to the key themes, with the expectation that it would have a positive impact upon collaboration. It is indicated that the members of a chain are all actors with whom the focal actor interacts directly or indirectly through its service providers, suppliers or customers, from the point of origin to consumption. Actors partake in the various value chain flows, including product, payment, information, agency support and promotion flows [28]. it is necessary to manage product flow to facilitate other flows, such as information and financial flows at the chain level to create knowledge sharing and dissemination mechanisms at the dyad level. The benefits of cross-functional collaboration between actors on which value to create and what information to share, for instance, is already apparent due to increased collaborative quality control and systems (e.g. HACCAP, Global GAP etc.), transactional framework and regulation positions (e.g. local authority or international authority), etc. [15]. The case studies found that all ten relationships focus on product flow to share product activities in the FFV chain, leading to information sharing for both dyadic actors. It is proposed that:

P2. Product flow of asset specificity, transaction frequency and actor position between dyadic actors at the chain level will have good effects on information sharing between them in their collaboration for a sustainable relationship.

Contract strategy is an approach to formal and informal agreements to set up the dyadic relationship with the highest mutual sharing of information and the lowest possible costs [34, 35]. This strategy is related to an economic approach that is linked to enhancing transactions between buyers and sellers based on maintaining incomplete contracts. This strategy will encourage various activities and resources allocation to help actors in sharing information for better actions towards best costs, prices and profits. Furthermore, dyadic relationships are the core of investments in time, money and effort, and they are means by which information and uncertain actions and performance are merged [15]. The case studies found that all ten relationships focus on the contracting strategy in formal or informal ways to share activities (e.g. planning quality protocols), allocate resources (e.g. adopting new ICT technology) and manage uncertainty (e.g. use of traceability systems), leading to information sharing for both dyadic actors. It is proposed that:

P3. The contract strategy of activities, resources and uncertainty management between dyadic actors at the dyad level will have good effects on information sharing between them in their collaboration for a sustainable relationship.

Price strategy is a way for dyadic actors in their collaboration to analyze costs and pricing processes along their functions, leading to sharing a set of information [15]. This mutual strategy focuses on pricing between buyers and sellers from inside the supply chain, affecting the price lists offered to end customers [19]. This economic approach is part of sustainability development to be integrated with mainstream information and management systems. Gathering and sharing data from various valuable sources leads to rich information availability, leading to better social interaction and environmental aspect along the chain [36]. All managers explained that they fully apply the concept of pricing in their actions with the dyadic actors and most of their partners are aware of the importance of efficient collaborative cost analysis for reintegrating the business functions for better benefits for economic and social issues. A sustainable relationship is highly vulnerable compared to other relationships due to external directions such as incorrect information, economic issues, off-season supply and demand and environmental regulation, as well as internal directions arising due to weak organizational structure (e.g. no expertise, poor data, insufficient information systems and information visibility). These directions have led dyadic actors to bond with each other in order to gain support in managing their internal and external effects [30, 28]. Hence, an efficient price strategy plays an important role in supporting actors against such chain-related ambiguities. It is proposed that:

P4. The price strategy of cost analysis, pricing processes and opportunism between dyadic actors at dyad the level will have good effects on information sharing between them in their collaboration for a sustainable relationship.

Revenue strategy is an approach to sharing costs and profits between dyadic actors in their operations strategy, methods and technologies in order to include the implementation of the supply chain paradigm and information management. In particular actors play the key role in equal value and return along the chain for activities that link widely dispersed producers to consumers. Revenue strategy is now viewed by many scholars as a powerful action for moving towards collaboration and for speeding sustainable results in the value chain. Revenue strategy between dyadic actors provides equal benefits, including revenue enhancements, cost reductions, and flexibility to cope with high demand uncertainties [37]. Literature and the case studies indicate that revenue strategy is important to establishing SBSRs based on information sharing, and it is a synergy for collaboration. It is proposed that:

P5. Revenue strategy of cost sharing, profit sharing and equal benefits between dyadic actors at the dyad level will have good effects on information sharing between them in their collaboration for a sustainable relationship.

All the case studies agreed that collaboration between dyadic actors has a positive impact on sustainability value chain performance, and that collaboration based on information sharing is not just based on close relationships, but must be supported by aligned goals and interaction development. A number of authors [e.g. 38, 39] have identified a positive link between collaboration and improved sustainable performance. Weak collaboration between dyadic actors may have a detrimental effect upon business performance, whilst effective collaboration should improve business performance. Each actor was asked about their actors' performance in terms of profit and access to markets, social factors (e.g. job creation, family work) and environmental factors (e.g. water pollution, chemical use, health hazards). The dyads A, B and C were the actors that most reflected sustainable performance and also achieved the highest indicators in terms of their industry norm and had a healthy market share, positive social impact and efficient environmental activities, whereas cases D and E both exhibited the least collaboration between dyadic actors and had the lowest profit and a weak market share, minimum social interaction and limited environmental results. According to Hsu et al. [4], actors should pay attention to both financial (e.g. profit) and non-financial (e.g. quality) criteria of business performance. Sustainability management includes considerations of social aspects and environmental issues of actor activities, as well as their interaction with economic performance. This is important considering that actors usually focus on these criteria and tend to neglect the sustainability criteria. In fact, high sustainability-performing collaboration included a few distinctive features, regarding the family business stability, hazard analysis, climate change, and longer interaction amongst value chain actors in the agricultural sector. These measures of business success indicate a positive association between information sharing in collaboration and sustainability performance. Therefore, it is proposed that:

P6. *Improvements in collaboration between dyadic actors based on information sharing will positively influence sustainability performance at the chain level*.

As can be seen in the conceptual framework in Figure 3, the direction of the variables in the conceptual framework should proceed from the actors' factors influencing information sharing to collaboration between dyadic actors, and then to overall sustainability value chain performance in the FFV supply chain.

5. Conclusions and Managerial Implications

The present research has explained the studied themes jointly and extended extant work by focusing on the sustainable relationship context. This work provides propositions that have been generated with support from the literature review and a multi- case study.

This research raises interesting areas of study. First, the conceptual framework (Figure 3) indicates significant opportunities for future studies. A key opportunity exists at the collaboration levels which are developed within the sustainable relationship context. Prior research has indicated that information sharing [e.g. 5, 10, 15] is needed at various levels of collaboration development and then improvement, raising empirical questions to examine each level, both dyad and chain. This study is qualitative in nature and the conceptual framework needs to be tested through further qualitative studies or quantitative studies involving large-scale surveys.

From a practical perspective, both dyadic actors who work at improving collaboration for sustainable relationships in the FFV supply chains can benefit from the conceptual framework. This framework offers a guideline to form and describe collaboration between actors along the value chain based on information sharing. Five antecedents to information sharing are highlighted that may be applied to improve collaboration at the dyad level between partners along the information flow that leads to better value creation in their functions including the product flow within the FFV supply chain. To improve information sharing between the dyadic actors, managers should identify good source of information, classify information types, apply a variety of sharing methods and indicate what value of information they need. Managers can apply contracting strategies, such as activities of supply scheduling and planning, price strategies, such as sharing the pricing process, and revenue strategies, such as distributing an equal return percentage. In this way, managers can have shared information (e.g. data or knowledge on quality control, demand, packaging etc.) in their value generation activities along the chain activities for sustainable value added in FFV supply chains.

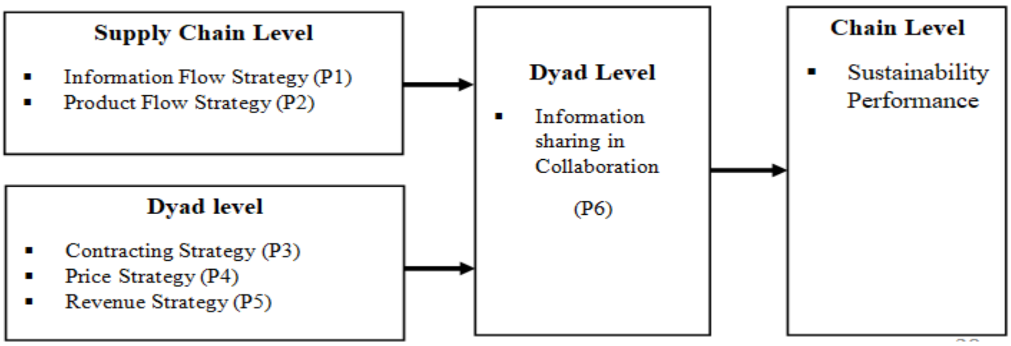

Figure 3. Conceptual framework: collaboration for sustainable relationships in FFV supply chain

References

[1] Porter, M. E. Competitive advantage: Creating and sustaining superior performance. New York: Free Press; 1985

[2] Aggarwal, S. and Srivastava, M. K., "Towards a grounded view of collaboration in Indian agri-food supply chains: A qualitative investigation", British Food Journal, Vol. 118, No.5,2016, 1085-1106

[3] Stewart, T. Intellectual capital: the new wealth of organisations. London: Nicholas Brealey;1998.

[4] Hsu, C.C., Kannan, V.R., Tan, K.C. and Leong, K.C., “Information sharing, buyer-supplier relationships, and firm performance: a multi-region analysis”, International Journal of Physical Distribution & Logistics Management, Vol. 38, No. 4, 2008, 296-310.

[5] Porter, M. and V. Millar, “How information gives you competitive advantage,” Harvard Business Review, Vol.63 No.4, 1985. 149–160.

[6]Francis, M.,“Application of the food value chain analysis meth od in the UK red meat industry”, Proceedings of the 9 th Inte rnational Symposium on Logistics, 104-109, UK, 2004.

[7] Xue, X., Shen, Q., Tan, Y., Zhang, Y., and Fan, H. (2011), “Comparing the value of information sharing under different inventory policies in construction supply chain”, International Journal of Project Management, Vol.29, No.7, 2011, 867-876.

[8] Niall, P. and Rich, N., “The relationship between lean operations and sustainable operations”, International Journal of Operations and Production Management, Vol. 35, No. 2, 2015, 282-315.

[9] Esfahbodi, A. Zhang, Y. Watson, G., “Sustainable supply chain management in emerging economies: Trade-offs between environmental and cost performance”, International Journal of Production Economics, Vol.181, 2016, 350–366.

[10] Bailey and Francis, “Managing information flows for improved value chain performance”, International Journal of Production Economics, Vol.111, No.1, 2008, 2-12.

[11] Cheng, J.H., “Inter-organizational relationships and information sharing in supply chains”, International Journal of Information Management, Vol. 31, No.4, 2011, 374-384.

[12] Pagell, M. and Shevchenko, A., “Why research in sustainable supply chain management should have no future”, Journal of Supply Chain Management, Vol. 50 No. 1, 2014, 44-55.

[13] Luzzini, D., Brandon-Jones, E., Brandon-Jones, A. and Spina, G., “From sustainability commitment to performance: the role of intra- and inter-firm collaborative capabilities in the upstream supply chain”, International Journal of Production Economics, Vol. 165, 2015, 51-63.

[14] Fearne, A., “The evolution of partnerships in the meat supply chain: insights from the British beef industry”, Supply Chain Management, Vol.3 No.4, 1998, 214-231.

[15] Jraisat, L., Gotsi, Manto and Bourlakis, M., “Drivers of information sharing and export performance in the Jordanian agri-food export supply chain: A qualitative study”, International Marketing Review, Vol. 30, No.4, 2013, 323-356.

[16] Porter, M. E., and Kramer, M. R., “Shared value: How to reinvent capitalism—and unleash a wave of innovation and growth”, Harvard Business Review, Vol.89, No.12, 2011, 62-77

[17] Ding, H., Guo, B., and Liu, Z., “Information sharing and profit allotment based on supply chain cooperation”, International Journal of Production Economics, Vol.133, No.1, 2011, 70-79.

[18] Tasca, A. L., Nessi, S. and Rigamonti, L., “Environmental sustainability of agri-food supply chains: An LCA comparison between two alternative forms of production and distribution of endive in northern Italy”, Journal of Cleaner Production, Vol.140, 2017, 725-741.

[19] Van Der Rhee, B., Van Der Veen, J.A., Venugopal, V. and Nalla, V.R., “A new revenue sharing mechanism for coordinating multi-echelon supply chains”, Operations Research Letters, Vol. 38, No. 4, 2010, 296-301

[20] Spekman, R. E., Jr, W. K. J. and Myhr, N., “An empirical investigation into supply chain management: A perspective on partnership”, Supply Chain Management: An International Journal, Vol.3, No. 2, 1998, 53-67.

[21] Rottman, J. W., “Successful knowledge transfer within offshore supplier networks: A case study exploring social capital in strategic alliances”, Journal of Information Technology, Vol. 23, 2008, 31-43.

[22] Williamson, O.E., “Transaction-cost economics: the governance of contractual relations”, Journal of Law and Economics, Vol. 22, No. 2, 1979, 233-261.

[23] Song, H., Turson, R., Ganguly, A. and Yu, K. "Evaluating the effects of supply chain quality management on food firms’ performance: The mediating role of food certification and reputation", International Journal of Operations & Production Management, Vol. 37, NO. 10, 2017, 1541-1562.

[24] Miles, M. B., Huberman, A. M., & Salda~na, J. Qualitative data analysis. A methods sourcebook, 3rd ed. Thousand Oaks, CA: SAGE Publications, Inc; 2014.

[25] Voss, C., Tsikriktsis, N. and Frohlich, M., “Case research in operations management”, International Journal of Operations & Production Management, Vol. 22, No. 2, 2002, 195-219

[26] Thiele, G.; Devaux, A.; Reinoso, I.; Pico, H.; Montesdeoca, F.; Pumisacho, M.; Andrade-Piedra, J.L.; Velasco, C.; Flores, P.; Esprella, R.; Thomann, A.; Manrique, K.; Horton, D., “Multi-stakeholder platforms for linking small farmers to value chains: Evidence from the Andes”, International Journal of Agricultural Sustainability, Vol.9, No.3, 2011, 423-433.

[27] Horvath, L., "Collaboration: the key to value creation in supply chain management", Supply Chain Management: An International Journal, Vol. 6, No. 5, 2001, 205-207

[28] Flynn, B.B., Huo, B. and Zhao, X., “The impact of supply chain integration on performance: a contingency and configuration approach”. Journal of Operation Management, Vol. 28, No.1, 2010, 58–71.

[29] Christopher, M. Logistics and Supply Chain Management - Strategies for Reducing Cost and Improving Service. 2nd edition., Prentice Hall; 1998.

[30] Taylor, D.H. and Fearne, A., “Towards a framework for improvement in the management of demand in agri-food supply chains”, Supply Chain Management: An International Journal, Vol.11, No.5, 2006, 379–384

[31] Mikkola, M, “Coordinative structures and development of food supply chains”, British Food Journal, Vol. 110, No. 2, 2008, 189-205.

[32] Jraisat, L. and Sawalha, I., “Quality control and supply chain management: a contextual perspective and a case study”, Supply Chain Management: An International Journal, Vol. 18, No. 2, 2013, 194-207.

[33] MacMillan, K., Money, K., Money, A., & Downing, S., “Relationship marketing in the not-for-profit sector: An extension and application of the commitment-trust theory”, Journal of Business Research, Vol.58, 2005, 806–818.

[34] Williamson, O. E., “Outsourcing transaction cost and supply chain management”, Journal of Supply Chain Management, Vol. 44, No.2, 2008, 5 – 15.

[35] Riordan, M., and Williamson, O., “Asset specificity and economic organization”, International Journal of Industrial Organization, Vol.3, 1985, 365-78.

[36] Williams, Z. and Moore, R., “Supply chain relationships and information capabilities: The creation and use of information

power", International Journal of Physical Distribution & Logistics Management, Vol.37, No.6, 2007, 469-483.

[37] Simatupang, T. M. and Sridharan, R., "The Collaboration Index: a measure for supply chain collaboration", International Journal of Physical Distribution & Logistics Management. Vol.35, No.1, 2005, 44-62.

[38] McAdam, R., Hazlett, S-A. and Anderson-Gillespie, K., "Developing a conceptual model of lead performance measurement and benchmarking: A multiple case analysis", International Journal of Operations & Production Management, Vol. 28, No. 12, 2008,1153-1185

[39] Acquaye, A., Genovese, A., Barrett, J. and Koh, S.C.L., "Benchmarking carbon emissions performance in supply chains", Supply Chain Management: An International Journal, Vol. 19, No. 3, 2014, 306-321.

JJMIE

Volume 13, Number 4, December. 2019
ISSN 1995-6665
Pages 291 - 299

Jordan Journal of Mechanical and Industrial Engineering

Applying Management Principles of Lean Manufacturing for Enhancing Efficiency and Effectiveness of Emergency Department Rooms

Mwafak Shakoor [a*], Mohamed Rafik Qureshi [b], Samar Jaber [a]

[a]Mechanical Engineering Department, American University of Madaba, P.O.Box 2882 Amman 11821, Jordan
[b]Industrial Engineering Department, King Khalid University, Abha 61421, Saudi Arabia

Received 25 November. 2019

Abstract

The lean manufacturing approach plays a vital role in reducing waste and enhancing productivity in the production environment and service setups. Lean manufacturing-based techniques might be employed in evaluating the efficiencies of different rooms in emergency departments (EDs) and hospitals. A lean thinking approach may be used in testing the usage of the existing facilities planned and constructed for patients' use. In the present study, the management principles of lean manufacturing-based methodology have been used to test the usage of the ED services. Two vital rooms of the ED viz. rapid response trauma (RR-Trauma) and rapid response medical (RR-Medical) are studied in terms of crowding and bed occupancy. Using the concept of takt time (TT), an individual department's efficiency and relative efficiency have been calculated to judge the effectiveness of the ED services. A case of a governmental, non-profit and teaching hospital in the southern region of Saudi Arabia has been studied to see the effect of staffed bed redistribution based on lean manufacturing concept. It has been revealed that ED is facing crowding and frequent critical ambulance diversion problems which require a management intervention to go for staffed bed redistribution to accommodate all of the patients' arrivals. Furthermore, the optimal allocation of resources is essentially be achieved to enhance the efficiency and effectiveness of ED rooms. Based on the lean manufacturing concept, the acceptable TT and efficiency for ED rooms are recommended.

Keywords: Cycle time (CT); Efficiency; Emergency department (ED); Lean manufacturing; Takt Time (TT).

1. Introduction

The emergency department (ED) plays a powerful function in a human being's risk management. There is an increasing risk of a sudden outbreak in the present age and an increased rate of injuries which places the burden on ED. To counteract the various natural diseases, scientists have developed remedies to cure most of the diseases in the present age. However new diseases are erupting from time to time thus makes everybody on their toes to develop a strategy to protect humanity. Also, man-made or natural disasters, injuries, epidemics of infectious diseases caused by viruses, etc. are the main reasons why emergency departments are crowded. The accidents are considered to be a major man-made threat to human beings around the globe. According to the World Health Organization (WHO), road traffic injuries caused an estimated 1.24 million deaths worldwide annually, which amounts to the accidental death of one person every 25 seconds. Furthermore, according to figures from statistics of Saudi Arabia, every second a car accident happens and on average 17 people are killed in accidents every day [1].

The epidemic eruption and increased accident rate pose great challenges to ED. The EDs are facing many challenges, some of which are very critical. The overcrowding problem in the ED is a major threat therefore, ambulance diversion problems can be faced due to the crowding problem in ED and boarding takes place which may put the patients in great danger. Also, in the case of accidents, sometimes the patients are brought in the critical situation warrants the medical aids in time, if not tackled quickly the patient may lose precious life.

One of the major problems faced by ED is overcrowding of patients and consequently ambulance diversion. Ambulance diversion is defined as the process of turning away the ambulance from the ED to another hospital due to insufficient staffed bed capacities or deficiency in the ED management process. Ambulance diversion poses a risk to any patient and endangers his or her life when needs immediate medical care.

The ED under study is part of a governmental, teaching and non – profit hospital located in Saudi Arabia. The ED in this hospital faces a serious overcrowding problem and ambulance diversion in the rapid response trauma (RR-Trauma) room and rapid response medical (RR-Medical) room. Therefore; ambulances are redirected to private

* Corresponding author e-mail: mmshakoor@yahoo.com

hospitals in the city due to the agreement between the Saudi Ministry of Health (MOH) and the private health sector. According to this agreement, the Ministry of Health is responsible for all the patients' care expenses in private hospitals. Hence, this situation will increase the cost of the provided healthcare services by the MOH. Furthermore, ambulance diversion is only taking place at RR-Trauma and RR-Medical. There is no ambulance diversion is taking place at the other ED rooms. The patients in such rooms have to wait or leave and seek services in other private hospitals at their expenses.

The lean management principles have gone far in the last decade and covered almost every field of production and service organizations. The vary introduction and implementation of the comparison analysis lean production system in Toyota has now a great impact on different areas of production and services. The various lean practices have shown that lean production methods are equally applicable to ED. Thus, lean management based concepts have been applied in ED rooms to resolve various issues faced regularly.

Looking at the ample potential and opportunities of lean implementations in services, the present research has been carried out with the following objectives:

1. To use the lean management based methodology in the service improvement of ED rooms of a governmental hospital.
2. To calculate the various efficiency of ED rooms and provide optimal redistribution of staffed bed to enhance efficiency and effectiveness

The paper is further organized as follows. Section 2 reviews the available literature on ED services and efficiency. Section 3 highlights the significance of cycle time (CT) and Takt Time (TT). Section 4 is about revisiting ED services of a government hospital. Section 5 discusses the results of the study, it also provides a comparative analysis of various ED rooms and staffed bed redistribution strategy. Section 6 provides a discussion on the present research. The paper ends with a conclusion in section 7.

2. Literature Review

In recent years, several researchers have studied the problem of patients' long waiting times in the healthcare sector in general and ED rooms in particular. The reduced waiting time and crowding in ED rooms will enhance service time effectiveness to improve the quality of delivered care services [2 – 7]. Keith et al. [8] researched on achieving wait time reduction in the ED. Their quality improvement team was able to achieve a large reduction in waiting time in the ED. Thereafter; Oredsson et al. [9] studied the worldwide problem of overcrowding in the ED. They used a scientific approach to explore the right intervention to improve patient flow in the ED.

Lean thinking principles have found its origin in the production area [10]. It has been applied to production and service management to enhance the productivity of resource utilization and many lean thinking studies have been carried out in a production environment. Braglia et al. [11] and Vendan and Sakthidhasan [12] used value stream mapping (VSM) lean tool in complex production systems. Matt and Rauch [13] studied the implementation of lean production principles in small-sized enterprises and Mandahawi et al. [14] assessed printing and cutting machines performance on the bases of customized Lean Six Sigma approaches at a paper manufacturing company. Marodina and Saurina [15] highlighted research areas and opportunities in lean production systems.

However, the applications of lean thinking principles have been extended to the healthcare sector. Many studies explored the application of these principles in healthcare organizations and ED to reduce waiting time and improve patients' flow [16 – 21]. Murrell et al. [22] applied lean thinking principles to develop a rapid triage and treatment (RTT) system in ED of community hospital and Holden [23] critically reviewed lean thinking in ED for understanding the effects of lean on ED work structures and processes, patient care, and employees, as well as the factors on which lean's success is contingent. Later on, Gill [24] used the application of VSM to eliminate waste in an emergency room.

In a process of ED services improvement, many researchers attempted to reduce the waiting times in the ED [25]. Mandahawiet al. [26] attempted to reduce waiting time in the ED using design for six sigma and discrete event simulation. Also,Vermeulen et al. [27] evaluated an ED using a lean process improvement program to reduce the length of stay (LOS).

The staffed bed redistribution has been an important research area for the researchers attempting to enhance the efficiency and effectiveness of the ED room. Akkerman and Knip [28] applied Markov chain theory and simulation experiments to carry out the staffed bed reallocation. Mehrolhasani et al. [29] applied a goal programming model for staffed bed reallocation. Khare et al. [30] applied computer simulation to decide the number of staffed beds in the ED. Diane et al. [31] used the application of lean thinking to redesign the ED. Teng-Kuan et al. [32] applied lean principles and simulation for the optimization for ED layout design

From the in-depth literature review, it has been found that using a lean thinking approach; efficiency can be calculated for various rooms of EDs for useful comparison. Thus, the present research attempts to bridge this gap.

3. Significance of CT and TT

As soon as the patient rushes in ED, the staff on duty takes due care in managing the existing emergency. The CT and TT are crucial in managing the number of patients rushing to ED. The increase in CT will increase the length of stay (LOS) and affect staffed bed availability. Thus, CT and TT become the important process analysis parameters required in determining the system efficiency and effective service rate. CT is the exact time required to serve a patient in ED, whereas a TT is the new time required to serve the increased demand of patients for the services. In the present study, TT is selected as a quantitative tool to measure the efficiency of the ED.

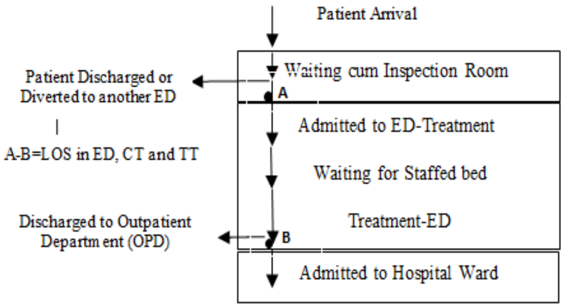

Figure 1. Patient Treatment in ED

Figure 1 shows the various parameters for the patients stay in ED for instance LOS, CT, TT, waiting for staffed bed, treatment time etc. These parameters are also presented in mathematical form in Equation (1-4) for calculating efficiency and effectiveness of ED rooms.

$$CT = \frac{Net\ Operation\ Time\ Period}{No\ of\ Patients\ treated} \quad (1)$$

$$TT = \frac{Net\ Operation\ Time\ Period}{Required\ number\ of\ patients\ to\ be\ treated\ per\ period} \quad (2)$$

Where:

$Net\ Operation\ Time\ Period$= Total available service time – Breaks (3)

Required service rate = Number of patients to be served

$$= \frac{Services\ provided\ to\ total\ patients}{Working\ periods\ per\ period}$$

(4)

Two different rooms of ED like RR – Trauma and RR – Medical rooms are considered for the present study. The TT in ED has been calculated by dividing operational time per period by the required number of patients to be treated per period. The TT can be used for all units in the value stream to adjust served patients to actual demand to serve more patients during peak hours.

3.1. Comparison of CT and TT

The crowd management in the ED is crucial and influenced by CT and TT. Cycle time is how long it should take to serve a patient in the ED. Thus CT includes value-added activities and non-value added activities hence warrants careful attention to achieve the desired service rate. The CT time depends on many parameters like number of activities to be performed, kind of medical procedure, the complexity of the task in various rooms, for instance, RR – Trauma and RR – Medical rooms. It also depends upon the availability of the doctor, nurse, technician, staffed bed, dressing room, body parameter measuring equipment etc. The TT is affected by patients' crowding requiring emergency services.

Various scenarios that can be found with their leading effects are listed in Table 1.

Table 1. Various scenario for CT and TT

Scenarios	Interpretation
CT=TT	The service line/production line is smooth and considered flawless and efficient.
CT<TT	The service capacity/production capacity is underutilized leading to waste and inefficiencies.
CT>TT	The presence of bottleneck in the service line/ production line cannot be ruled out.

4. Revisiting ED services of a government hospital

The ED under study is part of a governmental hospital based in the southern region of Saudi Arabia with a population of more than 350000. The ED consists of several rooms and this study is only concerned with RR – Trauma and RR – Medical rooms.

The study that conducted by Shakoor et.al. [33] has been further explored and results are further compared for the useful conclusion. Both RR – Trauma and RR – Medical rooms consist of 6 staffed beds for emergency patients and there is an extra staffed bed reserved for very critical cases that couldn't be diverted to other hospitals. It is noticed that the rooms under study facing a serious overcrowding problem and ambulance diversion.

In the present research, to determine and compare the efficiency of rooms under study, actual data for the length of stay (LOS), the maximum number of staffed beds occupied simultaneously each day and the total number of admitted patients are required. The required data is retrieved from the log book of the hospital. LOS represents the time that the patient reserves the staffed bed from the moment he or she admitted to the department until discharged. The collected data for RR-Trauma and RR-Medical rooms is summarized and tabulated in Table 2. The ED staffed bed occupancy rate is the ratio of the sum of the number of patients occupying staffed beds and the number of patients discharged in a day to the total number of staffed beds. The probability of ambulance diversion for RR–Trauma is 62.2% on day to day basis whereas the probability of ambulance diversion for RR-Medical is 9.58% on day to day basis. The RR-Trauma has high bed occupancy rate thus effects the ambulance diversion more as compared to RR-Medical.

Table 2: Number of Patients and LOS for RR-Trauma and RR-Medical rooms of ED

ED Rooms	Total No of Patients	LOS	Available Time (minutes)	Staffed bed Occupancy/year	Probability of ambulance diversion
RR – Trauma	1436	2123724	3153600	227	62.2%
RR – Medical	309	1173084	3153600	24	9.58%

Table 3. The Probability of the Bed Occupancy in the ED Rooms

Room	Maximum No of Staffed beds	The Probability of the Staffed bed Occupancy in the ED Rooms						
		4 or less	5	6	7	8	9	10
FOR	**9**	99.95%	0.05%	0.00%	0.00%	0.00%	0.00%	
FTR	**10**	99.17%	0.23%	0.14%	0.05%	0.14%	0.00%	0.28%
MOR	**9**	99.91%	0.00%	0.09%	0.00%	0.00%	0.00%	
MTR	**10**	98.29%	0.28%	0.19%	0.14%	0.14%	0.32%	0.65%
POR	**5**	97.78%	2.22%					
PTR	**5**	83.98%	16.02%					
RR MEDICAL	**6**	91.11%	2.22%	6.67%				
RR TRUMA	**6**	24.44%	13.33%	62.22%				

Table 4. Probability for a patient waiting or ambulance diversion upon arrival in the ED rooms.

Room	PTR	POR	MTR	FTR	MOR	FOR	RR-Medical	RR-Trauma
Probability	16.02%	2.22%	0.65%	0.28%	0.00%	0.00%	9.68%	62.22%

Table 3 shows the probability of staffed bed occupancy in ED rooms on day to day basis. The ED is equipped with Male Treatment Room (MTR), Female Treatment Room (FTR), Male Observation Room (MOR), and Female Observation Room (FOR), Pediatric Observation Room (POR), Pediatric Treatment Room (PTR), RR-Medical and RR-Trauma. The maximum number of staffed beds available for patients arriving in various rooms is different. The number of staffed beds ranges from 6 to 10 in ED rooms hence it is vital to know the staffed bed availability. The staffed bed availability maybe understood from the probability of the staffed bed occupancy rate on day to day basis. The staffed bed availability will be critically important to avert last-minute hustle and unnecessary ambulance diversion. Looking to the staffed bed usage of FOR, it has been revealed that the available 9 staffed beds have never been occupied at the same time during the whole year study period. Further, it has been seen the staffed bed utilization never been more that 5 staffed beds at the same time. If the utilization of staffed beds in the FOR, FTR and MOR rooms is compared with POR and PTR for example, it has been noted that the staffed beds in POR and PTR are continuously occupied as compared to the other rooms during the same period. Hence, distribution of the staffed bed must be revisited to enhance the efficiency and effectiveness of these staffed beds in the ED. Similar observations are also made for non-use of staffed bed during the study period so that the same can be reshuffled among the various ED rooms to enhance the efficiency and effectiveness. Table 4 provides the probability for a patient waiting or ambulance diversion in the ED rooms. The probability is ranging from 0.0% to a maximum of 62.22% for various rooms in the ED.

5. Results and Data Analysis

Based on the data collected from the hospital database for the two rooms of ED i.e. RR-Trauma and RR-Medical rooms, the actual available time/day was calculated for each room using the available facilities as shown in Table 2. Later on, the CT and TT were calculated for each room to compare the efficiency of each room with the other rooms. Cycle time is calculated as the ratio of the total actual time it takes the patients to get served to the total number of patients in a given time whereas the TT is calculated as the ratio of total available time to serve to the total number of patients in a given time. The CT and TT thus obtained are further used to calculate the efficiency of each room.

5.1. RR-Trauma Room vs. RR-Medical Room

- For the RR- Trauma room:

  $CT = \frac{2123724}{1436} = 1478.92$ min / patient

  $TT = \frac{3416400}{1436} = 2379.11$ min / patient

$Efficiency = E_{RR-Trauma} = \frac{\text{CT}}{\text{TT}} = \frac{1478.92 \text{ min./ patient}}{2379.11 \text{ min./ patient}} =$ 0.6216 i.e. 62.16%

- For the RR-Medical:

  $CT = \frac{1173084}{309} = 3796.39$ min. / patient

  $TT = \frac{3416400}{309} = 11056.31$ min. / patient

$Efficiency = E_{RR-Medical} = \frac{\text{CT}}{\text{TT}} = \frac{3796.39 \text{ min./ patient}}{11056.31 \text{ min./ patient}} =$ 0.3434 i.e. 34.34%

The CT, TT and calculated efficiency are represented for easy understanding in Figure2 and Figure3 respectively.

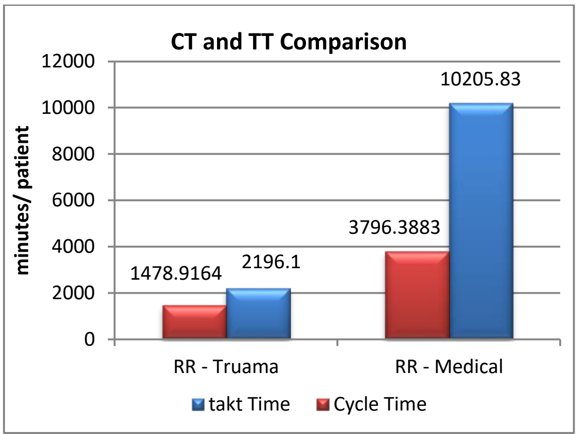

Figure 2. Comparing CT and TT of RR-Trauma and RR-Medical of ED Rooms

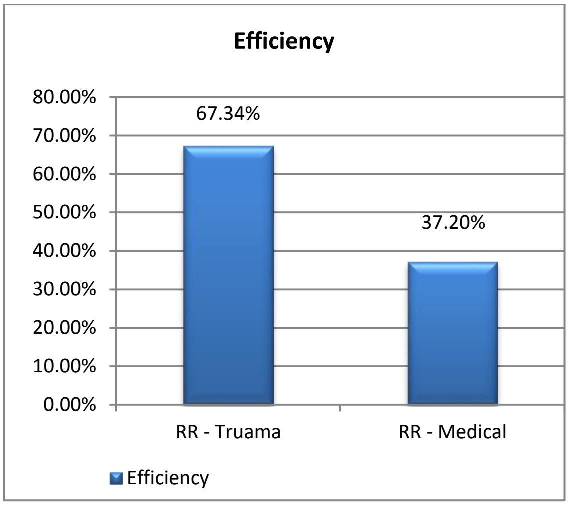

Figure 3. Efficiency Comparison of RR-Trauma and RR -Medical

A concept of relative efficiency $RE_{X/Y}$ as shown in Equation (5) is used to compare the efficiency between the two rooms X and Y as follows:

$$RE_{X/Y}=\frac{E_X}{E_Y} \quad (5)$$

Thus the $RE_{RR-\frac{Truama}{RR}-Medical}$ can be calculated as follow:

$$RE_{RR-Trauma/RR-Medical}=\frac{E_{RR-Trauma}}{E_{RR-Medical}}=\frac{0.6216}{0.3434}=1.81,$$

The relative efficiency implies that RR-Trauma room is 1.81 times more efficient than the RR- Medical room.

5.2. Comparison Analysis of the RR-Trauma Room and RR-Medical Room with the Other Rooms at the ED

On analyzing the data shown in Table 2 for LOS and staffed bed occupancy documented from the hospital log sheet, it has been observed that the staffed bed occupancy is more in RR-Trauma as compared to RR-Medical. Hence, it is more difficult to handle the patient's arrival in RR-Trauma as compared to RR-Medical. The probability of ambulance diversion is 62.2% which indicates that the ambulance has to be diverted considerably for more occasions as compared to RR-Medical. From Table 2, it is also evident that the number of patients handled in RR-Trauma are more as compared to RR-Medical. The CT and TT of RR-Trauma and RR-Medical maybe compared to understand the burden on the system. It has been seen that CT is less than the TT for both the Trauma rooms. It can be concluded that the ED room will be able to cope with the pressure of the arriving patients. Figure 2 shows the CT and TT for both RR-Trauma and RR-Medical and it may be compared to identify for the higher probability of ambulance diversion. The efficiency of RR-Trauma and RR-Medical maybe calculated and further compared for optimal resource utilization. It has been found that the RR-Trauma has higher efficiency i.e. 67.34% whereas the efficiency of RR-Medical is 37.20%. Figure 3 shows the efficiency comparison of RR-Trauma and RR-Medical.

Table 3 shows the probability of the staffed bed occupancy in the ED Rooms. The staffed beds' availability is ranging from 5 staffed beds to 10 staffed beds. Based on the hospital log sheet, it can be seen that 4 or less patients might be accommodated easily in all the ED rooms. Table 4 provides the probability of patient waiting or probable ambulance diversion in the ED rooms. The probability of waiting is more in Pediatric Treatment Room (PTR) and Pediatric Observation Room (POR) due to less number of staffed bed availability. Similarly, the treatment room occupancy is more compare to the observation room hence Male Treatment Room (MTR), and Female Treatment Room (FTR) show more patient waiting. The waiting time is minimum in Male Observation Room (MOR) and Female Observation Room (FOR). It has been observed that the observation rooms in male and female rooms can handle maximum 4 patients without any waiting. There is less ambulance diversion for RR-Medical as compared to RR-Trauma. Table 5 shows the efficiency, CT and TT of the ED rooms. The efficiency is maximum for PTR followed by POR. The efficiency of MTR and FTR are 50.32% and 41.45%.The efficiency of observation room for male and female is comparatively low. The efficiency of MOR is 18.97% and whereas efficiency of FOR is 17.73%. RR-Medical and RR-Trauma has the efficiency of 67.34% and 67.34% respectively.

The CT and TT for various ED rooms maybe calculated for comparison purposes as shown in Figure 4. It has been observed that CT is comparatively less than the TT in all the ED rooms. It has also been observed that the CT and TT of RR-Trauma and RR-Medical are the maximum. Whereas, the CT and TT are less in case of PTR.

Table 5: Efficiency, CT and TT of the different rooms of the ED

Room	Present Staffed beds	Available Time (minutes)	LOS (minutes)	No of Patients	CT	TT	Efficiency
PTR	5	2628000	2462436	25856	95.24	101.64	93.70%
POR	5	2628000	2065608	7981	258.82	329.28	78.60%
MTR	10	5256000	2645060	8274	319.68	635.24	50.32%
FTR	10	5256000	2178826	5816	374.62	903.71	41.45%
MOR	9	4730400	897556	1512	593.62	3128.57	18.97%
FOR	9	4730400	838482	1547	542.01	3057.8	17.73%
RR MEDICAL	6	3153600	1173084	309	3796.39	10205.83	37.20%
RR TRAUMA	6	3153600	2123724	1436	1478.92	2196.1	67.34%

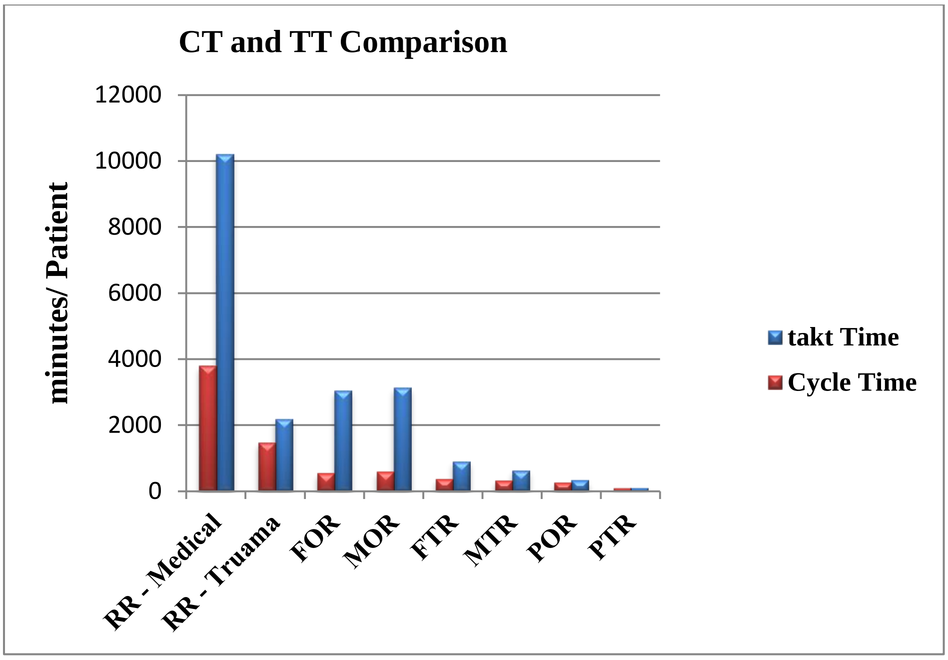

Figure 4: Comparison of CT and TT for the different rooms of the ED

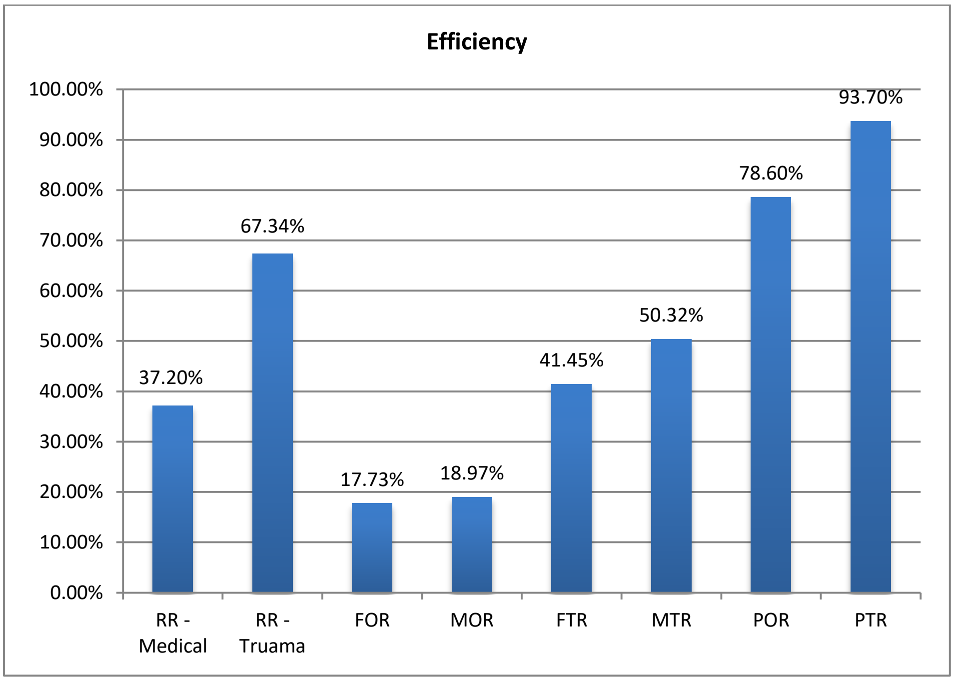

Figure 5: Efficiency comparison for the different ED rooms

5.3. Analysis of staffed Beds Redistribution in the ED Rooms

Looking to the underutilization of some rooms in the ED, the staffed bed redistribution is essential for the enhancement of efficiency and effectiveness. Based on the utilization probability as shown in Table 2 and Table 3, the staffed beds maybe redistributed for the optimal utilization. Based on the probabilities shown in Table 3 and Table 4, the allocated staffed beds maybe changed to enhance efficiency and effectiveness of ED room. As per Table 5, the number of staffed beds allocated for the MOR is 9 and proposed beds are reduced to 5, thus 4 staffed beds are transferred to other ED room to strengthen the resource utilization. Similarly FOR has 9 staffed beds, PTR and POR has 5 staffed beds, MTR and FTR has 10 staffed beds, RR medical and RR Trauma has 6 staffed beds, can be redistributed. The new proposed staffed beds distribution is shown in Table 5. Due to the proposed staffed bed redistribution, the TT and efficiency can be determined. The new proposed staffed beds along with TT and efficiency are shown in Table 6.

Table 5: Staffed bed redistribution with probabilities of accommodating more patients in the ED rooms

Room	Proposed Staffed beds for the Room	4 or less	5	6	7	8	9	10	11
FOR	5	99.95%	0.05%						
FTR	8	99.17%	0.23%	0.14%	0.05%	0.42%			
MOR	5	99.91%	0.09%						
MTR	10	98.29%	0.28%	0.19%	0.14%	0.14%	0.32%	0.65%	
POR	5	97.78%	2.22%						
PTR	7	83.98%	3.38%	2.50%	10.14%				
RR MEDICAL	9	91.11%	2.22%	3.34%	1.11%	2.22%	0.00%		
RR TRUMA	11	24.44%	13.33%	12.22%	28.90%	14.44%	4.44%	2.22%	0.00%

Table 6: Effects redistribution of staffed beds on the parameters of ED rooms

	Room	FOR	FTR	MOR	MTR	POR	PTR	RR - Medical	RR - Trauma
ED Parameters	Proposed staffed beds	5	8	5	10	5	7	9	11
	TT	1698.77	722.97	1738.1	635.24	329.28	142.3	16159.22	4209.19
	Efficiency	31.91%	51.82%	34.15%	50.32%	78.60%	93.70%	23.49%	35.14%

Based on the staffed bed redistribution, the FOR and MOR rooms at ED will face a reduced crowding. Both ED rooms will be able to negotiate the patients' arriving flow. The staff at ED will be able to deliver quality care by timely assessing patients and providing treatment without unnecessary patient waiting. From Table 6, it is revealed that the arriving patients at FOR and MOR rooms at ED will have to face a low probability of waiting. Therefore, it maybe recommend the acceptable TT and efficiency for ED rooms preferably below 1700 minutes/ patient and 30% respectively.

6. Discussion

As it is well understood that lean at ED helps in establishing value-added activities (for example wound cleaning and repair) by eliminating non-value-added activities (for example triage) in accomplishing immense patients' care. It also strives to remove *Muda* (waste) from the process by smoothly balancing *Mura* (un-level workload) among ED staff and *Muri* (unreasonable burden) on equipment thus lean management methodologies may prove to be useful for the managers in ascertaining the required efficiency, reduce waiting time for patients seeking quality care and predicting ambulance diversion to meet the patients' expanded population. The knowledge of lean management in general and TT in particular will enable managers to revisit the ED activities at *Gemba* (workplace) to ensure a new framework, implement suitable changes, develop methods and time standards for smooth workflow (staff and patient movement) to implement for continuous improvement at ED. The knowledge of CT, TT will also help managers to handle the work pressure which will help in negotiating the error and service quality. The probability of ambulance diversion is an important parameter to decide the crowding in the ED rooms. The ambulance diversion may also be controlled by managing the TT. Thus, based on the staffed bed occupancy during the year a probability of non-availability of staffed bed and TT will decide the ambulance diversion to another ED of other private hospitals. The probability patients' arrival and TT at the ED rooms will also ensure the minimum staffed bed to handle the patients rush at the ED rooms. By calculating the TT and probability of staffed bed occupancy in ED rooms, a decision making policy concerning the minimum number of staffed beds maybe useful in maintaining the balance between the quality care services to ailing patient and optimum resource utilization.

It has been noticed that the ED rooms are not optimally utilized throughout the year due to the variation in the patients' arrival. Hence based on the logbook data of the hospital, the redistribution of staffed bed has been carried out to enhance the efficiency and effectiveness of ED rooms. Based on the lean principles, it has been proposed that the number of staffed beds maybe 5 for optimal resource utilization. Similarly, the FTR may have 8 staffed beds, MOR may have 5 staffed beds, MTR may have 10 staffed beds, POR may have 5 staffed beds, PTR may have 7 staffed beds, RR Medical may have 9 staffed beds, and RR Trauma may have 11 staffed beds. This staffed bed redistribution will enhance the efficiency and effectiveness of ED rooms. It will also help in saving the precious life of ailing patients seeking immediate care. The frequent ambulance diversion will also affect the breakeven point of the hospital operation which will make hospital service most costly. It will also pose a hurdle in becoming a competitive healthcare services provider. Using management principles of lean manufacturing the TT management is feasible. The reduced TT will further help in reducing the cycle time. On managing TT within a controllable limit, it is also further possible to enhance the efficiency and effectiveness of ED rooms. The patient arrival rate maybe accurately forecasted to take complete control of ED rooms.

6.1. Case of RR- Trauma Room

Retrieved data from the hospital database revealed that in 62.22% of the year days, there was a probability of ambulance diversion from the RR-trauma room due to the occupancy of all staffed beds simultaneously by patients in this room. Also, in 27% of the year days, there was a probability of not accommodating very critical cases because the seventh staffed bed that reserved for these cases is occupied. This situation surfaced out the serious and critical problem in managing the patients' crowd in this room of the ED. Therefore, this situation requires an urgent intervention to increase the number of staffed beds in this room in order to accommodate all arrived patients and save their lives.

In this room, the CT<TT (i.e. 1478.92<2379.11), cycle time is 1478.92 minutes/ patient, whereas TT is 2379.11 minutes/ patient. Also, the RR-Trauma's room efficiency ($E_{RR-Trauma}$)is calculated as the ratio of CT to TT, and found to be $\mathrm{E}_{\mathrm{RR-Trauma}}$= 62.16% which is considered to be a high value for healthcare facilities as in ED.

6.2. Case of RR-Medical Room

Also, the retrieved data revealed that in 9.58% of the year days, there was a probability of ambulance diversion from the RR-medical room. In addition to that, in 27% of the year days, there was a probability of not accommodating very critical cases. It is evident that the RR-medical room has a crowding and ambulance diversion problems but the situation in this room still much better than the situation in the RR-trauma room. The RR-medical room requires an increase in the number of staffed beds in order to reach the conclusion of a zero ambulance diversion.

Furthermore, in this room, the CT<TT (i.e. 3796.39 <11056.31), cycle time is 3796.39 minutes per patient, whereas TT is 11066.31 minutes per patient. Also, the efficiency of the RR-Medical room ($\mathrm{E}_{\mathrm{RR-Medical}}$) has been found as 34.34% which is considered to be an acceptable value but still need to be reduced in order to reach a zero ambulance diversion. Looking at the efficiency calculations, it has been observed that the efficiency of the RR-Trauma room is 81% greater than the RR- Medical room.

7. Conclusion

It is very essential to understand the role of CT and TT in order to increase the efficiency and effectiveness and to reduce crowding at the ED rooms. In the ideal situation for ED services, the CT should equal the TT. It may be interpreted as service warranted does not show any exigency nor need any additional action as there is no pressure on its administration and management. However, this situation is hardly prevailing in the ED rooms. When CT is more than the TT, it results in severe crowding at ED rooms. It is observed that on frequent crowding the patients have to wait in receiving the critical care services in ED. In the present case, it was revealed that there was a shortage of staffed beds in ED rooms. In such a scenario, the patient's life is put to great danger. The decision-making becomes crucial in a patient's movement and subsequent ambulance diversion. Frequent crowding and ambulance diversion may threaten to lose customer faith and loyalty. Thus, private healthcare organizations may face losing customers and market share in the end. The frequent ambulance diversion will be a costly affair as it will put pressure on the hospital overhead. The government may also face extra burdens due to added liability. On the other hand, the TT and probability-based staffed bed distribution will further reduce the number of totals diverged patients to other hospitals in a year which will help in saving lives and cost. From the present case study, it may be recommended that the acceptable TT and efficiency for ED rooms preferably should be below 1700 minutes/ patient and 30% respectively. The practicing managers at ED may follow this benchmarking in managing patients' flow to avert crowding. Finally, CT and TT must be considered as the top priority in ED services. The ED staffed beds maybe redistributed using the lean concepts to enhance patient's flow and to optimize the resource utilization to offer world-class services.

Compliance with Ethics Requirements

Mwafak Shakoor declares that he has no conflict of interest.

Also, this article does not contain any studies with human or animal subjects.

References

[1] Health Statistics Annual Book. Ministry of Health, Saudi Arabia, http://www.moh.gov.sa/en/Ministry/Statistics/book/flash/1433/MOH_Report_1433.html, accessed on 1 – 12 – 2014, 2012.

[2] S. David, M. Yariv,"Ways to reduce patient turnaround time and improve service quality in emergency departments", Journal of Health Organization and Management, Vol. 19 (2005), No. 2, 88 –105.

[3] E.W. Dickson, S. Singh, D.S. Cheung, C.C. Wyatt, A.S. Nugent,"Application of lean manufacturing techniques in the Emergency Department", The Journal of Emergency Medicine, Vol. 37 (2009), No. 2, 177–182.

[4] N. Xiao, R. Sharman, H.R. Rao, S. Dutta, "A simulation-based study for managing hospital emergency department's capacity in extreme events", International Journal of Business Excellence, Vol. 5 (2012), No. 1- 2, 140–154.

[5] J.F. Bard, Z. Shu, D.J. Morrice, D.E. Wang, R. Poursani, L. Leykum, "Improving patient flow at a family health clinic", Health Care Management Science, Vol. 19 (2016), No. 2, 170 – 191

[6] Y. He, L. Ting, G. Kremer, "Performance comparison of four triage–based patient flow interventions in the emergency department", International Journal of Collaborative Enterprise, Vol. 4 (2014), No. 1–2, 115–135.

[7] Z. Sepehri, S.M. Arabzad, S.M. Sajadi, "Analyzing performance of emergency department by simulation: the case of Sirjan Hospital", International Journal of Services and Operations Management, Vol. 20 (2015), No. 3, 289 – 301

[8] A.W. Keith, B.T.B. Chan, M. Strenger, "Achieving wait time reduction in the emergency department", Leadership in Health Services, Vol. 23 (2010), No. 4, 304–319.

[9] S. Oredsson, H. Jonsson, J. Rognes, L. Lind, K.E. Göransson, A. Ehrenberg, K. Asplund, M. Castrén, N. Farrohknia, 2011. "A systematic review of triage-related interventions to improve patient flow in emergency departments", Scandinavian Journal of Trauma, Resuscitation and Emergency Medicine, Vol. 19 (2011), 43, DOI: 10.1186/1757-7241-19-43

[10] J. Womack, D. Jones,"Lean Thinking". Simon & Schuster, New York, NY, 1996.

[11] M. Braglia, G. Carmignani, F. Zammori,"A new value stream mapping approach for complex production systems",

International Journal of Production Research, Vol. 44 (2006), No. 18–19, 3929–3952.

[12] S. P. Vendan, K. Sakthidhasan, "Reduction of Wastages in Motor Manufacturing Industry", Jordan Journal of Mechanical and Industrial Engineering, Vol. 4 (2010), No. 5, 579 – 590

[13] D.T. Matt, E. Rauch,"Implementation of lean production in small sized enterprises", ProcediaCIRP, Vol. 12 (2013), 420–425.

[14] N. Mandahawi, R.H. Fouad, S. Obeidat, "An Application of Customized Lean Six Sigma to Enhance Productivity at a Paper Manufacturing Company", Jordan Journal of Mechanical and Industrial Engineering, Vol. 6 (2012), No. 1, 103 – 109

[15] G.A. Marodina, T.A. Saurina, "Implementing lean production systems: research areas and opportunities for future studies", International Journal of Production Research, Vol. 51 (2013), No. 22, 6663–6680.

[16] M.A. Gomez, J.A. Hirsch, P. Stingley, E. Byers, R.M. Sheridan,"Applying the lean management philosophy to neurointerventional radiology", Journal of Neurointerventional Surgery, Vol. 2 (2010), No. 1, 83–86.

[17] J.E. Johnson, A.L. Smith, K.A. Mastro, "From Toyota to the bedside: nurses can lead the lean way in health care reform", Nursing Administration Quarterly, Vol. 36 (2012), No. 3, 234–242.

[18] P. Mazzocato, R.J. Holden, M. Brommels, H. Aronsson, U. Bäckman, M. Elg, J. Thor, "How does lean work in emergency care? A case study of a lean-inspired intervention at the Astrid Lindgren Children's hospital, Stockholm, Sweden", MBC Health Service Research, Vol. 12 (2012), No. 1, 12–28.

[19] J.S. Toussaint, L.L. Berry,"The promise of lean in health care", Mayo Clinic Proceedings, Vol. 88 (2013), No. 1, 74–82.

[20] S. Timmons, F. Coffey, P. Vezyridis, "Implementing lean methods in the emergency department: The role of professions and professional status", Journal of Health Organization and Management, Vol. 28 (2014), No. 2, 214–228.

[21] Abdelhadi, M. Shakoor, "Studying the efficiency of inpatient and outpatient pharmacies using lean manufacturing", Leadership in Health Services, Vol. 27 (2014), No. 3, 255 – 267

[22] K.L. Murrell, S.R. Offerman, M. B. Kauffman,"Applying lean: implementation of a rapid triage and treatment system", Western Journal of Emergency Medicine, Vol. 12 (2011), No. 2, 184–191.

[23] R.J. Holden, "Lean thinking in emergency departments: A critical review", Annals of Emergency Medicine, Vol. 57 (2011), No. 3, 265–278.

[24] P.S. Gill, "Application of value stream mapping to eliminate waste in an emergency room", Global Journal of Medical Research, Vol. 12 (2012), No. 6, 51–56.

[25] R.R. Willem, "Improving healthcare delivery with lean thinking: action research in an emergency department". (2014)

[26] N. Mandahawi, S. Al-Shihabi, A.A. Abdallah, Y.M. Alfarah,"Reducing waiting time at an emergency department using design for six sigma and discrete event simulation", International Journal of Six Sigma and Competitive Advantage, Vol. 6 (2010), No. 1-2, 91–104

[27] M.J. Vermeulen, T.A. Stukel, A. Guttmann, H.R. Brian, M. Zwarenstein, B. Golden, A. Nigam, G. Anderson, R.S. Bell, M.J. Schull, "Evaluation of an emergency department lean process improvement program to reduce length of stay", Annals of Emergency Medicine, Vol. 64 (2014), No. 5, 427 – 438, DOI: 10.1016/j.annemergmed.2014.06.007

[28] R. Akkerman, M. Knip,"Reallocation of Beds to Reduce Waiting Time for Cardiac Surgery", Health Care Management Science, Vol 7 (2004), No. 2, 119 – 126.

[29] M.H. Mehrolhasani, S. Khosravi, and M. Tohidi,"Reallocation of Shafa Hospital Beds in Kerman Using Goal Programming Model", Electron Physician, Vol. 8 (2016), No. 8, 2733–2737.

[30] R.K. Khare, E.S. Powell, G. Reinhardt, M. Lucenti, "Adding More Beds to the Emergency Department or Reducing Admitted Patient Boarding Times: Which Has a More Significant Influence on Emergency Department Congestion?", Annals of Emergency Medicine, Vol. 53 (2009), No. 5, 575-585.

[31] L.K. Diane, D.I. Ben-Tovim, J. Bassham,"Redesigning emergency department patient flows: Application of Lean Thinking to health care", Emergency Medicine Australasia, Vol. 18 (2006), No. 4, 391 – 397.

[32] W. Teng-Kuan, T. Yang, C-Y. Yang, Chan, "Lean principles and simulation optimization for emergency department layout design", Industrial Management & Data Systems, Vol. 115 (2015), No. 4, 678-699.

[33] M. Shakoor, W. Abu Jadayil, N. Jabera, S. Jaber, "Efficiency Assessment in Emergency Department Using Lean Thinking Approach", Jordan Journal of Mechanical and Industrial Engineering, Vol. 11 (2017), No. 2, 97-103

المملكة الأردنية الهاشمية

الجامعة الهاشمية

المجلة الأردنية
للهندسة الميكانيكية والصناعية

JJMIE

مجلة علمية عالمية محكمة

تصدر بدعم من صندوق البحث العلمي

http://jjmie.hu.edu.jo/

ISSN 1995-6665

المجلة الأردنية للهندسة الميكانيكية والصناعية

المجلة الأردنية للهندسة الميكانيكية والصناعية: مجلة علمية عالمية محكمة تصدرعن الجامعة الهاشمية بالتعاون مع صندوق دعم البحث العلمي والابتكار- وزارة التعليم العالي والبحث العلمي في الأردن.

ترسل البحوث إلى العنوان التالي

رئيس تحرير المجلة الأردنية للهندسة الميكانيكية والصناعية

الجامعة الهاشمية
كلية الهندسة
قسم الهندسة الميكانيكية
الزرقاء - الأردن

هاتف : 3903333 5 00962 فرعي 4147

Email: jjmie@hu.edu.jo

Website: www.jjmie.hu.edu.jo